A survey on deep learning in medical image registration: new technologies, uncertainty, evaluation metrics, and beyond

Junyu Chen^{a,1,*}, Yihao Liu^{b,1}, Shuwen Wei^{b,1}, Zhangxing Bian^b, Shalini Subramanian^a, Aaron Carass^b, Jerry L. Prince^b, Yong Du^a

ARTICLE INFO

Article history: Received xxxx Received in final form xxxx >Accepted xxxx Available online xxxx

Communicated by xxxx

ABSTRACT

Deep learning technologies have dramatically reshaped the field of medical image registration over the past decade. The initial developments, such as regression-based and U-Net-based networks, established the foundation for deep learning in image registration. Subsequent progress has been made in various aspects of deep learning-based registration, including similarity measures, deformation regularizations, network architectures, and uncertainty estimation. These advancements have not only enriched the field of image registration but have also facilitated its application in a wide range of tasks, including atlas construction, multi-atlas segmentation, motion estimation, and 2D-3D registration. In this paper, we present a comprehensive overview of the most recent advancements in deep learning-based image registration. We begin with a concise introduction to the core concepts of deep learning-based image registration. Then, we delve into innovative network architectures, loss functions specific to registration, and methods for estimating registration uncertainty. Additionally, this paper explores appropriate evaluation metrics for assessing the performance of deep learning models in registration tasks. Finally, we highlight the practical applications of these novel techniques in medical imaging and discuss the future prospects of deep learning-based

field of image regis tasks, including atla 2D-3D registration. recent advancement cise introduction to we delve into innov and methods for est appropriate evaluati els in registration ta techniques in medical image registration.

1. Introduction

Medical image registration involves estimating the optimal spatial transformation to align the structures of interest in a pair of fixed and moving images. The choice of spatial transformation depends on the specific application and can be categorized as either rigid/affine or non-rigid/deformable. be categorized as either rigid/affine or non-rigid/deformable. In rigid/affine registration, all spatial coordinates are transformed using the same rigid/affine matrix. On the other hand, non-rigid/deformable registration employs independent transformations for individual local regions of spatial coordinates. Both types of registration are of great importance to many medical imaging tasks. Rigid registration is commonly used when the rigid body assumption holds. For example, it is used to align a structural scan—e.g., magnetic resonance image (MRI) or computed tomography (CT)—with a functional scan—e.g., functional magnetic resonance image (fMRI) or positron emission tomography (PET)—of the same patient for attenuation correction (Hofmann et al., 2008) or interpretation of functional activities (Studholme et al.,

2000). On the other hand, deformable image registration (DIR) is often used in cases where more complex, spatially varying deformations are needed. Examples of such applications include constructing deformable templates for a patient cohort (Christensen et al., 1996; Ganser et al., 2004) or registering atlases to a patient image for multi-atlas segmentation (Reed et al., 2009; Cabezas et al., 2011; Aljabar et al., 2009).

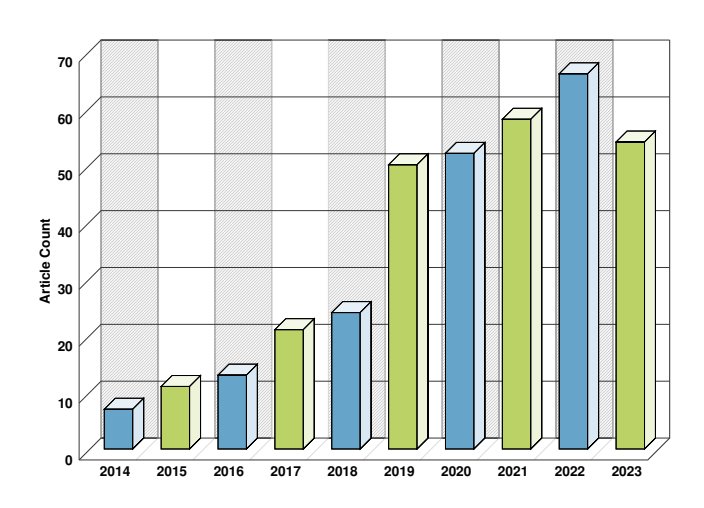
Traditionally, image registration has been accomplished by iteratively solving an optimization problem (e.g., demons (Vercauteren et al., 2009), LDDMM (Beg et al., 2005), SyN (Avants et al., 2008), DARTEL (Ashburner, 2007), and Elastix (Klein et al., 2009). These methods are well-established and supported by strong mathematical theory but come with notable limitations. Firstly, they are computationally intensive and tend to be slow, as they involve solving a distinct optimization problem for every pair of moving and fixed images, leading to redundancy across optimizations. Secondly, the objective function related to transformation parameters (such as displacement fields or control points) typically exhibits non-linearity, creating a nonconvex optimization dilemma. To address this, attempts have been made to simplify the problem, for instance, by linearizing the objective function (Sun et al., 2013), convexifying the optimization (Esser, 2010; Heinrich et al., 2014; Rajchl et al.,

^aDepartment of Radiology and Radiological Science, Johns Hopkins School of Medicine, MD, USA

^bDepartment of Electrical and Computer Engineering, Johns Hopkins University, MD, USA

^{*}Corresponding author. E-mail address: jchen245@jhmi.edu.

¹Contributed equally to this work.



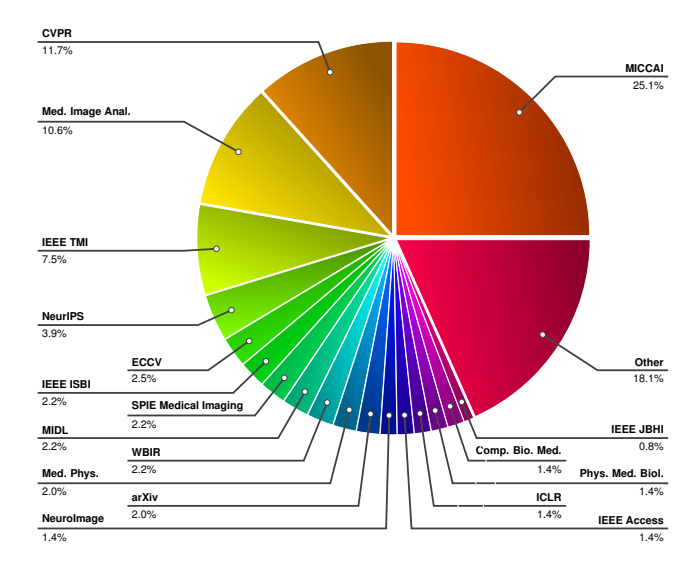


Fig. 1. Statistics of the articles investigated in this survey paper. The left panel displays a histogram of the number of papers by year; the vast majority of the surveyed papers were proposed within the last five years. The right panel illustrates the sources of the investigated articles, demonstrating that our survey draws from sources associated with the field of medical image analysis.

2016), or adopting discretized registration techniques (Glocker et al., 2008, 2011; Heinrich et al., 2012b, 2014). However, these approaches often increase computational costs and might lead to a less realistic problem, given the inherently non-convex nature of image registration (Sotiras et al., 2013). Several review papers have covered traditional medical image registration methods extensively (Maintz and Viergever, 1998; Hill et al., 2001; Shams et al., 2010; Fluck et al., 2011; Sotiras et al., 2013; Oliveira and Tavares, 2014; Viergever et al., 2016). Interested readers can refer to these references for more information on these methods.

In the last decade, deep learning-based methods have shown promise in improving the accuracy and efficiency of image registration. Unlike traditional methods, deep learning-based methods train a general network by optimizing a global objective function on a training dataset. Then in the testing phase, the trained network is directly applied to each image pair with fixed network weights without further optimization. Deep learningbased methods offer a threefold advantage: First, the diversity within the training dataset acts as an implicit regularization, effectively smoothing the loss landscape by averaging out noisy or misleading gradients that may lead to suboptimal local minima. Secondly, the optimization of non-convex problems is highly dependent on the initial starting point. The use of pretrained weights (i.e., transfer learning), combined with advanced optimization algorithms, enhances deep learning methods' capacity to locate global minima. Lastly, the capability to process image pairs through a single forward pass during inference, avoiding iterative optimization, results in a significant speed advantage over traditional optimization-based methods. Initially, image registration network architectures were mostly encoder-based, serving either as feature extractors to replace hand-crafted features in optimization-based registration methods (Wu et al., 2013) or as regressors for estimating transformation parameters from local image patches (Miao et al., 2016). However, following the success of U-Net (Ronneberger et al.,

2015) in medical imaging, learning-based deformable registration methods began to incorporate an encoder-decoder architecture within a supervised learning framework (Yang et al., 2017; Rohé et al., 2017; Sokooti et al., 2017; Uzunova et al., 2017), often requiring ground truth deformation fields for direct supervision. Concurrently, the advent of spatial transformer networks (Jaderberg et al., 2015) heralded a shift towards unsupervised and end-to-end learning for deformable registration employing the encoder-decoder framework, which has now become the dominant approach (Vos et al., 2017; Li and Fan, 2018; Balakrishnan et al., 2019; Kim et al., 2021; Chen et al., 2022c). On the other hand, learning-based rigid/affine registration methods continue to adopt encoder-only networks (Miao et al., 2016; Hu et al., 2018; De Vos et al., 2019; Chen et al., 2021e, 2022c; Mok and Chung, 2022a), with the output being the rigid or affine parameters. In the context of supervised learning for these deep learning-based methods, the ground truth is typically a transformation matrix for rigid/affine registration tasks, while a dense displacement field is used for deformable registration tasks. While there are papers that provide general reviews of learning-based registration methods (Fu et al., 2020a; Chen et al., 2021d; Xiao et al., 2021; Zou et al., 2022), it is important to note that these reviews may not be fully upto-date due to the rapid advancement of the field of deep learning. Recent advancements, including learning-based similarity metrics and regularizers, novel network architectures, and innovative evaluation metrics and uncertainty estimation methods, have demonstrated promising potential for medical image registration. This paper provides a timely review of learningbased methods in medical image registration, highlighting the latest technologies that have been proposed and discussing their respective characteristics and applications. In addition, we investigate and formally define registration uncertainty for deep learning-based image registration and address the appropriate evaluation metrics for these methods that have been overlooked in previous review papers. For simplicity, we refer to deep learning-based methods as learning-based methods throughout the paper.

In this paper, we surveyed over 250 articles on learningbased medical image registration. As depicted in Fig. 1, the focus is primarily on recent advancements proposed in the last five years. Our search covers well-established medical imaging journals, such as Medical Image Analysis, IEEE Transactions on Medical Imaging, Medical Physics, and NeuroImage, as well as conference proceedings related to medical imaging and image registration, such as MICCAI, IPMI, WBIR, CVPR, ECCV, ICCV, and NeurIPS. A comprehensive list of opensourced code from the papers reviewed in this study has been organized and is available at https://bit.ly/3QgFJ9z. The remainder of the paper is organized as follows: Section 2 offers a brief overview of the fundamentals of learning-based image registration. Section 3 explores widely-used loss functions for learning-based registration methods which resemble objective functions in traditional methods, and discusses other novel loss functions enabled by deep learning. Section 4 investigates network architectures developed for medical image registration, with a focus on recent developments. Section 5 delves into methods for estimating registration uncertainty in learningbased registration. Section 6 considers appropriate evaluation metrics for learning-based methods and examines methods for quantifying the regularity of generated deformation fields. Section 7 provides an enumeration of commonly used public benchmark datasets for medical image registration. Section 8 summarizes recent applications of learning-based registration in medical imaging. Finally, Section 9 discusses current challenges and provides future perspectives for deep learning in medical image registration.

2. Fundamentals of Learning-based Image Registration

Image registration aims to estimate the optimal coordinate transformation that minimizes an energy function of the form:

$$\hat{\phi} = \arg\min_{\phi} E(I_f, I_m \circ \phi) + \lambda R(\phi), \tag{1}$$

where I_f and I_m denote the fixed and moving image, respectively, ϕ represents the deformation field that maps I_m to I_f , and R is a functional of ϕ . The first term in the energy function measures the image similarity between the fixed image and the transformed moving image. The second term enforces regularization on the deformation field, with λ being a hyperparameter that determines the trade-off between image similarity and deformation field regularity. The purpose of the image similarity measure is to quantify the discrepancy between the fixed image and the transformed moving image. The regularization term is typically used in DIR, as it allows for the integration of prior knowledge about the desired characteristics of the deformation field, such as spatial smoothness. Moreover, regularization prevents the deformation field from exhibiting physically implausible behaviors, such as "folding" or rearranging of voxels (Rohlfing, 2011). This is particularly important for medical images because such unrealistic behavior does not accurately reflect the way that organs deform in reality and may lead to a misinterpretation of the registration results. Regularization is often not required for rigid/affine registration because the deformation field is guaranteed to be spatially uniform.

2.1. Supervised vs. Unsupervised Learning

Learning-based registration methods can be broadly categorized as supervised and unsupervised. In the machine learning paradigm, supervised learning typically refers to the use of extrinsic information during learning (such as labels) whereas unsupervised methods are concerned with discovering properties intrinsic to the data. Both supervised and unsupervised learning-based registration methods require a training stage that uses pairs of inputs and their corresponding target outputs. Supervised registration methods use ground truth transformations as target output during the training process. Unsupervised methods refer to those that do not require ground truth transformations. Yet, methods that employ landmark correspondences or anatomical label maps during their training phase are still categorized under supervised learning. This is because landmark correspondences are a sparse representation of the ground truth transformations, and matching label maps act as a surrogate for evaluating registration performance. When this extrinsic information is used alongside the image data to aim learning, these methods are referred to as semi-supervised. In certain contexts, the term "unsupervised" might be misleading. A more precise term could be "self-supervised" to underscore the training aspect of deep learning. However, for the purposes of clarity and consistency in this discussion, we will use conventional terminology and refer to methods that do not require supervision from extrinsic information as unsupervised.

During the early stages of development, the majority of learning-based registration methods were supervised. The ground truth transformations required for the training process are typically generated using traditional registration methods, such as (Yang et al., 2017; Rohé et al., 2017; Cao et al., 2017; Hu et al., 2018; Fan et al., 2019b). However, generating groundtruth transformations this way is a time-consuming process, which is a notable drawback of such methods. In addition, since these networks are trained to mimic the function of traditional methods, their registration performance may not surpass that of the methods they are based on. In some cases, post-processing of the deformation fields may be required to further improve registration accuracy (Yang et al., 2017). Alternatively, artificial deformations can also be used as ground truth transformations in certain cases (Miao et al., 2016; Krebs et al., 2017; Sokooti et al., 2017; Eppenhof and Pluim, 2018b; Eppenhof et al., 2018).

More recently, the introduction of spatial transformer networks (Jaderberg et al., 2015) has led to a shift towards developing unsupervised methods that do not rely on ground-truth transformation (Vos et al., 2017; Li and Fan, 2018; De Vos et al., 2019; Balakrishnan et al., 2019; Dalca et al., 2019b; Mok and Chung, 2020a,b, 2021b; Kim et al., 2021; Chen et al., 2022b, 2021b). These methods use the difference between the deformed moving image and the fixed image to update the network, enabling end-to-end training. By removing the reliance on ground truth transformation, these methods offer greater

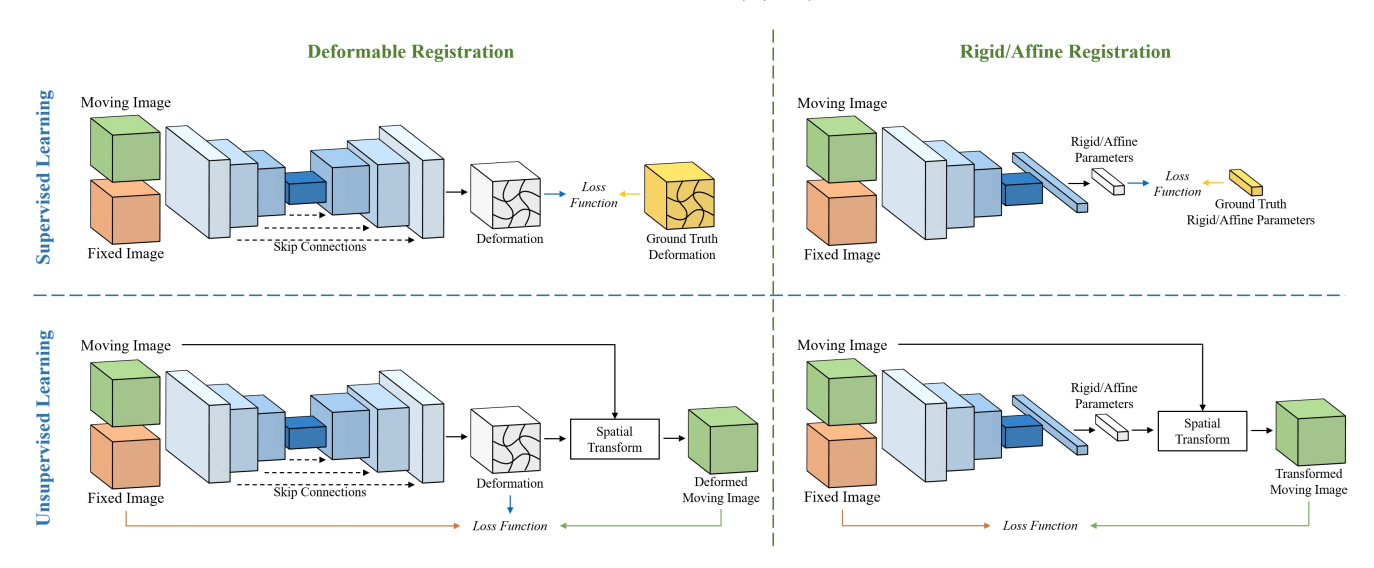


Fig. 2. Overview of learning-based image registration. The top panel depicts the common pipeline for supervised learning in medical image registration, which necessitates ground truth transformations. The bottom panel demonstrates the unsupervised learning pipeline, wherein the network learns to perform registration using only input images. The left panel presents the learning-based DIR pipeline, typically employing an encoder-decoder-style network architecture. The right panel exhibits the learning-based rigid/affine registration, which usually involves only an encoder.

flexibility in modeling different properties of the deformation fields (*e.g.*, smoothness, invertibility).

2.2. Paradigm for Learning-based Registration

Recent progress in the field of learning-based medical image registration has been focusing on exploring different ways to improve registration accuracy, such as through modifications to network architectures, loss functions, and training methods, which will be discussed in detail in subsequent sections. Despite these efforts, the fundamental principles of learning-based registration have remained unchanged. Figure 2 illustrates the conventional paradigms of learning-based rigid/affine and DIR. Typically, these paradigms consist of the following components:

- 1. Moving and fixed images as input
- 2. A deep neural network
- 3. The spatial transformer (for unsupervised methods)
- 4. A loss function

The way in which moving and fixed images are inputted into deep neural networks (DNNs) varies depending on the architecture of the network. They can either be concatenated and sent in as a single input (*e.g.*, VoxelMorph (Balakrishnan et al., 2019)) or each image can be processed separately by the DNN, with the feature maps being combined in a deeper stage (*e.g.*, Quicksilver (Yang et al., 2017)).

The architecture of DNNs can vary depending on the specific task they are designed to perform and the learning method they will undergo. For affine/rigid registration methods, DNN encoders are used for feature extraction and fully connected layers are used to output the parameters of the predicted transformation. DIR methods use DNNs with both an encoder and decoder, and the result is a deformation field of equal sizes to the input images. In the supervised setting, the network output is

compared to ground truth transformations (generated from synthetic transformations or traditional image registration methods) or landmark correspondences using a loss function. In the unsupervised setting, the predicted transformation is used by the spatial transformer (Jaderberg et al., 2015) to warp the moving image, and the transformed image is then evaluated against the fixed image using a loss function that incorporates an image similarity measure. When anatomical label maps for the fixed and moving images are available, the warped moving label map can also be produced by using the predicted transformation and the spatial transformer. An anatomy loss can be computed using the warped moving label map and the fixed label maps to provide extra guidance during network training.

There is a diverse range of loss functions to choose from, depending on the learning mode. These are thoroughly discussed in Section 3. The networks are trained by globally optimizing the loss function during the training stage using a training dataset. The trained networks are then applied to unseen testing images for inference.

Due to the self-supervised nature of image registration, the difference between the transformed moving image and the fixed image can be further reduced at test time. This is commonly known as *instance-specific optimization* (Balakrishnan et al., 2019; Siebert and Heinrich, 2022; Mok and Chung, 2022b; Heinrich and Hansen, 2022; Chen et al., 2020). Specifically, the network weights can be optimized during test time to reduce the dissimilarity of each fixed and moving image pair in the test dataset and further boost the performance. Registration networks can also be specifically designed to produce diffeomorphic transformations, which are highly desirable in DIR methods and will be discussed further in the next subsection.

2.3. Diffeomorphic Image Registration

Many learning-based DIR methods follow a small deformation model (Balakrishnan et al., 2019; Kim et al., 2021; De Vos

et al., 2019; Sokooti et al., 2017; Mok and Chung, 2021b; Heinrich, 2019; Hu et al., 2018). In this model, ϕ in Eqn. 1 is approximated by a displacement field, d, expressed as $\phi = id + d$, where the displacement is added to the identity transform, id. Since ϕ may not be a one-to-one mapping, this model does not guarantee the invertibility of the deformation. In some cases, the "inverse" transformation is roughly approximated by subtracting the displacement (Ashburner, 2007). In many applications (e.g., Avants et al. (2008); Oishi et al. (2009); Christensen et al. (1997)), diffeomorphic image registration is highly desirable because it provides transformation invertibility and topological preservation. Diffeomorphic transformations are defined as smooth and continuous one-to-one mappings with a smooth and continuous inverse (i.e., positive Jacobian determinants). They are achieved mainly through two approaches: the timedependent velocity field (Beg et al., 2005; Avants et al., 2008) or the time-stationary velocity field (Arsigny et al., 2006; Ashburner, 2007; Vercauteren et al., 2009; Hernandez et al., 2009) approach.

The time-dependent velocity field approach involves integrating sufficiently smooth velocity fields that change over time. The diffeomorphism is established by using a velocity field $v^{(t)}$ at time t, and evolving it through (Beg et al., 2005):

$$\frac{d\phi^{(t)}}{dt} = v^{(t)}(\phi^{(t)}). \tag{2}$$

The diffeomorphic transformation is achieved by starting with an identity transformation, *i.e.* $\phi^{(0)} = id$, and integrating over the unit time period:

$$\phi^{(1)} = \phi^{(0)} + \int_0^1 v^{(t)}(\phi^{(t)})dt. \tag{3}$$

Time-varying models for learning-based registration offer the promise of capturing complex and large deformations while preserving diffeomorphic mappings that ensure biologically realistic transformations. However, such models entail certain challenges. Achieving the time-dependent diffeomorphic mapping can be done by either integrating a sequence of small, sufficiently smooth (first-order differentiable) velocity fields as proposed by the original LDDMM (Beg et al., 2005), or by estimating an initial velocity field and subsequently deriving the time-varying velocity fields via geodesic shooting (Miller et al., 2006; Zhang and Fletcher, 2019). Implementing the former within a DNN framework necessitates the network to estimate a series of displacement fields at discrete time points, usually at high resolution, which leads to increased memory requirements. On the other hand, it is numerically difficult to enforce a deformation field to follow a geodesic by geodesic shooting, making end-to-end training challenging without adapting the geodesic shooting method to modern DNN libraries. Such challenges have limited the implementation of time-varying diffeomorphic mapping in current learning-based registration models. Only a handful of studies (Ramon et al., 2022; Pathan and Hong, 2018; Shen et al., 2019; Yang et al., 2016, 2017; Han et al., 2021; Wang and Zhang, 2020; Wang et al., 2023b; Wang and Zhang, 2022), have integrated this into a DNN framework. Out of these, only three studies have embedded geodesic shooting into an end-to-end learning framework for medical image registration (Shen et al., 2019; Wang et al., 2023b; Wang and Zhang, 2022).

The time-stationary velocity field approach considers velocity fields that remain constant throughout time. By using this setting, the evolution of the diffeomorphism in Eqn. 2 can be rewritten as:

$$\frac{d\phi^{(t)}}{dt} = v(\phi^{(t)}),\tag{4}$$

where the velocity field, v, is now independent of time. Dalca et al. (2019b) were the first to use this setting in a DNN model through the *scaling-and-squaring* method (Arsigny et al., 2006; Ashburner, 2007). This method has since become dominant in learning-based diffeomorphic registration models (Mok and Chung, 2020a; Chen et al., 2022b; Mok and Chung, 2020b; Han et al., 2023; Zhang et al., 2021a; Qiu et al., 2021; Zhao et al., 2021a; Krebs et al., 2019). The scaling-and-squaring method considers the velocity field as a member of the Lie algebra and the deformation field as a member of the Lie group. The relationship between the velocity field and diffeomorphism is governed by the principle that one-parameter subgroups in the Lie group can be equivalently represented via an exponential map (Arsigny et al., 2006; Vercauteren et al., 2009; Ashburner, 2007), which is mathematically expressed as:

$$\phi = \exp(v) = \exp(2^{-N}v)^{2^{N}}, \tag{5}$$

which is equivalent to integrating along the velocity field over the unit time period (in this case, N time steps). An alternative perspective is that the Jacobian determinant of a deformation resulting from exponentiating the velocity field is always positive, similar to how the derivative of the exponential of a real number is always positive (Ashburner, 2007). For further information on the implementation of this method, we direct interested readers to the references cited (Ashburner, 2007; Arsigny et al., 2006; Dalca et al., 2019b). It is important to note that the scaling-and-squaring method cannot guarantee a foldingfree transformation in the digital domain when measured by the finite difference approximated Jacobian determinant. This is because the scaling-and-squaring method involves bilinear or trilinear interpolation that is inconsistent with the piecewise linear transformation assumed by the finite difference based Jacobian determinant computation (Liu et al., 2022b).

3. Loss Functions

Table 1 provides a compilation of unsupervised DIR models, summarizing the similarity and auxiliary loss functions, as well as other details.

The topic of similarity measures is only touched upon briefly in this section and is in itself a wide area of active research, interested readers may find the review articles by Santini and Jain (1999) and Unnikrishnan and Hebert (2005) to be a useful resource. See the text for complete details and discussion.

3.1. Supervised Learning

In supervised learning, where the ground truth transformation is used, the loss function is typically easy to define, with Table 1. A compilation of unsupervised deformable image registration models (models are listed in alphabetical order). The table summarizes the models'

choices of similarity and auxiliary loss functions, regularization techniques, accuracy measures, and regularity measures.

	Similarity Loss				Aux	Aux. Loss Regularizer						ularity measures. Accuracy Measure					Regularity Measure					
	MSE	ГСС	Correlation	NGF	MI	MIND-SSC	Anatomy	Landmark	Diffusion	Curvature	Bending	Jacobian	Consistency	TRE	MSE	SSIM	Dice	HdD	$\%$ of $ J_{\phi} \le 0$	of $ J_{\phi} \le 0$	std.($ J_{\phi} $)	Δ 7.
AC DM'D (Zhanatal 2022)			O			Σ		1		Ŭ			ŭ							#	٥,	
AC-DMIR (Khor et al., 2023)	•	•					•		•		•	•					•	_	•			
ADMIR (Tang et al., 2020)		•							•			_		•			•	•				
AMNet (Che et al., 2023)		•							•			•					•		•			
Attention-Reg (Song et al., 2022)							•		•					•			•				•	
Baum et al. Baum et al. (2022)							•				•			•			•					
BIRNet (Fan et al., 2019b)	•																•					
CondLapIRN (Mok and Chung, 2021b)		•							•								•		•		•	
CycleMorph (Kim et al., 2021)	•	•							•				•		•	•	•		•			
de Vos et al. (De Vos et al., 2020)					•						•						•	•	•			
Deformer (Chen et al., 2022c)		•							•								•		•		•	
DiffuseMorph (Kim et al., 2022)		•							•						•	•	•		•			
DIRNet (De Vos et al., 2017)		•															•					
		•									•						•					
OLIR (De Vos et al., 2019)											•	_				_		•	•		•	
ONVF (Han et al., 2023)		•							•			•				•	•		•			
OTN (Zhang et al., 2021a)	•								•								•		l		•	
Oual-PRNet (Hu et al., 2019b)		•							•								•					
Oual-PRNet++ (Kang et al., 2022)		•							•								•	•	•			
AIM (Kuang and Schmah, 2019)		•							•			•					•			•		
an et al. (Fan et al., 2019a)									•					İ				•		•		
Fourier-Net (Jia et al., 2023)	•	•							•								•	•	•			
SDiffReg (Qin and Li, 2023)		•							•	•							•		•		•	
GraformerDIR (Yang et al., 2022b)		•							•	_		•					•		•		•	
		•							-			•		•			•					
Ian et al. (Han et al., 2022)		•		_					•	_				•				_				
ering et al. (Hering et al., 2021)				•				•		•							•	•	•			
yperMorph (Hoopes et al., 2022a)	•	•					•		•						•		•				•	
DIR (Wolterink et al., 2022)		•									•	•		•						•		
n2grid (Liu et al., 2022c)	•								•								•		•	•		
rebs et al. (Krebs et al., 2019)		•							•					i	•		•	•	i .			
apIRN (Mok and Chung, 2020b)		•							•								•		İ	•	•	
KU-Net (Jia et al., 2022)		•					•		•								•	•	•		•	
i et al. (Li and Fan, 2018)		•					_		•								•		-		_	
iu <i>et al.</i> (Liu et al., 2019)	•								_								•					
	•																					
MAIRNet Gao et al. (2024)						•				•							-					
IIDIR (Qiu et al., 2021)					•				•								•		•			
IodeT (Wang et al., 2023a)		•							•								•		•			
IS-DIRNet (Lei et al., 2020)		•		•					•		•			•	•							
IS-ODENet (Xu et al., 2021)	•								•						•		•					
IICE-Trans Meng et al. (2023)		•							•			•					•		•			
ODEO (Wu et al., 2022b)		•							•			•					•		•			
C-Reg (Yin et al., 2023)		•					•		•								•	•	•			
C-SwinMorph (Liu et al., 2022a)		•					_		•								•	_	_			
		•				_	_		•				•								_	
DD-Net 2.5D (Heinrich and Hansen, 2020)						•	•		•								•				•	
DD-Net 3D (Heinrich, 2019)						•	•		•								•		l		•	
IViT (Ma et al., 2023)		•							•								•			•		
2Net (Joshi and Hong, 2023)	•			•								•			•		•			•		
DHNet (Zhou et al., 2023)		•							•								•	•	•			
hao et al. (Shao et al., 2022)	•								•						•				i i	•	•	
pineRegNet Zhao et al. (2023)		•								•							•		•			
VF-R2Net (Joshi and Hong, 2022)		_								_		•			•		•		1	•		
YMNet (Mok and Chung, 2020a)		•							•			•					•					
		•										•	•				•			-		
ymTrans (Ma et al., 2022)	•								•								•			•		
with Morph (Hoffmann et al., 2021)							•		•								•		•			L
M-DCA (Chen et al., 2023a)		•					•		•								•		•		•	
M-TVF (Chen et al., 2022a)	•	•					•		•	1				1		•	•	•	•		•	
ransMatch (Chen et al., 2023c)	•	•							•								•		•		•	
ansMorph (Chen et al., 2022b)	•	•					•		•		•					•	•		•			
T-V-Net (Chen et al., 2021b)	•								•								•		•			1
oxelMorph (Balakrishnan et al., 2019)	•	•					•		•								•		•	•		
oxelMorph-diff (Dalca et al., 2019)		_					•										•					H
	•					_	•		-								•		•			
oxelMorph++ (Heinrich and Hansen, 2022)						•		•	•					•						•	•	
R-Net (Jia et al., 2021)	•								•								•	•	•			
TN (Zhao et al., 2019)			•						•			•	•				•		•		•	
Morpher (Shi et al., 2022)		•					•		•				•				•		•			
hang et al. (Zhang et al., 2020)	•								•			•					•		•			

the mean square error (MSE) (Miao et al., 2016; Krebs et al., 2017; Eppenhof et al., 2018; Rohé et al., 2017; Cao et al., 2017; Fan et al., 2019b), the equivalent end-point-error (EPE), and mean absolute error (MAE) (Yang et al., 2017; Sokooti et al., 2017) being the most popular choices. Recently, Terpstra et al. (2022) highlighted that a loss based on ℓ^2 (equivalent to MSE or EPE) does not distribute errors symmetrically across deformation directions when calculated separately for each direction. To address this, they introduced \perp -loss, which considers the interplay between directions. In this method, the x and y direc-

tions of the deformation field are viewed as the real and imaginary components of a complex image, thereby creating a polar representation of deformations. \perp -loss quantifies the phase error between the predicted and actual complex image representations of the deformation fields. When combined with Euclidean distance, forming the $\perp + \ell^2$ loss, it ensures symmetric error distribution across both deformation directions. The authors demonstrated that a network trained with a combination of \perp -loss and ℓ^2 loss outperforms a network trained with ℓ^2 loss alone in terms of registration performance. However, the appli-

cability of this method to 3D or 4D registration tasks remains to be further explored, given the challenge of representing additional dimensions within a 2D complex image framework.

3.2. Unsupervised & Semi-supervised Learning

In unsupervised learning, where there is no ground truth transformation to reference, regularization is usually used to enforce smoothness in the transformation. As a result, the loss function is often similar to the energy function used in traditional methods (*i.e.*, Eqn. 1), which includes an image similarity measure and a transformation regularizer. The following subsections provide a summary of commonly used and recently proposed loss functions for image registration.

3.3. Similarity Measure

Mono-modality. The choice of image similarity measure can vary depending on each specific application. For mono-modal registration, MSE is still a popular choice and has the advantage of having a straightforward probabilistic interpretation of the Gaussian likelihood approximation (Dalca et al., 2019b; Chen et al., 2022b; Kim et al., 2021; Balakrishnan et al., 2019; Meng et al., 2022a; Jia et al., 2021; Liu et al., 2022c). However, a disadvantage of MSE is that it averages the difference across all voxels in the image, making it sensitive to local intensity variations within the image. Local correlation coefficient (LCC) is known to be more robust to local intensity variations and has been found to be superior in brain MR registration applications (Avants et al., 2008). LCC has been extended as a loss function for training learning-based models, with the local window computation often being done through convolution operations (Kuang and Schmah, 2019; Chen et al., 2022b; Kim et al., 2021; Balakrishnan et al., 2019; Zhang, 2018; Mok and Chung, 2020a,b, 2021b). One disadvantage of LCC is its higher computing cost in comparison to MSE, which is mainly attributable to the comparatively large convolution kernel size (typically chosen between $5 \times 5 \times 5$ and $9 \times 9 \times 9$ voxels (Avants et al., 2008; Balakrishnan et al., 2019; Mok and Chung, 2020a)). To improve the computational efficiency, Gaussian weighted LCC can be used and implemented as three 1D convolutions. The locality is controlled by the standard deviation of the Gaussian window. However, the computation time complexity is independent of the standard deviation, because the 1D Gaussian kernel can be approximated by a fast recursive filter (Cachier and Pennec, 2000). The structural similarity index (SSIM) (Wang et al., 2004) has also been demonstrated to be an effective loss function for mono-modal image registration (Chen et al., 2020; Mahapatra et al., 2018a; Sandkühler et al., 2018). SSIM takes into account luminance, contrast, and structure. It can be thought of as an extension of the LCC, with the structure term in SSIM being the square root of LCC. This allows SSIM to capture more information about the similarity of two images beyond just the degree of correlation between them. The mono-modality loss function can also be adapted for multi-modality registration by leveraging image synthesis techniques. Liu et al. (2023b) introduced a network architecture that accepts two images from different modalities to estimate a deformation field. Rather than employing a loss function designed for multi-modality images, the authors integrate an image-to-image translation network. This network aims to match the modality of the moving image with that of the fixed image, thereby facilitating the use of a mono-modality loss. To ensure that the image-to-image translation network is solely responsible for modifying intensity without compensating for spatial transformations, a specialized training scheme is implemented.

Multi-modality. For multi-modal applications, traditional methods often use mutual information (MI) (Viola and Wells III, 1997), correlation ratio (Roche et al., 1998), selfsimilarity context (SSC) (Heinrich et al., 2013b), or normalized gradient fields (NGF) (Haber and Modersitzki, 2006) as similarity measures. Both MI and correlation ratio evaluate the relationship between the two images by calculating intensity statistics, such as intensity histograms, to measure statistical dependence. However, the standard method for calculating intensity histograms, which involves counting, is not differentiable, so a Parzen window formulation (Thévenaz and Unser, 2000) is often used to allow the loss to be backpropagated during network training. Parzen-window-based MI has been employed as a loss function in many multi-modal applications (Qiu et al., 2021; De Vos et al., 2020; Nan et al., 2020; Guo, 2019; Hoffmann et al., 2021), but it can be relatively difficult to implement and also sensitive to factors such as the number of intensity bins and the smoothness of the window function. Meanwhile, local MI (LMI) has been adapted for deep learning-based image registration to incorporate detailed spatial information Guo (2019). The calculation of MI in general often requires a vectorized approach to bypass loop operations for speed and automatic differentiation, which significantly increases memory consumption as the spatial dimension must expand to accommodate the number of bins used. Therefore, LMI is typically implemented using non-overlapping square patches to conserve memory, although overlapping patches are also feasible Guo (2019). As far as we are aware, the correlation ratio has not been used in learning-based medical image registration. It should be noted that these intensity-statistic-based measurements do not take into account local structural information, making them more suitable for rigid/affine registration and less suitable for deformable registration applications (Pluim et al., 2000; Heinrich et al., 2013b). SSC is another commonly used loss function for multi-modal applications, and it is an improvement on the modality-independent neighborhood descriptor (MIND) (Heinrich et al., 2012a). Both SSC and MIND operate by calculating the descriptor between a voxel and its neighboring voxels within a given image, turning an image of any modality into a feature representation of these descriptors. The similarity is determined by summing the absolute differences between the descriptors of the two images. As SSC and MIND consider local structural information, they are not limited in the same way as MI or correlation ratio, making them more useful for multimodal deformable registration (Hansen and Heinrich, 2021; Mok and Chung, 2021a; Yang et al., 2020; Xu et al., 2020; Blendowski et al., 2021). Note that SSC and MIND generate descriptors by analyzing the spatial intensity distribution within a localized area surrounding each voxel, making them sensitive to local orientations (i.e., they are not rotationally invariant). Consequently, when large rotations are expected between image pairs, one should calculate SSC and MIND for a warped moving image, instead of applying the warp to the SSC and MIND descriptors of the moving image. NGF compares images by focusing on the intensity changes, or edges, in the images. The similarity between the two images is determined by the presence of intensity changes at the same locations, regardless of the modalities of the images being compared. NGF was originally developed for multi-modal applications like brain MR T1-to-T2 and PET-to-CT (Haber and Modersitzki, 2006). However, it is now mostly used in learning-based registration models for lung CT registration (Hering et al., 2019, 2021; Mok and Chung, 2021a). This is because the complex structure of the lung, including bronchi, fissures, and vessels, can hinder accurate registration (Hering et al., 2021). NGF focuses on edges rather than intensity values, making it a more suitable measure for this pur-

Recent Advancements. There have been many efforts to improve upon or propose new loss functions due to some limitations of the aforementioned similarity measures. Czolbe et al. (2021, 2023) leveraged a ConvNet feature extractor to obtain image features from the deformed and fixed images, and then computed the LCC between these features as a similarity measure. The benefit of this approach is that the features produced by the ConvNet feature extractor have less noise, resulting in a more consistent similarity measure in areas with noise which leads to a smoother transformation. Haskins et al. (2019) were the first to propose using a ConvNet to learn a similarity measure for image registration. However, this method relies on having ground truth target registration error for the training dataset to learn such a similarity measure. Ronchetti et al. (2023) used a ConvNet followed by the inner product operation to approximate LC² similarity (Fuerst et al., 2014). They showed that the trained network can be used for loss function in multi-modal registration. Grzech et al. (2022) went one step further and introduced a technique for learning a similarity measure using a variational Bayesian method. The method involves initializing the convolution kernels in the network architecture to model MSE and LCC, and then using variational inference to learn a similarity measure that optimizes the likelihood of the images in the dataset when aligning them to the atlas. Building on the success of adversarial networks in computer vision (Makhzani et al., 2015; Goodfellow et al., 2020), researchers have developed a number of techniques for image registration that leverage adversarial training (Fan et al., 2019a; Mahapatra and Ge, 2020; Luo et al., 2021). These methods can be used standalone or in conjunction with a traditional similarity measure.

3.4. Deformation Regularizer

A deformation regularizer, as the terminology implies, is used for DIR, with its usage being not necessary for rigid/affine transformations. For DIR algorithms, producing smooth deformations is not only a desirable property but a necessary requirement: while diffeomorphic transformations may not be required for certain applications, smoothness remains imperative in almost all cases to avoid trivial solutions such as re-

arranging voxels (Rohlfing, 2011), with which an almost perfect similarity measure can be achieved but result in unrealistic transformation (also see Section 6). The regularizer can be considered as a prior in a maximum a posteriori (MAP) framework, while the similarity measure acts as the data likelihood (e.g., in the case of MSE, the data likelihood becomes a Gaussian likelihood). The diffusion regularizer is a commonly employed deformation regularizer, as demonstrated by its frequent appearance in Table 1. This regularization computes the squared ℓ^2 -norm of the gradients of the displacement field, effectively penalizing the disparities between adjacent displacements. Other alternatives for regularization include using the ℓ^1 -norm instead of the ℓ^2 -norm to impart equal penalties on the neighboring disparities, or penalizing the second derivative of the displacements, commonly referred to as bending energy (Rueckert et al., 1999). It is important to note that since bending energy and curvature-based regularizers penalize the second derivatives, thereby zeroing out any affine contributions, pre-affine alignment prior to the deformable registration step may not be necessary, as demonstrated in (Ding and Niethammer, 2022; Fischer and Modersitzki, 2003b). These conventional regularizers enforce an isotropic regularization on the displacement field (Pace et al., 2013). As a result, they discourage discontinuities in the displacements in applications where sliding motion may occur in organs, such as registering exhale and inhale CT scans of the lung. Historically, various improvements have been made to address this issue, including the isotropic Total Variation (TV) regularization (Vishnevskiy et al., 2016), anisotropic diffusion regularization (Pace et al., 2013), and adaptive bilateral filtering-based regularization (Papież et al., 2014). However, these regularization techniques have not been widely adopted in learning-based image registration.

Recent Advancements. Enforcing spatial smoothness alone is insufficient to ensure the regularity of the transformations. A different strategy is to penalize the "folding" of voxels directly during training, in addition to applying the aforementioned regularizers to enforce smoothness in the deformation. These foldings can be evaluated using local Jacobian determinants, where the magnitude of the Jacobian determinant indicates if the volume is expanding or shrinking near the voxel location. A non-positive Jacobian determinant represents a locally non-invertible transformation. Several regularization methods based on local Jacobian determinants have been proposed to penalize such transformations (Kuang and Schmah, 2019; Mok and Chung, 2020a). Meanwhile, with the advent of deep learning, new methods have emerged that leverage the deep learning of deformation regularization from data. One such method by Niethammer et al. (2019), introduced a method that learns a spatially-varying deformation regularization using training data. Spatially-varying regularization offers the advantage of accommodating variations in deformation that may be required for different regions within an image, such as the movement of the lungs in relation to other organs (e.g., rib cage) due to respiratory processes. The technique proposed by Niethammer et al. involves training a registration network to produce not only a deformation field but also a set of weight maps, each of which corresponds to the weight of a Gaussian smoothing kernel in a multi-Gaussian kernel configuration. The weighted multi-Gaussian kernel is then applied to the deformation field via convolution. To further impose spatial smoothness, an optimal mass transport (OMT) loss function was introduced to encourage the network to assign larger weights to Gaussian kernels with larger variances. While this method was developed for a time-stationary velocity field setting, Shen et al. (2019) later expanded upon it by incorporating it into a timevarying velocity field setting. In this setup, a different set of weight maps are produced for each time point. More recently, Chen et al. (2023b) introduced a weighted diffusion regularizer that applies spatially-varying regularization to the deformation field. The neural network generates a weight volume, assigning a unique regularization weight to each voxel and thus allows for spatially-varying levels of regularization strength. As the diffusion regularizer is related to Gaussian smoothing, using spatially-varying strengths of diffusion regularization can be considered equivalent to employing a multi-Gaussian kernel, as originally proposed by Niethammer et al. (2019). This is because the convolution of multiple Gaussian kernels still results in a Gaussian kernel. To promote the overall smoothness of the deformation, they further applied a log loss to the weight volume, which encourages the maximum regularization strength when possible. In a different approach, Wang et al. (2022) employed a regression network to learn the optimal regularization parameter for an optimization-based method, specifically Flash (Zhang and Fletcher, 2019). Flash is a geodesic shooting method in the Fourier space that requires only the initial velocity field to compute the time-dependent transformation. Wang et al. generated ground truth optimal regularization parameters by assuming the prior of the initial velocity field given the regularization parameter as a multivariate Gaussian distribution. Using gradient descent, they obtained the optimal regularization parameter for each image pair through MAP estimation. A ConvNet regression encoder then estimates the optimal regularization parameter based on the image pair. This approach achieved registration performance comparable to Flash while significantly improving runtime and memory efficiency. Alternatively, Laves et al. (2019) were inspired by the deep image prior (Ulyanov et al., 2018). They used a randomly initialized ConvNet as a regularization prior. They then fed a random image (i.e., a noise image) as input and the network gradually transformed it into a smooth deformation field through iterative optimization. The deep image prior provided by the ConvNet enables the network to produce a smooth deformation in the early iterations, then gradually adds non-smooth highfrequency deformations. As a result, early stopping is used for the network to generate a smooth deformation field without the need for explicitly encouraging smoothness in the loss function.

Transformations can also be implicitly regularized by imposing invertibility constraints. This is achieved by using a symmetric consistency loss or cycle consistency loss. Symmetric consistency typically uses a single DNN to output both the forward and reverse deformation fields, which transform the moving image to the fixed image and vice versa, respectively. The similarity between the warped image and the target im-

age is then calculated and backpropagated to update the network (Mok and Chung, 2020a; Liu et al., 2022a). Alternatively, a consistency loss can be calculated by composing the networkgenerated forward and backward deformation fields, and then comparing the outcome with the identity transformation (Greer et al., 2021; Tian et al., 2022). The underlying concept is that, theoretically, an invertible mapping should cancel itself when composed with its inverse. Such an approach by itself imposes invertibility but does not explicitly enforce spatial smoothness over the deformation field. Greer et al. (2021) demonstrated that incorporating such a loss within a DNN framework implicitly imposes spatial regularity and inverse consistency on the deformation field without necessitating an additional regularizer to enforce smoothness. The authors showed that the errors of the DNN in computing the inverse, combined with the implicit bias of DNN favoring more regular outputs, enable such a consistency loss to entail a H^1 – or Sobolev-type regularization over the deformation field, thereby implicitly enforcing spatial smoothness. Later, Tian et al. (2022) expanded on this regularizer and proposed to regularize deviations of the Jacobian of the composition from the identity matrix. This improved regularizer led to faster convergence while offering greater flexibility, while maintaining an approximated diffeomorphic transformation. Greer et al. (2023) introduced a simple method to ensure DNN-based registration models are inverse consistent by construction. They began by defining the output of the registration network as a member of a specified Lie group that inherently supports inverse consistency. Specifically, suppose a DNN f generates a deformation field, this is mathematically represented as:

$$f[I_m, I_f] := \exp(g(I_m, I_f)).$$
 (6)

The DNN ensures the generated deformation field retains inverse consistency when $g(I_f, I_m) = -g(I_m, I_f)$, as demonstrated by:

$$f[I_m, I_f] \circ f[I_f, I_m] \equiv \exp(g(I_m, I_f)) \circ \exp(-g(I_m, I_f)) = id. \tag{7}$$

To ensure $g(I_f, I_m)$ meets this condition, the authors propose:

$$g(I_f, I_m) := M_{\theta}(I_f, I_m) - M_{\theta}(I_m, I_f),$$
 (8)

where M_{θ} is an arbitrary DNN with parameters θ . This approach structurally guarantees that the deformation field generated by the DNN maintains inverse consistency. The authors recognize that their previous two-stage approach (Greer et al., 2021; Tian et al., 2022), which initially estimates the deformation field at a coarse level and subsequently refines it with an additional field, does not guarantee inverse consistency due to the interleaving of inverses. To address this, they introduced a TwoStepConsistent operator that works on the square root of $\exp(g(I_m, I_f))$. This operator can also be adapted for multi-step registration methods, which involve compositions as described later in Section 4.10. The updated model has been evaluated on both synthetic and real-world brain MRI datasets and has shown significantly more precise inverse consistency compared to models that employ penalty-based approaches for ensuring inverse consistency (Greer et al., 2021; Tian et al., 2022).

On the other hand, cycle consistency employs two identical networks, where the first network generates a forward deformation field that deforms the moving image and the second network produces a reverse field that aims to warp the deformed image back to the original moving image (Zhao et al., 2019; Kuang, 2019; Kim et al., 2021). Both consistency losses have been shown to improve the registration performance and provide regularization to the deformation field. However, since this regularization is not explicitly applied to the deformation fields, a separate deformation regularizer is often required in addition to the consistency loss.

Regularization terms in the objective function frequently necessitate tuning additional hyperparameters (e.g., λ in Eqn. 1) to effectively balance the trade-off between the image similarity measure and the regularity of the deformation field. In a recent study (Dou et al., 2023), the authors observed that the similarity and regularity losses often conflict in terms of optimization direction. They proposed a layer-wise gradient surgery process that modifies the gradient of the total loss whenever the inner product of the gradients from these two components is less than zero. This gradient surgery process focuses solely on the direction of the regularization loss gradient, thereby eliminating the need to adjust its weighting.

3.5. Auxiliary Anatomical Information

The overlap of anatomical label maps of the fixed and transformed moving images is a widely used evaluation metric for image registration. Hence, to improve registration performance on this metric, learning-based methods often apply the estimated deformation to the moving label map during training to compute an extra anatomy loss between the fixed and transformed moving label map. Various loss functions used in image segmentation tasks, such as Dice loss, cross-entropy, and focal loss (see Ma et al. (2021) for a comprehensive review of such loss functions), can be borrowed as the choice of anatomy loss. Despite the availability of different loss functions, Dice loss remains the most commonly used loss function in learning-based image registration, as evidenced by Table 1. This is likely because Dice loss is confined within the range of [0, 1], like LCC, which makes it easier to adjust hyperparameters when used in conjunction with LCC. Auxiliary anatomical information can also be introduced in the registration network through multitask learning (Estienne et al., 2019; Qin et al., 2018). In particular, Tan et al. (2023) showed that such strategy is more effective than the direct application of anatomy loss.

Recent Advancements. Building on the concept of integrating segmentation loss while training the registration network, additional auxiliary data related to anatomical prior knowledge can also be included during the training process. When anatomical landmarks are present in both the moving and fixed images, the transformation generated by the DNN can be applied to the landmarks of the moving image. The resulting transformed landmarks can then be compared with the landmarks of the fixed image to create a loss. This landmark supervision has been utilized in optimization-based registration methods to improve performance, as demonstrated in a number of studies (Ehrhardt et al., 2010; Polzin et al., 2013; Rühaak et al.,

2017; Heinrich et al., 2015; Fischer and Modersitzki, 2003a). Hering et al. (2021) were the first to incorporate landmark supervision into a DNN framework by comparing the MSE between the transformed and target landmarks, which resulted in a substantial improvement in the target registration error of the landmark. Subsequently, (Heinrich and Hansen, 2022) confirmed the superiority of landmark supervision on multiple benchmark datasets in their work. It is worth mentioning that the landmarks can be generated automatically before or during the training stage without manual labeling using automatic landmark detection algorithms (Heinrich et al., 2015; Rühaak et al., 2017; Polzin et al., 2013), making it straightforward to integrate into most learning-based registration frameworks.

The combination of anatomy loss and deformation regularization without an intensity-based similarity measure is also common, and in these cases, the anatomy loss serves as a modality-independent similarity measure (Hu et al., 2018; Song et al., 2022; Blendowski et al., 2020). However, the drawback of using anatomy loss without a similarity measure is clear: it does not penalize deformations in areas where anatomical labels are missing or ambiguous. Thus, to achieve accurate and realistic deformations, the anatomical labels should be as detailed as possible, ideally with a unique label for each organ or structure. However, obtaining such detailed labels is often challenging as anatomical label maps in medical imaging are usually manually delineated, which is a time-consuming and expensive process.

4. Network Architectures

The application of ConvNets has been the dominant trend in learning-based image registration since its inception. Among different ConvNets architectures, the U-Net-like architectures (Ronneberger et al., 2015), which were initially designed for image segmentation tasks, have played an important role. Many noteworthy ConvNet-based registration models, including RegNet (Sokooti et al., 2017), DIRNet (De Vos et al., 2017), QuickSilver (Yang et al., 2017), VoxelMorph (Balakrishnan et al., 2019; Dalca et al., 2019b), VTN (Zhao et al., 2019), DeepFlash (Wang and Zhang, 2020), and CycleMorph (Kim et al., 2021), have demonstrated promising performance in various registration applications. More recently, registration neural networks have witnessed notable advancements beyond the conventional ConvNet designs, owing to the progress of DNN architectures in computer vision and the development of architectures that are specifically tailored for registration tasks. Notably, models such as Transformers, diffusion models, and Neural ODEs are gaining increasing attention in the field of image registration. Table 2 summarizes the types of network architectures along with the associated anatomies and modalities of the methods outlined in Table 1. This section provides a comprehensive overview of the recent advancements in network architectures.

4.1. Adversarial Learning

The majority of adversarial learning applied to image registration relies on the foundational principles of generative adversarial networks (GANs). The concept of GANs is derived

 $Table \ 2. \ A \ summary \ of \ the \ anatomy, \ modality, \ and \ network \ infrastructure \ of \ the \ methods \ outlined \ in \ Table \ 1.$

Method	Anatomy	Modality	Network Infrastructure
AC-DMiR (Khor et al., 2023)	Brain / Uterus	MRI	Transformer
ADMIR (Tang et al., 2020)	Brain	MRI	CNN
AMNet Che et al. (2023)	Brain	MRI	CNN
Attention-Reg (Song et al., 2022)	Prostate	US / MRI	CNN (Self Attention)
BIRNet (Fan et al., 2019b)	Brain	MRI	CNN
Baum et al. (Baum et al., 2022)	Prostate	MRI / Transrectal Ultrasound	CNN
CondLapIRN (Mok and Chung, 2021b)	Brain	MRI	CNN
CycleMorph (Kim et al., 2021)	Faces / Brain / Liver	Photographs / MRI / CT	CNN
de Vos et al. (De Vos et al., 2020)	Breast	MRI	CNN
Deformer (Chen et al., 2022c)	Brain	MRI	CNN
DiffuseMorph (Kim et al., 2022)	Faces / Brain / Cardiac	Photographs / MRI	DDPM
DIRNet (De Vos et al., 2017)	Cardiac	MRI	CNN
DLIR (De Vos et al., 2019)	Cardiac / Chest	MRI / CT	CNN
DNVF (Han et al., 2023)	Brain	MRI	DNVF
DTN (Zhang et al., 2021a)	Brain	MRI	CycleGAN-like
Dual-PRNet (Hu et al., 2019b)	Brain	MRI	CNN / Siamese
	Brain	MRI	•
Dual-PRNet++ (Kang et al., 2022)			CNN / Siamese
FAIM (Kuang and Schmah, 2019)	Brain / Balvia	MRI MBI / CT	CNN
Fan et al. (Fan et al., 2019a)	Brain / Pelvis	MRI / CT	GAN
Fourier-Net (Jia et al., 2023)	Brain	MRI	CNN
FSDiffReg Qin and Li (2023)	Cardiac	MRI	DDPM
GraformerDIR (Yang et al., 2022b)	Brain / Cardiac	MRI	CNN
Han et al. (Han et al., 2022)	Brain	MRI / CT	CycleGAN
Hering et al. (Hering et al., 2021)	Lung	CT	CNN
HyperMorph (Hoopes et al., 2022a)	Brain	MRI	CNN
IDIR (Wolterink et al., 2022)	Lung	CT	INRs
im2grid (Liu et al., 2022c)	Brain	MRI	CNN
Krebs et al. (Krebs et al., 2019)	Cardiac	MRI	CNN
LapIRN (Mok and Chung, 2020b)	Brain	MRI	CNN
LKU-Net (Jia et al., 2022)	Brain	MRI	CNN
Li et al. (Li and Fan, 2018)	Brain	MRI	CNN
Liu <i>et al.</i> (Liu et al., 2019)	Brain	MRI	CNN / Siamese
MAIRNet Gao et al. (2024)	Pelvis / Spine	MRI / CT	CNN
MIDIR (Qiu et al., 2021)	Brain	MRI	CNN
ModeT (Wang et al., 2023a)	Brain	MRI	Transformer
MS-DIRNet (Lei et al., 2020)	Abdomen	CT	CNN
· · · · · · · · · · · · · · · · · · ·	Brain	MRI	Neural-ODE
MS-ODENet (Xu et al., 2021)			
NICE-Trans Meng et al. (2023)	Brain	MRI	Transformer
NODEO (Wu et al., 2022b)	Brain	MRI	Neural-ODE
PC-Reg (Yin et al., 2023)	Brain / Abdomen	MRI / CT	Transformer
PC-SwinMorph (Liu et al., 2022a)	Brain	MRI	CNN
PDD-Net 2.5D (Heinrich and Hansen, 2020)	Abdomen	CT	CNN
PDD-Net 3D (Heinrich, 2019)	Abdomen	CT	CNN
PIViT (Ma et al., 2023)	Brain	MRI	Transformer
R2Net (Joshi and Hong, 2023)	Brain / Lung / Cardiac	MRI / CT	Neural-ODE
SDHNet (Zhou et al., 2023)	Brain / Liver	MRI / CT	CNN / Student – Teacher
Shao et al. (Shao et al., 2022)	Abdomen	Endoscopic	CNN
SVF-R2Net (Joshi and Hong, 2022)	Brain	MRI	CNN
SpineRegNet Zhao et al. (2023)	Spine	MRI / CT	CNN
SYMNet (Mok and Chung, 2020a)	Brain	MRI	CNN
SymTrans (Ma et al., 2022)	Brain	MRI	Transformer
SynthMorph (Hoffmann et al., 2021)	Brain	MRI	CNN
TM-DCA (Chen et al., 2023a)	Brain	MRI	Transformer
TM-TVF (Chen et al., 2022a)	Faces / Brain	Photographs / MRI	Transformer
TransMatch (Chen et al., 2023c)	Brain	MRI	Transformer
TransMorph (Chen et al., 2022b)	Brain / Abdomen	MRI / CT	Transformer
ViT-V-Net (Chen et al., 2021b)	Brain	MRI	Transformer
VoxelMorph diff (Dalag et al., 2019)	Brain	MRI	CNN
VoxelMorph-diff (Dalca et al., 2019b)	Brain	MRI	CNN
VoxelMorph++ (Heinrich and Hansen, 2022)	Chest / Abdomen	CT	CNN
VR-Net (Jia et al., 2021)	Cardiac	CT	CNN
VTN (Zhao et al., 2019)	Brain / Liver	MRI / CT	CNN
VAA	Brain / Cardiac	MRI / CT	Transformer
XMorpher (Shi et al., 2022) Zhang et al. (Zhang et al., 2020)	Brain	MRI	CNN

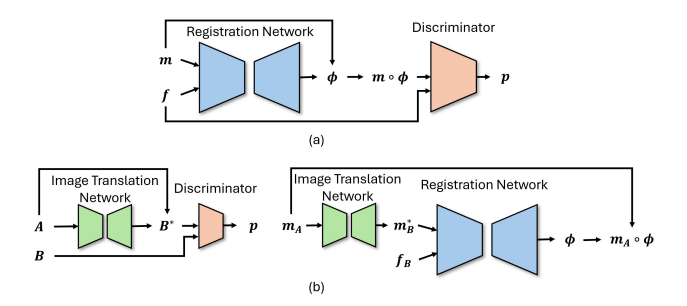


Fig. 3. Visual representation of adversarial learning in medical image registration, with m and f denoting the moving and fixed images, respectively. Here, ϕ represents the deformation field, p indicates a pseudo-probability generated by the discriminator, and A and B correspond to two different modalities. Panel (a) demonstrates how adversarial learning serves as a metric for image similarity, as similarly employed in Fan et al. (2018), Yan et al. (2018), Mahapatra et al. (2018a,b), and Mahapatra and Ge (2020). Panel (b) shows the application of adversarial learning to multi-modal image registration, synthesizing different image modalities into the same modality for registration, as seen in Xu et al. (2020), Wei et al. (2019), Zhang et al. (2021a), and Han et al. (2022).

from a two-player zero-sum game involving a generator and a discriminator (Goodfellow et al., 2020). The objective of the generator is to generate new samples by learning the data distribution, while the discriminator functions as a binary classifier, aiming to accurately distinguish between real and generated samples. In the context of image registration, the registration network acts as the generator, producing a deformation field and subsequently warping the moving image. Meanwhile, the discriminator functions as an image similarity measure, distinguishing between the warped image and the fixed image. This offers the advantage of alleviating the need for an explicit similarity measure, making the approach adaptable to both monoand multi-modality applications.

Figure 3 summarizes the designs of adversarial-based DNNs used for medical image registration. In early applications of adversarial learning to image registration, Fan et al. (2018) and Yan et al. (2018) adhered to the aforementioned approach. The former utilized the generator to produce a deformation field, while the latter employed a ConvNet encoder to generate affine transformation parameters. Subsequently, a binary discriminator served as a similarity measure between the transformed and fixed images. In a similar vein, Mahapatra et al. (Mahapatra et al., 2018a,b; Mahapatra and Ge, 2020) applied adversarial learning to multi-modal image registration, with the additional implementation of CycleGAN (Zhu et al., 2017; Qin et al., 2019) to further ensure the inverse consistency of the generated deformation field. Elmahdy et al. (2019) proposed incorporating anatomical label maps into a Wasserstein-GAN (WGAN) to enhance the segmentation performance of the registration network. Their generator was a U-Net-based network that generated a deformation field, which warped both the moving image and the associated anatomical label map. The discriminator's role was to evaluate the alignment between the warped and fixed image, as well as the warped and fixed label maps. In their approach, image and anatomical similarity measures were still employed, while the discriminator served as an additional measure of the alignment. Similar approaches can be

found in Duan et al. (2019), Li and Ogino (2019), and Luo et al. (2021), where the authors used the discriminator in conjunction with image similarity measures as additional alignment indicators. In another study, Fan et al. (2019a) proposed a GAN-based registration framework applicable to both monoand multi-modality registration. Their generator was also a registration network based on U-Net, with the discriminator serving as the sole measure of image alignment. However, the definition of positive pairs sent to the discriminator deviated from previous methods. Ideally, in mono-modality registration, a positive pair would consist of identical images, but this strict requirement is impractical. Given this observation, the authors proposed that the positive pair comprise the fixed image and an alpha-blended image created from the fixed and moving images. For multi-modality registration, a positive pair consisted of pre-aligned multi-modal images from the same patient. The method was evaluated on mono-modal brain MRI registration and multi-modal pelvic MR and CT registration tasks, demonstrating favorable performance compared to the state-of-the-art at the time.

Given the promising results GANs have demonstrated in image translation, i.e., synthesizing one image modality into another, researchers have made efforts to leverage their capabilities in addressing multi-modal image registration (Xu et al., 2020; Wei et al., 2019; Zheng et al., 2021; Han et al., 2022; Zhong et al., 2023). This approach involves first synthesizing multi-modal images into the same modality and then applying a registration network to perform the image registration task. In (Xu et al., 2020), the authors tackled the challenge of multimodal registration of CT and MR images using a CycleGANbased approach to translate CT images into MR images. To ensure that the translated images maintained anatomical consistency with the original images, the authors introduced additional loss functions, including MIND and identity loss, alongside the standard CycleGAN loss. They then employed a threestage registration framework to align the original and translated images. In the first stage, a U-Net-based registration network learned the multi-modal registration between CT and MR images. In the second stage, a network with the same architecture learned the mono-modal registration between the translated CT and the target MR images. Finally, the deformation fields created by both registration networks were fused using a convolutional layer to produce the final deformation field. A similar concept was presented in Wei et al. (2019), where mutual information was used instead of MIND to enforce structural consistency. Zheng et al. (2021) integrated an image translation network within a GAN-based image registration framework, where the modality of the moving image was first translated to the modality of the target image before a registration network was applied to register the two images. The discriminator in this approach acted as an image similarity metric for both the registration and image translation networks. Additionally, this approach employed a symmetric pipeline that reversed the order of the moving and fixed images, ensuring symmetric consistency in the resulting synthesized and deformation images. More recently, Han et al. (2022) proposed tackling the multimodal registration between CT and MR images using a dualchannel framework. Within each channel, an imaging modality was transformed into a target modality using a probabilistic CycleGAN, which was then followed by a registration network that predicted the deformation in the target modality. The deformation fields from both channels were then fused, taking advantage of the uncertainty weighting generated by the synthesis networks. This proposed dual-channel framework can be trained end-to-end, resulting in improved registration accuracy and faster runtime compared to baseline methods.

Adversarial learning has also been employed for knowledge distillation, enabling the transfer of information from a larger teacher network to a smaller student network (i.e., in terms of the number of parameters). Tran et al. (2022) aimed to compress the size of a registration network by transferring information from a computationally expensive VTN (Zhao et al., 2019) to a smaller registration network with only one-tenth of its parameters. The training process for the student network involved calculating a correlation-based image similarity measure (Zhao et al., 2019) between the warped image generated by the student network and the fixed image. Meanwhile, a discriminator was used to differentiate the deformation field created by the student network and the pre-trained teacher network. After training, the teacher network was discarded, and only the lightweight student network was used for inference. Despite having only one-tenth of the network parameters, the lightweight registration network demonstrated comparable performance to baseline learning-based methods with larger parameter sizes, in terms of both anatomical overlaps and deformation smoothness.

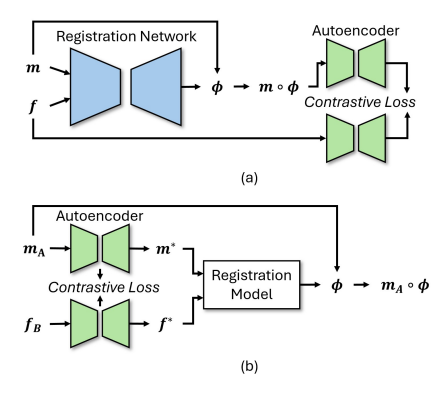


Fig. 4. Visual representation of contrastive learning in medical image registration, with m and f, respectively, denoting the moving and fixed images, ϕ denoting the deformation field, and A and B corresponding to two different modalities. Panel (a) illustrates the application of contrastive learning as a similarity metric for comparing the deformed moving image to the fixed image, as seen in Hu et al. (2019a) and Dey et al. (2022). Panel (b) depicts the use of contrastive learning to transform images from different modalities into a unified feature representation, upon which the registration model operates, as similarly employed in Pielawski et al. (2020), Wetzer et al. (2023), and Casamitjana et al. (2021).

4.2. Contrastive Learning

The principle of contrastive learning enables DNNs to learn by comparing various examples instead of focusing on single data points independently. This comparison process typically involves examining positive pairs of similar inputs and negative pairs of dissimilar inputs. For a comprehensive understanding of this concept and a detailed overview of the evolution of contrastive learning, we recommend interested readers refer to Le-Khac et al. (2020). Figure 4 provides a broad illustration of the contrastive learning designs used in medical image registration applications. In the context of image registration, contrastive learning could be particularly beneficial as an alternative to using explicit image similarity metrics, which can be challenging to optimize due to their task-specific nature. For example, different similarity metrics may be preferred for lung CT registration versus brain MRI registration or multi-modal versus monomodal registration tasks. Whereas, contrastive learning empowers the DNN to determine whether two images are registered or not without relying on a specific image similarity metric (e.g., Fig. 4 (a)), making it a more versatile approach for handling different registration tasks.

Hu et al. (2019a) were the pioneers in applying contrastive learning to multi-modal affine registration, concentrating on the inter-patient alignment of 2D CT and MR scans for patients with Nasopharyngeal Cancer. Their method involved using an automatic keypoint detecting algorithm to identify keypoints in the CT and MR scans. Subsequently, they extracted a patch centered on each keypoint and employed a Siamese network to minimize the contrastive loss, which minimized the distance between corresponding keypoints and maximized the distance between non-corresponding keypoints. In the testing phase, after establishing correspondences between all keypoints in the CT and MR scans, the optimal affine transformation parameter was determined by means of least-squares fitting. In another study, Pielawski et al. (2020) applied contrastive learning to transform multi-modal images into similar contrastive representations with equivariant properties. Their method used two independent U-Nets to learn the representations for each modality such that the InfoNCE-based (Oord et al., 2018) loss between the learned representations is minimized. This minimization can be understood as maximizing the mutual information between the two learned representations. Finally, conventional affine registration methods were used to align the learned representations as if they had undergone a mono-modal registration task. Wetzer et al. (2023) later investigated the contrastive learning approach proposed in Pielawski et al. (2020) to determine whether applying contrastive learning supervisions to the U-Nets' intermediate layers could improve multi-modal image registration performance. However, they concluded that the best representations for the evaluated registration task were achieved when the contrastive loss was applied only to the features of the final layers. Casamitjana et al. (2021) proposed a contrastive learning-based approach for multi-modal deformable registration. They introduced a synthesis-by-registration method, where they trained a registration network for mono-modal registration on the target modality domain, and then froze the network's weight for training an image synthesis network using a loss function that leverages the registration network. The image synthesis network's ability to accurately translate the moving image into the target modality directly influenced the performance of the registration network. To enhance synthesis performance and ensure geometric consistency, a PatchNCE-based (Park et al., 2020)

contrastive loss was used, maximizing the mutual information between pre- and post-synthesis images at the patch level. This method demonstrated promising results in multi-modal brain MRI registration applications, outperforming both MI-based registration and other image synthesis-based registration methods. Dey et al. (2022) also addressed the multi-modal registration task using contrastive loss. In their method, featureextracting autoencoders were first pre-trained for each modality to derive modality-specific features. These autoencoders were then used on the deformed moving image and the fixed image to extract features for a PatchNCE-based (Park et al., 2020) contrastive loss. In order to optimize contrastive learning, a single positive pair was sampled, corresponding to the multi-scale feature patches of the same spatial location across both modalities, while multiple negative pairs were sampled, corresponding to the feature patches of different spatial locations.

Until now, the methods based on contrastive learning have been centered on multi-modal image registration. However, Liu et al. (2023a) proposed the integration of contrastive learning in the intermediate stages of the network architecture for monomodal brain MRI registration. In their method, two identical ConvNet encoders of shared weights were applied to the moving and fixed images, each followed by a fully-connected layer to project ConvNet extracted features onto a latent space where the contrastive loss is applied. The positive pair for computing the contrastive loss consists of the unregistered moving and fixed image pair, while any other pair apart from the current image pair under registration is considered a negative pair. In an extension of their work, Liu et al. (2022a) proposed to compute the contrastive loss in a similar way, but between patches of the moving and fixed images. However, it is important to note that the positive pair used in these two methods contained structural dissimilarities as it was the unregistered image pair, as opposed to the registered images used in the methods mentioned earlier. The authors argued that this was because the image contents, including the number of brain structures, were consistent for brain registration. Nonetheless, further research is needed to fully uncover the potential of these methods.

4.3. Transformers

One of the key factors in designing ConvNets is the size of the receptive fields. While incorporating consecutive convolutional layers and pooling operations can increase the theoretical receptive fields of ConvNets, its effective receptive fields are still limited (Luo et al., 2016). This makes them less effective at capturing long-range spatial correspondence, which is important to image registration since it aims to identify the correspondence between different parts of the images. In contrast, Transformers are widely acknowledged for their superior ability to capture long-range dependencies and achieve exceptional performance when trained on large datasets (Li et al., 2023a). Transformers differ from ConvNets in that they employ the selfattention mechanism, in which each local part of an image is compared in relation to the other parts, guiding the network on where to focus. Originally developed for natural language processing tasks (Vaswani et al., 2017), Transformers have recently become prevalent in various computer vision applications (Dosovitskiy et al., 2021a; Liu et al., 2021b, 2022e; Chen

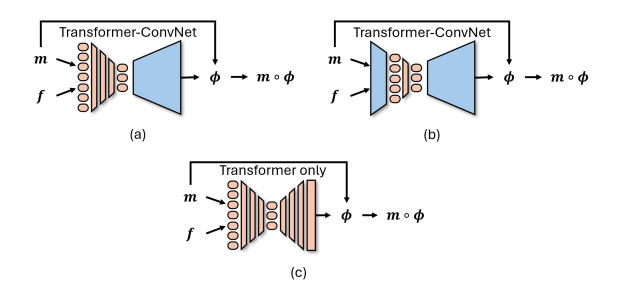


Fig. 5. Graphical representation of Transformers used in medical image registration, with m and f indicating the moving and fixed images, respectively, and ϕ representing the deformation field. Panel (a) displays a Transformer-ConvNet hybrid architecture, where Transformers function as encoders for extracting features, coupled with a ConvNet decoder for generating the deformation field. A similar framework is adopted in Chen et al. (2021b, 2022b, 2023b), and Zhang et al. (2021a). Panel (b) shows a design where a Transformer is sandwiched between ConvNets, with the initial ConvNet acting as a feature extractor and the Transformer applies self- or cross-attention between image features, and the subsequent ConvNet decoder producing the deformation field. This configuration is adopted in Zhang et al. (2021a), Chen et al. (2022c), and Song et al. (2022). Panel (c) illustrates the architecture where Transformers serve as both the encoder and decoder, a design adopted in Shi et al. (2022).

et al., 2021a; Yuan et al., 2021; Dong et al., 2022; Carion et al., 2020). Inspired by their success, many Transformer-based models have been proposed and have demonstrated promising performance in medical imaging applications. Figure 5 provides a graphical illustration of the Transformer-based DNNs used in medical image registration. For a comprehensive review of the current Transformer-based models in medical imaging in general, interested readers are directed to a review paper by Li et al. (2023a). Despite their potential, Transformers have certain drawbacks, such as larger computational complexity and a lack of inductive bias when compared to ConvNets, hindering the training process. To address these shortcomings, Transformers are commonly used in conjunction with Conv-Nets in medical image registration applications. Initially, the field saw the introduction of self-attention-based Transformers for these tasks. More recently, cross-attention-based Transformers emerged, demonstrating potential advantages. Given that registration involves identifying correspondences between images, cross-attention, which focuses on the features of one image in relation to another, may enhance this identification process. We start by examining self-attention-based Transformers and then proceed to discuss the developments in crossattention-based Transformers specifically designed for medical image registration.

Self-attention. Chen et al. (2021b) were the first to adopt Transformers for registration-based tasks. They proposed ViT-V-Net, which employs a ConvNet for extracting high-level features, followed by a Vision Transformer (ViT) (Dosovitskiy et al., 2021b) and a ConvNet decoder to generate a dense displacement field. Subsequently, they proposed TransMorph (Chen et al., 2022b), which employs a Swin Transformer (Liu et al., 2021b) in the encoder, replacing the ConvNet feature extractor and ViT. TransMorph is capable of both affine registration and deformable registration. The study provided empirical evidence that Transformer-based models have larger effective

receptive fields than baseline ConvNets. In inter-subject and atlas-to-subject brain MRI registration, as well as XCAT-to-CT abdomen registration applications, TransMorph achieved significantly improved registration performance when compared to top-performing traditional and ConvNet-based registration models. Zhang et al. (2021a) proposed DTN, which consists of two encoder branches with identical architecture. Each branch contains a ConvNet feature extractor and a ViT. In DTN, the moving and fixed images are first fed consecutively into one encoder branch, then concatenated and sent to the other branch. The encoder outputs are then concatenated and sent to a Conv-Net decoder to produce a deformation field. Mok and Chung (2022a) introduced a Transformer encoder, C2FViT, specifically designed to tackle the affine registration problem. Their Transformer architecture was inspired by ViT, but with augmented patch embedding and feed-forward layers to introduce locality into the model. C2FViT adopts a coarse-to-fine strategy with an image pyramid for affine registration. The registration process is carried out in multiple stages of ViTs with identical architectures, each corresponding to a different resolution of the fixed and moving images. The affine parameters are estimated in each stage, and the moving image is affinetransformed using the parameters from the previous stage to refine the registration progressively. C2FViT was evaluated on several benchmark datasets and demonstrated superior performance compared to multiple ConvNet-based and traditional affine registration methods. Chen et al. (2022c) proposed a Deformer module, which leverages the attention mechanism on feature maps produced by a ConvNet encoder. The authors argued that the Deformer module facilitated the image-to-spatial transformation mapping process by estimating the displacement vector prediction as a weighted sum of multiple bases. Employing a coarse-to-fine strategy, the proposed model outperformed both the ConvNet and Transformer models in the comparative analysis. Yin et al. (2023) introduced PC-Reg, which uses a Swin Transformer similar to that in TransMorph (Chen et al., 2022b) but incorporates modifications in patch partitioning through two convolutional residual blocks. The processed features are subsequently directed to a specially designed Conv-Net decoder tasked with predicting the a deformation field. The decoder estimates the final deformation field using a coarse-tofine approach, progressively upsampling the lower-resolution field and employing a separate module at each scale to refine the field by estimating the residuals. This refinement module draws inspiration from the predictor-corrector method commonly used in numerical methods for differential equations. PC-Reg shows promising results, performing competitively in brain MRI and abdominal CT registration tasks.

Cross-attention. Song et al. (2022) introduced Attention-Reg, a model that adopts cross-attention to correlate features extracted from multi-modal input images by a ConvNet encoder. To expedite the training process, they applied a contrastive pretraining strategy to the ConvNet feature extractor, allowing for the extraction of similar features from different modality images. The Dice loss was used as the multi-modal similarity measure, and they developed both rigid and deformable variations of the model. The results showed that Attention-Reg per-

formed favorably against several learning-based rigid and deformable registration models. Similarly, Shi et al. (2022) introduced XMorpher, a full Transformer architecture featuring dual parallel feature extractors that exchange information via a cross-attention mechanism. The cross-attention module developed in their study is based on a Swin Transformer, where attention is computed between base windows of one image and searching windows of another image with differing sizes. This cross-attention mechanism exhibited improved performance compared to self-attention-based Transformers and ConvNet models. Chen et al. (2023a) made further improvements to the cross-attention technique used in XMorpher. They proposed a novel deformable cross-attention module that enables tokens to be sampled from regions beyond the conventional rectangular window, while also reducing computational complexity. A lightweight ConvNet was introduced to deform the sampling window in a reference. The attention is then computed between the tokens sampled from the deformed window in the reference and those sampled from a rectangular window in a base. This enables tokens sampled from a larger reference region to guide the network on where to focus within each local window in the base. The proposed network includes two encoding paths. In one path, the moving and fixed images are used as the base and reference, respectively. In the other path, the roles of the base and reference are switched, with the moving image used as the reference and the fixed image used as the base. A ConvNet decoder then fuses the features extracted from the two encoders to generate a deformation field. Their method was evaluated on brain MRI registration tasks, and it performed favorably against self-attention, cross-attention, and ConvNet-based models. Adopting a similar strategy of incorporating cross-attention for image registration, Chen et al. (2023c) developed TransMatch. This model employs a Transformer encoder with dual-stream modules, each alternating between windowed self-attention and cross-attention to enhance the matching of image features through dot-product attention. This process aims to establish more accurate spatial correspondences both between and within images. A ConvNet decoder subsequently processes the concatenated features from both streams to estimate a deformation field. TransMatch was evaluated on mono-modal brain MRI image registration tasks, where it outperformed both traditional ConvNets and self-attention-based Transformers. Liu et al. (2022c) proposed im2grid, a model that uses cross-attention to explicitly guide the neural network in comprehending the coordinate system for image registration, which is usually learned implicitly from data. Their approach uses ConvNet encoders to independently extract hierarchical features from the fixed and moving images. Subsequently, their proposed coordinate translator block computes a softmax score function by comparing the extracted fixed image feature at a voxel location with the features of the moving image within a search window. Spatial correspondence between the voxel location in the fixed and moving images is established by linearly combining the coordinates of all voxel locations weighted by the score function. Their approach is implemented as cross-attention with coordinates as one of the inputs. This model was evaluated on inter-patient brain MRI registration tasks using publicly available datasets and demonstrated superior performance compared to the comparative ConvNets and Transformer-based models. Wang et al. (2023a), inspired by the im2grid introduced in Liu et al. (2022c), aimed to calculate matching scores to weight deformations but also enhanced the the weighting process by noting that feature maps at coarse-level resolutions typically exhibit different motion modes. Specifically, the authors developed a motion decomposition Transformer, named ModeT. This Transformer decomposes the feature maps of the moving and fixed images into multi-head feature representations using a linear projection layer followed by LayerNorm. Cross-attention is then applied between the feature at each spatial location in the fixed image and the features of the neighboring locations in the moving image, employing a technique similar to that used in Liu et al. (2022c). This process yields a series of deformation fields, with the count equaling the number of heads used. Subsequently, a competitive weighting module, which consists of a shallow ConvNet ending with a SoftMax activation function, is applied to the sequence of deformation fields. These fields are then aggregated to form a deformation field at each resolution. Finally, the final deformation field at the full resolution is generated by sequentially composing the upsampled deformation fields from each resolution. This model was tested on brain MRI image registration tasks and showed superior performance compared to several state-of-the-art methods at the time. In Khor et al. (2023), the authors proposed AC-DMiR for joint learning of registration and segmentation. Specifically, AC-DMiR adopts two Transformer-based backbone networks, similar to the one used in TransMorph (Chen et al., 2022b), to generate initial predictions: a deformation field for registration and segmentation for the warped moving image. Subsequently, the feature maps from the registration and segmentation networks are coupled via cross-task attention modules. These modules employ cross-attention to focus on features from one task to another, followed by self-attention and a decoder to estimate the final deformation field. This integration allows the correlation of anatomical variations and alignment information from the segmentation network with the registration network, thereby enhancing the estimation of the deformation. When compared to traditional ConvNet-based and other Transformer-based methods, AC-DMiR shows enhanced registration accuracy in terms of Dice coefficients and comparable deformation regularity on both Brain MRI and Uterus MRI image registration tasks.

The mechanisms of Transformers have inspired various ConvNet designs in computer vision, leading to a debate on whether Transformers could replace ConvNets for imagerelated tasks (Li et al., 2023a). ConvNet models such as ConvNeXt (Liu et al., 2022d) and RepLKNet (Ding et al., 2022b) have built upon Transformer concepts and demonstrated performance comparable to Transformers. Inspired by these models, Jia et al. (2022) proposed a U-Net with increased kernel sizes to expand the effective receptive field of the U-Net. Their method compared favorable against several Transformer-based registration methods. Currently, ConvNets still possess inherent advantages over Transformers, such as their invariance to input image sizes and the incorporation of inductive bias due to the nature of

the convolution operation. Therefore, there has been a growing interest in advancing ConvNets using Transformer concepts in computer vision. It is anticipated that further research in this area will lead to improved ConvNet architectures for medical image registration applications.

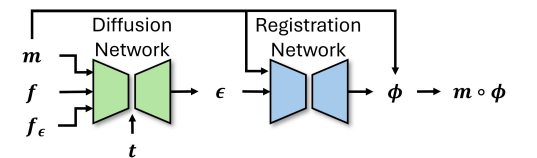


Fig. 6. Visual depiction of the diffusion model in medical image registration, where m and f are the moving and fixed images, respectively, ϕ is the deformation field, ϵ symbolizes the score function, and t represents an imaginary time step in the diffusion process. This approach adopts a diffusion model to create a conditional score function associated with the time step. This function, in conjunction with the moving image, facilitates the generation of continuous deformations going from the moving image to the fixed image. This approach is adopted in Kim et al. (2022).

4.4. Diffusion Models

In recent years, diffusion models (Sohl-Dickstein et al., 2015; Ho et al., 2020) have garnered significant research interest in computer vision. Initially designed for generative tasks, such as image synthesis, inpainting, and super-resolution, diffusion models have now been widely explored in various applications in the field of medical image analysis (see Kazerouni et al. (2023) for a survey). In contrast to other generative models like GANs and VAEs, which are either confined to data with limited variability or generating low-quality samples (Ho et al., 2020; Kazerouni et al., 2023), diffusion models have no such restrictions, making them an attractive alternative. The goal of diffusion models is to use the known forward process of gradual diffusion of information caused by noise to learn the reverse process of recovery of information from noise. The forward process is similar to the behavior of particles in thermodynamics, where particles spread (i.e., diffuse) from areas of high concentration to those of low concentration (Kirkwood et al., 1960; Sohl-Dickstein et al., 2015). The existing diffusion models use iterative steps of diffusion, which can include up to several thousand steps, to carry out the diffusion process. As a result, inference with these models, which requires the reverse diffusion process, is time-consuming. To date, only a few studies have incorporated diffusion models into medical image registration (Kim et al., 2022; Qin and Li, 2023), and Fig. 6 provides a graphical representation of these diffusion model-based models. In (Kim et al., 2022), the authors proposed Diffuse-Morph, which involves a diffusion network and a deformation network. The diffusion network learns a conditional score function (i.e., the added noise), while the deformation network uses the latent feature in the reverse diffusion process to estimate the deformation field. The registration process of DiffuseMorph is a one-step procedure as the fixed image is the target image at the end of the reverse diffusion process (i.e., t = 0), and it is already given. As a result, there is no need for time-consuming reverse diffusion steps to synthesize a target image from the moving image. Furthermore, DiffuseMorph offers the added capability of producing continuous deformations through the interpolation of the learned latent space. The method demonstrated promising results when compared to several ConvNet-based methods on a publicly available Cardiac MRI dataset and a human facial expression dataset. However, since their forward process adopts the strategy of adding Gaussian noise to the fixed image, their diffusion network learns a conditional score function for the fixed image. This score function is then used in the registration network, rather than directly inputting the fixed image, allowing the score function to carry semantic information. This results in a method that differs from the conventional diffusion models. In (Qin and Li, 2023), the authors proposed an alternative diffusion model based on (Kim et al., 2022) for medical image registration, where the score function is used as a weighting map for the image similarity measure. However, this formulation deviates from conventional diffusion models, where the score function is typically modeled as Gaussian noise.

4.5. Neural ODEs

Inspired by Euler's method for discretizing the derivative of ordinary differential equations (ODEs) into discrete time step updates, Chen et al. (2018) proposed a new family of DNN models called Neural ODEs. In their method, DNN elements that progressively update their input (*e.g.*, residual connections, or recurrent networks) are interpreted as updates of time steps in Euler's method. Consequently, a chain of these elements in a neural network is essentially a solution of the ODE with Euler's method of the form:

$$\frac{dh(t)}{dt} = f_{\theta}(h(t), t), \tag{9}$$

and

$$h(t+1) = h(t) + f_{\theta}(h(t), t),$$
 (10)

where h(t) represents the t-th element, which may be a residual block or a network. The final output at t = T can be computed by integrating f over the time interval [0, T], which is evaluated by a numerical solver taking many small time steps, thus approximating a neural network with infinite depth.

The first application of the NeuralODE framework for medical image registration was introduced by Xu et al. (2021). They proposed MS-ODENet, which parameterizes h at the final time point T (i.e., h(T)) as the deformation field that warps the moving image to the fixed image, and $\frac{dh(t)}{dt}$ as the small increment of deformation produced by a network at state t from the preceding state h(t-1). To alleviate the computational burden of numerical solvers and accelerate the runtime, they proposed solving ODEs at different resolutions in a coarse-to-fine manner. However, the loss function, consisting of a similarity measure and a deformation regularizer, is applied only to the final deformation field h(T). Similarly, Wu et al. (2022b) proposed NODEO, which formulated h(t) as the voxel movement at time t and the trajectory of the movement as the solution to the ODE. Drawing inspiration from dynamical systems, they expressed the ODE as $\frac{dh(t)}{dt} = \mathcal{K}v_{\theta}(h(t), t)$, where \mathcal{K} is a Gaussian smoothing kernel, v_{θ} denotes the velocity of the voxel movement produced by a neural network, and the initial condition h(0) is an identity. It is noteworthy that this formulation

bears similarities to LDDMM (Beg et al., 2005), an influential optimization-based method that considers image registration as an energy-minimizing flow of particles over time. In contrast to MS-ODENet (Xu et al., 2021), which applies loss solely to the deformation at t = T, NODEO optimizes image similarity at each t while minimizing the energy of the flow and encouraging spatial smoothness and regularity of the velocity fields through the Gaussian kernel, diffusion regularizer, and Jacobian determinant loss. The authors compared NODEO to various widely-used traditional methods and a ConvNet model on brain MRI registration tasks. It demonstrated superior registration performance measured by Dice while attaining diffeomorphic registration. Joshi and Hong (2023) introduced R2Net, which integrates both time-varying and time-stationary velocity fields using a neural ODE approach. This method employs Lipschitz continuous residual networks to estimate smooth intermediate velocity fields from an initial momentum, which is predicted by a U-Net-based ConvNet. The underlying theory relies on the Cauchy-Lipschitz theorem, positing that Lipschitz continuous integration ensures a well-defined mapping within the space of diffeomorphisms. The Lipschitz continuous residual networks comprise N blocks, each corresponding to a time step in the integration process. In the time-stationary configuration, these N blocks share weights, contrasting with the time-varying setting where the weights are not shared for each block. R2Net was evaluated against both optimization-based and learning-based diffeomorphic registration methods. It showed competitive performance, producing notably smoother deformations compared to the other methods.

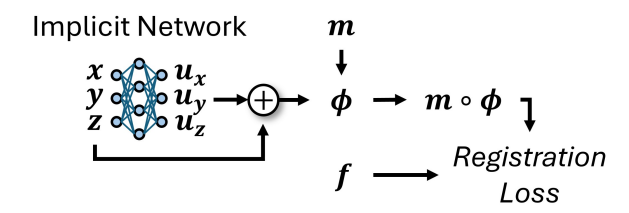


Fig. 7. Graphical depiction of implicit neural representations in medical image registration, with m and f denoting the moving and fixed images respectively, and ϕ denotes the deformation field. The set $\{x,y,z\}$ represents the grid in three distinct spatial dimensions, while the associated u's indicate the displacement vectors. Implicit neural representations are typically employed within a pair-wise optimization framework. In this setup, the DNN (typically an MLP) receives coordinates from an image grid as input and outputs the corresponding displacement vector for those coordinates. These vectors are then iteratively refined through the pair-wise optimization of the registration objective function. Similar frameworks are found in Han et al. (2023), Wolterink et al. (2022), Byra et al. (2023), and van Harten et al. (2024).

4.6. Implicit Neural Representations

Image registration can be formulated as an implicit problem of the form:

$$C(\mathbf{x}, \psi) = 0, \ \psi : \mathbf{x} \to \psi(\mathbf{x}), \tag{11}$$

where $\mathbf{x} \in \mathbb{R}^{2,3}$ is the 2D or 3D spatial coordinate (*i.e.*, from an integer grid), and ψ represents a neural network that maps each coordinate \mathbf{x} to a value of interest, subject to the constraint C. In the context of image registration, ψ typically maps the coordinate \mathbf{x} to its deformation $\psi(\mathbf{x})$, while C comprises a similarity

measure and a deformation regularizer. The neural network ψ can be considered as an implicit function of x, defined by the relation modeled by C (Eqn. 11). This concept is commonly referred to as implicit neural representations (INRs) in computer vision (Sitzmann et al., 2020; Mescheder et al., 2019; Niemeyer et al., 2019; Mildenhall et al., 2021). Although x's used during training are discrete, the implicit function $\psi(x)$ parameterized by a neural network, often a multi-layer perceptron (MLP), is a continuous and differentiable function. As a result, INRs provide a more compact representation of a continuous function and facilitate smooth manipulation of that function. Note that the input to the MLP is an image grid, which remains invariant across different image datasets. Consequently, INRs are commonly used in pairwise optimization-based registration (Han et al., 2023; Wolterink et al., 2022; Byra et al., 2023; van Harten et al., 2024), as graphically illustrated in Fig. 7.

Han et al. (2023) proposed to parameterize a continuous deformation field using a MLP introduced in (Sitzmann et al., 2020), given an integer grid representing the spatial coordinates of the voxels. The MLP thus serves as the implicit function of the integer grid. Since the MLP is not conditioned on the images and the only input is the coordinates that are deterministic for all images of the same resolution, optimization of the MLP is carried out iteratively and pair-wise for each image pair (similar to how the traditional registration methods are performed). To further improve the registration performance, the authors proposed a cascade framework that combines the benefits of learning-based registration DNNs with the optimizationbased INRs provided by the MLP. Within this framework, the learning-based DNN predicts an initial deformation field, while the MLP produces the residual deformation that refines the initial deformation field, leading to an enhanced overall registration performance. Leveraging the capability of INRs to represent continuous image grids, Wolterink et al. (2022) introduced an implicit DIR model that facilitates continuous differentiation of the deformation. This feature is crucial for calculating deformation regularization terms, such as the first derivative in diffusion regularizer and the second derivative in bending energy. This approach marks a significant shift from conventional DLbased registration models, which typically predict a discrete deformation field and hence rely on finite differences for differentiation. The authors explored various activation functions within the MLP framework and found that periodic activation functions enable the network to represent high-frequency signals necessary for capturing small local deformations. In contrast, ReLU activation functions tend to favor low-frequency functions. The proposed model showed promising results on the DIR-LAB dataset, surpassing DL-based methods. However, it demonstrated slightly inferior performance compared to traditional optimization-based methods on this dataset. Building on this foundation, Byra et al. (2023) further refined the model by proposing the decomposition of a moving image into a residual image and a support image. The residual image accounts for image artifacts and texture patterns that differ from the fixed image, whereas the support image aids in enhancing registration performance. These images are estimated using two implicit networks designed to minimize an exclusion loss, which encourages the gradient structures of these networks to be decorrelated, as suggested by Gandelsman et al. (2019). Image registration is then conducted by jointly minimizing a reconstruction loss, ensuring that the sum of the support and residual images reconstructs the moving image, along with two image dissimilarity measures applied to the deformed moving and support images against the fixed image, a deformation regularizer, and the exclusion loss. This method was evaluated on in situ hybridization image registration, where it demonstrated improved performance over both the earlier proposed INRs-based and CNNbased models, as well as traditional optimization-based methods. In van Harten et al. (2024), the author used IRN to parameterize the temporal motion of the intestine. Instead of using spatial coordinates from an integer grid, they align the coordinate system with the tangent space of the anticipated dominant motion, which conforms to the orientation of the intestines. The authors contend that this adjustment simplifies the complexity of the IRN and leads to better registration performance. It is important to note to recognize that these aforementioned INRsbased registration methods, much like traditional approaches, suffer from a common limitation: the optimization is conducted on a pairwise basis without learning from a larger dataset. As a result, these methods are unable to take advantage of the guidance offered by anatomical label maps when such maps are unavailable during the inference process. Meanwhile, Sun et al. (2022) applied INRs to a task of organ shape registration. Their approach was based on the idea of DeepSDF (Park et al., 2019), where an auto-decoder maps a latent code representing a unique organ shape and the 3D coordinates of a sampled point to a signed distance function (SDF). The value of an SDF determines whether the point lies inside (< 0), outside (> 0), or on the surface (= 0) of the shape, consequently providing an implicit description of the organ shapes. The resulting SDF is a continuous function, and the auto-decoder serves as the implicit neural representation of the discrete coordinates. To register points from different organ shapes, the authors modeled the trajectory of the point movement in space as the solution to an ODE, akin to the formulation proposed in NODEO (Wu et al., 2022b). In this formulation, the time derivative corresponds to the velocity of the point movement at time t. The authors solved this ODE using a NeuralODE solver (as briefly discussed in section 4.5), resulting in a diffeomorphic mapping between shapes.

4.7. Hyperparameter Conditioning

Inspired by HyperNetworks (Ha et al., 2017) and Hyperparameter Optimization (Franceschi et al., 2018), recent research has introduced methods that integrate hyperparameters directly into the architecture of the registration DNNs, which is graphically depicted in Fig. 8. This allows for the capturing of a wide range of hyperparameters within a single training process, consequently speeding up the hyperparameter tuning process without requiring multiple networks to be trained from scratch for each hyperparameter value. In the training process of these methods, a distinct hyperparameter value is randomly selected, and the network generates a deformation field associated with that value. Subsequently, the registration loss is calculated us-

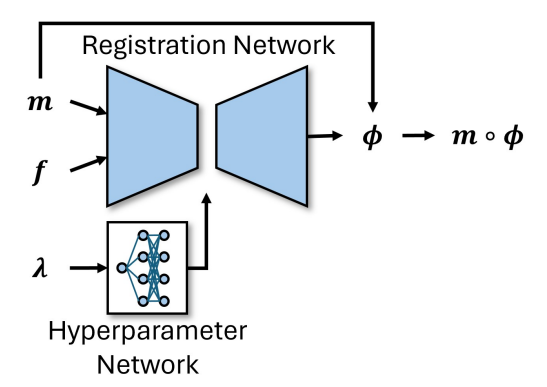


Fig. 8. Illustration of hyperparameter conditioning applied in medical image registration, with m and f denoting the moving and fixed images, respectively, and ϕ indicating the deformation field. Here, λ is the hyperparameter for tuning the loss function, commonly associated with the regularization hyperparameter to control the smoothness of the deformation field. The purpose of this strategy is to facilitate the adjustment of hyperparameters at test time, circumventing the need for time-intensive retraining. Hyperparameters can either be integrated directly into the network architecture (Mok and Chung, 2021b; Chen et al., 2023b) or input into a separate DNN that then produces the parameters for the registration network (Hoopes et al., 2022a).

ing the same hyperparameter value, which is then used to update the network parameters. The hyperparameter being conditioned typically relates to the weight of the deformation regularizer, which affects the smoothness of the deformation produced by the network.

Hoopes et al. (2022a) introduced HyperMorph, which is based on the concept of HyperNetworks (Ha et al., 2017). HyperMorph comprises two ConvNets: a hypernetwork and a U-Net-like registration network (i.e. VoxelMorph (Balakrishnan et al., 2019)). The hypernetwork estimates the weights of the U-Net based on the provided hyperparameter value for the diffusion regularizer, while the U-Net generates a deformation field to warp the moving image. In each training step, the hyperparameter value is randomly sampled from a uniform distribution, and the loss is computed using the same sampled value. After training, the best-performing hyperparameter value is acquired using gradient descent. In this process, the network weights are fixed, and an optimizer iteratively updates the hyperparameter based on a target objective function (commonly the Dice score) applied to a validation dataset. In a parallel work, Mok and Chung (2021b) proposed conditioning the regularization hyperparameter through conditional instance normalization (Dumoulin et al., 2017). In this approach, the feature map statistics within the regularization network are normalized and shifted according to two affine parameters. These affine parameters are generated by a lightweight mapping network, which takes the sampled hyperparameter value as input. Later, Chen et al. (2023b) expanded the conditional instance normalization to a conditional layer normalization for application in Transformerbased registration models. The training processes in both (Mok and Chung, 2021b; Chen et al., 2023b) are similar to the one used in HyperMorph, where the hyperparameter value is sampled from a uniform distribution and then employed for loss computation. However, it is worth noting that Mok and Chung (2021b) and Chen et al. (2023b) obtain the best-performing hyperparameter value through a grid search, whereas HyperMorph acquires it via gradient descent.

4.8. Anatomy-aware Networks

Given the widespread success of DNN methods in medical image segmentation, anatomical label maps can now be relatively easily obtained using a segmentation network. As a result, some registration models have started to incorporate this prior anatomical information into their design to enhance registration accuracy, moving beyond simply using them as components of a loss function during training.

In Su and Yang (2023), the authors proposed using anatomical label maps to extract a set of nonuniformly spaced control points, sampled along the contours of anatomical structures. These control points allow for more precise deformation of anatomical structures, particularly at their boundaries, compared to uniformly distributed control points on image grids. The method involves extracting intensity features, which are generated by a ConvNet encoder, alongside spatial features, both of which are aligned with the positions of the sampled control points. In another approach, to facilitate a spatially discontinuous deformation, which is important for many registration applications as delineated in Section 3, Chen et al. (2021f) proposed an alternative approach. Rather than employing a discontinuity-permitted deformation regularization (as briefly mentioned in Section 3), the authors proposed using anatomical label maps to segregate the moving and fixed images into different regions of interest and subsequently generate deformation fields for each region using multiple registration networks. These deformation fields are then combined to yield a final deformation via addition. However, this method has an immediate drawback in necessitating the anatomical label maps throughout both the training and inference stages. When label maps are not available, this method becomes infeasible.

4.9. Correlation Layer

Optical flow is the name given by the computer vision community to image registration. In learning-based optical flow, it is common to employ a correlation layer (Dosovitskiy et al., 2015) to aid neural networks in pinpointing explicit correspondences between points in images. This involves computing the correlation between the neighboring features of a spatial location in the moving image and the neighboring features of a range of spatial locations in the fixed image. The correlation is computed between two feature patches centered at \mathbf{x}_m and \mathbf{x}_f in the moving and fixed images, respectively, using the following equation:

$$c(\mathbf{x}_m, \mathbf{x}_f) = \sum_{\mathbf{o} \in [-k,k]} \langle F_m(\mathbf{x}_m + \mathbf{o}), F_f(\mathbf{x}_f + \mathbf{o}) \rangle, \qquad (12)$$

where F_m and F_f denote the feature patches of the moving and fixed images, respectively, and k defines the patch size. The selection of locations \mathbf{x}_m and \mathbf{x}_f is based on a maximum displacement d, meaning that for each \mathbf{x}_m , the range of \mathbf{x}_f is limited to the locations that are at most d distance away. The output of the correlation layer is a set of correlation values that represent the

correlation between one feature patch in the moving image and another feature patch in the fixed image. The output has a size of $H \times W \times D \times d$, where $H \times W \times D$ represents the size of the feature maps.

Although the concept of directing networks with explicit correspondences between voxels or patches has been employed in computer vision since 2015, it was only recently embraced in medical image registration. This delay can be attributed to the potential computational challenges introduced by Eqn. 12. Since medical images are typically volumetric, the search space for each voxel location would be in a 3D volume, quickly becoming unmanageable as the search distance *d* grows. (Heinrich, 2019) was the first to implement a correlation layer in their network design by introducing the PDD-net. Instead of calculating the scalar product between two features as done in Eqn. 12, PDD-net computes the correlation as the mean squared error between feature patches centered at each control point in the moving and fixed images:

$$c(\boldsymbol{x}_m, \boldsymbol{x}_f) = \sum_{\boldsymbol{o} \in [-k,k]} \|F_m(\boldsymbol{x}_m + \boldsymbol{o}) - F_f(\boldsymbol{x}_f + \boldsymbol{o})\|^2.$$
 (13)

Moreover, in their correlation layer, the search distance is represented by a 3D matrix, d^3 , with each element in the vector, d, defining a discrete displacement distance from the current center of the feature patch. This correlation layer produces a 6D matrix, where the first three dimensions outline the shape of the feature maps, and the final three dimensions describe the shape of the search space. Due to the sparsity of the control points in comparison to the image size, the computational burden of this correlation layer remains relatively low. The correlation layer is applied to features independently extracted from the moving and fixed images using a ConvNet that incorporated deformable convolutional layers as introduced in Heinrich et al. (2019). Subsequently, min-convolutions and mean-field inference are employed to spatially smooth the dissimilarities produced by the correlation layer. A softmax operation is then applied to the 6D matrix, converting the dissimilarities into pseudo-probabilities. The displacement field is subsequently generated by multiplying the probabilities with the displacement distance in d^3 , resulting in a weighted average of these probabilistic estimates for the 3D displacement field. The deformation field is then trilinearly interpolated to align with the image resolution. Heinrich and Hansen (2020) later extended this approach by proposing a 2.5D approximation of the quantized 3D displacement, significantly reducing the memory burden of the original Pdd-net. Instead of creating a 6D dissimilarity matrix, they generated three 5D matrices (i.e., the 2.5D dissimilarity matrices), with each matrix representing the dissimilarities computed for two out of the three dimensions. The 2.5D probabilities produced at the end of the network are interpolated to 3D using B-splines. To minimize the error during the conversion from 2.5D to 3D, a two-step instance normalization is applied for each pair of test scans using gradient descent. More recently, Heinrich and Hansen (2022) further expanded the concept of probabilistic displacement and incorporated keypoint supervision into VoxelMorph (Balakrishnan et al., 2019) through the introduction of VoxelMorph++. They advanced

VoxelMorph in two respects: probabilistic displacement via heatmap prediction and multi-channel instance optimization using one-hot embeddings of the anatomical label maps generated by a segmentation network. In their model, high-level features are initially extracted from the VoxelMorph decoder, and feature vectors are then sampled at given keypoint locations. These feature vectors are converted into larger heatmap patches through a convolution block followed by a softmax operation. Consequently, each heatmap represents the probabilistic displacements of the corresponding keypoint. The final displacement field is generated as the sum of the displacements weighted by the heatmap. During the testing phase for each image pair, an instance optimization strategy (Siebert et al., 2021a) refines the displacement field using the supervision provided by the anatomical labels generated from a segmentation network. The methods discussed in this subsection were evaluated on abdomen and lung CT datasets, where large deformations are necessary for accurate registration. The architectures proposed in these methods proved to be efficient and demonstrated superior performance compared to traditional methods and learningbased networks that only generate dense displacement fields.

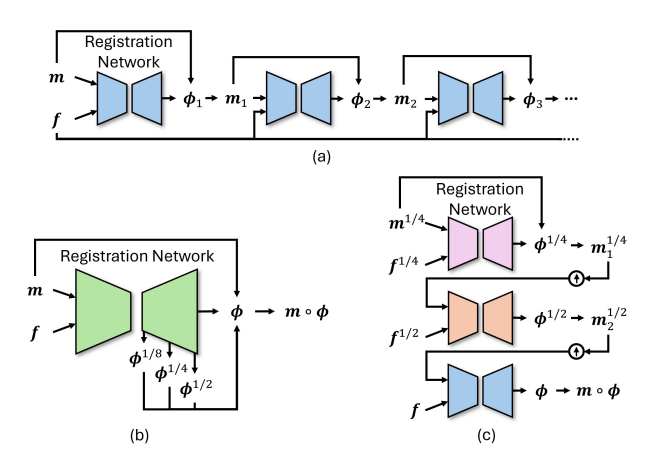


Fig. 9. This illustration depicts progressive and multi-scale registration network designs employed in medical image registration, where m and f represent the moving and fixed images, respectively, and ϕ denotes the deformation field. The subscripts indicate the intermediate deformed moving images at respective stages, while the superscripts specify the resolution fraction of the image or the deformation field. Panel (a) outlines the framework for progressive image registration, e.g., VTN (Zhao et al., 2019). Panels (b) and (c) demonstrate two distinct approaches to multi-scale registration employed in learning-based methods. The former incorporates a multi-scale aggregation of deformation fields within a single network (e.g., im2grid (Liu et al., 2022c)), whereas the latter uses an independent network for each scale (e.g., DLIR (De Vos et al., 2019) and LapIRN (Mok and Chung, 2020b, 2021b)). The designs for progressive and multi-scale registration are intended to emulate the optimization strategy commonly used in traditional methods, which typically involve iterative and multiscale updates of the deformation field.

4.10. Progressive and Pyramid Registration

Recent research has also demonstrated that employing a network to progressively warp a moving image towards a fixed image, or performing registration through a multi-scale image pyramid employing a coarse-to-fine technique, may significantly improve registration performance. Figure 9 graphically summarizes these two types of architectures, in which panel (a)

illustrates the progressive registration framework, while panels (b) and (c) depict the multi-scale registration frameworks. Zhao et al. (2019) introduced the VTN, which leverages cascade registration networks to align moving images with fixed images. Drawing inspiration from FlowNet2.0 (Ilg et al., 2017), each subnetwork is responsible for aligning the current moving image with the fixed image, with the resulting warped image sent into the subsequent subnetwork as the new moving image. The final deformation field is the composition of the intermediate deformation fields produced by the subnetworks. This approach has been shown effective in handling large displacements. Similar trends of adopting a progressive registration framework are evident in the development of image registration models, which have shown enhanced registration performance (Jia et al., 2021; Chen et al., 2022a; Lara-Hernandez et al., 2023). Chen et al. (2022a) proposed a method for progressive image registration within a single network. Their method employs multiple convolution blocks in the decoding stage, each responsible for aligning the current moving image to the fixed image. In Jia et al. (2021), the authors introduced VR-Net, an end-to-end learning framework that unfolds the iterative optimization process. First, the nonlinear objective function (i.e., Eqn. 1) is linearized with respect to the deformation by applying a first-order Taylor series expansion. Subsequently, an auxiliary variable is introduced to decouple the objective function into two convex problems. This approach mirrors earlier methods that used quadratic relaxation applied to the variational problem (Chambolle, 2004; Steinbrücker et al., 2009; Heinrich et al., 2014), where one subproblem focuses on optimizing similarity and the other concentrates on the regularization of the deformation. VR-Net employs a sequence of network blocks that iteratively updates and refines the deformation field, with each block refining the output from the previous one, effectively mirroring the iterative update process for the decoupled objective function. In Lara-Hernandez et al. (2023), the authors adopt a similar strategy to that of VTN (Zhao et al., 2019) by employing a sequence of intermediate registration networks that progressively warp the moving image towards the fixed image. The authors augmented the VTN framework for dynamic myocardial perfusion CT registration by introducing a contrast loss specifically designed to focus on the dynamic changes in contrast agent concentration within the heart. The proposed method surpasses several established optimization-based registration methods for this particular task.

Concurrently, there have been efforts to apply progressive registration using a multi-scale image pyramid approach. Given the widespread adoption of hourglass-shaped network architectures in image registration, convolution blocks within the decoder generate deformation fields at multiple resolutions in a coarse-to-fine manner. These deformation fields at different resolutions are subsequently upsampled and composited to form the final deformation field. Notable methods that adopt this scheme include (Jiang et al., 2020; Kang et al., 2022; Liu et al., 2022c; Lv et al., 2022). In addition to network architecture, the coarse-to-fine training scheme has also been adopted in learning-based image registration. Taking inspiration from conventional registration methods that often employ multiple

stages with varying resolutions, De Vos et al. (2019) pioneered a multi-scale training strategy for deformable image registration. Their approach involves sequentially training the Conv-Net in each stage for a specific image resolution by optimizing the image similarity measure. Notably, a B-spline framework is adopted thus alleviating the need for a deformation regularizer. During training, the weights of the preceding Conv-Nets are held fixed, and after training, the registration is performed through a single pass of input images to the multi-stage ConvNets. Eppenhof et al. (2019) proposed a novel progressive and multi-scale training scheme for learning-based image registration. Instead of training a large network on the registration task all at once, they first train smaller versions of the network on lower-resolution images. The resolution of the training images is then gradually increased, and additional convolutional layers are added to increase the network size. A similar approach is employed by Berg et al. (2023). Mok and Chung (2020b) proposed LapIRN, which adopts a similar pyramid training scheme. However, unlike the previous training approach, which progressively increases the image resolution and network size of the same network, LapIRN employs three different networks, each producing a deformation field for a specific resolution. Each network is equipped with a skip connection that propagates feature embeddings from a lower-resolution network to a higher-resolution network. The networks are trained in a coarse-to-fine manner, with each network producing a deformation field that refines the upsampled deformation field from the previous resolution. However, using multiple networks to generate a pyramid of deformation fields can be computationally inefficient and increase the network size, which can hinder training. To address this issue, Hu et al. (2020) proposed a self-recursive contextual network that employs a single feature extractor to produce features at different resolutions. Then, a weight-sharing deformation generator and receptive module are then used to recursively generate and refine deformation fields in a coarse-to-fine manner. Since the network weights are shared between resolutions, this method reduces the computational burden and the size of the network, resulting in more efficient training. Zhou et al. (2023) proposed a novel network architecture to leverage progressive registration at both single and multi-scale resolution. The proposed method iteratively refines the deformation field generated from the previous iteration, with each iteration composing deformation fields of various resolutions to form the new deformation field. Meng et al. (2023) introduced NICE-Trans, a novel approach to address both affine and deformable registration simultaneously using a coarse-to-fine framework. The model features dual-path ConvNet-based encoders that independently extract features from the moving and fixed images across multiple scales. A Transformer-based decoder is employed to estimate affine parameters at its bottleneck, along with multiple displacement fields at various resolutions of the decoder. The final displacement field is derived by summing the upsampled affine grids and the multi-scale displacements. NICE-Trans has shown superior performance compared to previous DL-based DIR methods, which often rely on optimization-based methods for affine registration as a preprocessing step or require a separate affine network to pre-align the images prior to the DIR network.

In Ma et al. (2023), the authors developed a single Transformer-based network architecture for image registration that integrates both progressive and multi-scale strategies. The architecture features a dual-stream ConvNet decoder that independently extracts multi-scale features from both moving and fixed images. Recognizing that large deformations are typically captured at coarser scales, the network employs a series of Swin Transformer-based blocks (Liu et al., 2021b) at the bottleneck scale. These blocks progressively refine the deformation fields through successive additions, where each field is updated based on the output from the previous block, which takes in the deformed moving features together with the fixed image features. Subsequently, additional blocks that include upsampling and a convolution layer further refine the deformation field from the bottleneck to the full scale. The model was rigorously validated to identify the optimal number of progressive updates, with findings indicating that 2 to 3 updates are adequate to achieve satisfactory registration accuracy for the brain MRI and liver CT registration tasks it was evaluated on. For these tasks, the proposed method surpassed several contemporary registration models, including those based on ConvNets and Transformers.

The registration methods discussed in this subsection have demonstrated the efficacy of decomposing the registration process into multiple steps, where each step refines the deformation fields from the previous step. These approaches have consistently shown significant performance gains while enforcing a smoother deformation field for image registration tasks compared to using a single network to generate a deformation field all at once.

5. Uncertainty in Learning-based Registration

DNNs are capable of learning complex representations. However, their predictions are typically deterministic and assumed to be accurate, which is usually not the case. Estimating the uncertainty is important for evaluating what the models learn from the data and helps reduce risk in decision-making based on the model prediction. In medical image analysis, uncertainty estimation has been widely used in tasks such as image segmentation, image classification, and image registration. For example, registration uncertainty empowers surgeons to evaluate the surgical risk tied to the registration model's prediction, thereby avoiding undesirable consequences. Prior to the deep learning-based registration, traditional registration uncertainty is based on the framework of probabilistic registration, where the probabilistic distribution of the transformation parameters is estimated.

In this section, we focus on reviewing the **recent advance-ments** in estimating registration uncertainty through deep learning methods, though many concepts have been drawn from traditional registration uncertainty estimation methods. We start with the general framework for estimating uncertainty using deep learning methods. Next, we formally define the different types of registration uncertainty and elaborate on how the uncertainty estimation methods are used in learning-based reg-

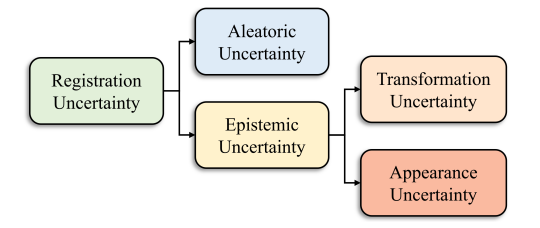


Fig. 10. Various types of registration uncertainty can be estimated using DNNs.

istration. Finally, we provide a summary of the methods used for evaluating the quality of uncertainty estimation.

5.1. Bayesian Deep Learning

As shown in Fig. 10, in general, uncertainty can be categorized into two types: aleatoric and epistemic uncertainty (Kendall and Gal, 2017). Aleatoric uncertainty, also known as data uncertainty or inherent uncertainty, refers to the inherent randomness or variability present in observed data. It can be thought of as the variability of the data given the underlying true data generation model due to factors such as measurement errors, sensor noise, or the intrinsic stochastic nature of the data generation process. Epistemic uncertainty, also known as model uncertainty or knowledge uncertainty, refers to variability present in the model structure, model parameters, and model assumptions. It arises due to our limited knowledge or understanding of the underlying model. Aleatoric uncertainty may be reduced by improving the data quality, while epistemic uncertainty may be mitigated by improving model selection, refining parameter estimation, or acquiring additional relevant information.

To predict aleatoric and epistemic uncertainty using deep learning, we train a model W using data set D that takes an input x to generate an output y(x, W) and a variance prediction $\sigma^2(x, W)$. Aleatoric uncertainty describes the uncertainty that is inherent in the training data D. It is expressed as follows:

$$u_a = E_{p(W|D)} \left[\sigma^2(x, W) \right], \tag{14}$$

where E represents taking the average of $\sigma^2(x, W)$ over the distribution p(W|D). Epistemic uncertainty describes the uncertainty of the model W. It is represented as follows:

$$u_e = V_{p(W|D)}[y(x, W)],$$
 (15)

where V represents taking the variance of y(x, W) over the distribution p(W|D). Directly computing aleatoric uncertainty using Eqn. 14 and epistemic uncertainty using Eqn. 15 is usually impractical, as it requires the integration of high dimensional numerical functions. Instead, these uncertainties are approximated from a set of outputs by using the model weights W sampled from the posterior distribution p(W|D).

In theory, the posterior distribution p(W|D) can be obtained through Bayes' rule,

$$p(W|D) = \frac{p(D|W)p(W)}{p(D)},\tag{16}$$

where p(W) is an assumed prior. However, it is not feasible to obtain p(D) in the denominator due to the intractable integral. As an alternative, variational inference is used to approximate p(W|D) as a distribution $q_{\theta}(W)$ with parameter θ by minimizing the Kullback-Leibler (KL) divergence between them. This process can be simplified as follows:

$$\hat{\theta} = \arg\min_{\theta} D_{KL} \left[q_{\theta}(W) || p(W) \right] - E_{q_{\theta}} \left[\log p(D|W) \right], \quad (17)$$

where D_{KL} represents KL divergence and $E_{q_{\theta}}$ represents taking the average over the distribution $q_{\theta}(W)$. With this, the aleatoric uncertainty in Eqn. 14 and the epistemic uncertainty in Eqn. 15 can be approximated by sampling W from $q_{\hat{\theta}}(W)$.

Many sampling methods can be used for uncertainty estimation, including Monte Carlo dropout, bootstrap, and snapshot techniques. The Monte Carlo dropout sampling method operates under the assumption that $q_{\theta}(W)$ follows a Bernoulli distribution (Gal and Ghahramani, 2016). It leverages dropout layers during the testing phase to perform multiple forward inferences. This method is widely used in learning-based registration models, likely due to its straightforward implementation (Yang et al., 2016, 2017; Madsen et al., 2020; Chen et al., 2022b; Xu et al., 2022). Bootstrap sampling, a traditional method, involves training the registration model multiple times on independent training sets to produce multiple inferences (Kybic, 2009). Snapshot sampling uses the cyclic learning rate in one training process for perturbing the model to converge to multiple different local minimums (Huang et al., 2017). It has shown that snapshot sampling performs better uncertainty estimation than other methods for the medical image registration use case (Gong et al., 2022).

5.2. Registration Uncertainty Estimation for DNN

Both aleatoric and epistemic uncertainty are present in image registration. Aleatoric uncertainty in image registration may arise from factors such as image noise, image artifacts, lack of image features or image contrast, and natural anatomical variation between images. There may be two types of aleatoric uncertainty in image registration. One is that given the underlying true deformation field, two aligned images may not be exactly the same due to different image noise, image artifacts or natural anatomical variation between images. Another type is that multiple deformation fields may align two images with similar performance due to lack of image features or image contrast. On the other hand, epistemic uncertainty represents the limitations inherent in the modeling process. In image registration, this relates to the limited ability of the model to precisely capture the complex deformation field. This form of uncertainty can be attributed to factors like inadequate training data, choices in model architecture, or the inherent complexity posed by the inverse problem of estimating the deformation fields. The following subsections provide details on each type of uncertainty.

5.2.1. Aleatoric Uncertainty

In medical image registration, the output of the network is usually a deformation field $\phi(I_f, I_m, W)$ as a function of the fixed image I_f , the moving image I_m and the model W. To help

the model estimate the aleatoric uncertainty inherent from data, the model needs to predict a variance $\sigma(I_f, I_m, W)$ of the output. Assuming the deformation field ϕ follows a voxel-wise Gaussian distribution, the model W can be trained by minimizing the loss function.

$$\mathcal{L} = \sum_{p} \frac{(\phi(p) - \phi^{*}(p))^{2}}{\sigma^{2}(p)} + \log \sigma^{2}(p), \tag{18}$$

where ϕ^* is the ground truth for the deformation field. However, in unsupervised learning-based image registration, the ground truth deformation ϕ^* is unavailable, and the loss may be calculated in the image domain (i.e., in the form of image similarity measure) rather than directly comparing the deformation fields as in Eqn. 18. To overcome this issue, the aleatoric uncertainty for image registration is frequently estimated using a variational inference strategy, which optimizes a global neural network to produce posterior of deformation fields (Dalca et al., 2019b; Grzech et al., 2020, 2022; Wei et al., 2021a; Smolders et al., 2022; Croquet et al., 2021; Krebs et al., 2019). This approach circumvents the direct computation of the intractable posterior $p(\phi|I_f;I_m)$ by introducing an approximate posterior $q_{\theta}(\phi)$, where the parameter θ can be predicted by a network based on the inputs I_f and I_m . The KL divergence between the two posteriors is then minimized, which maximizes the evidence lower bound (ELBO):

$$\hat{\theta} = \arg\min_{\theta} D_{KL} \left[q_{\theta}(\phi) || p(\phi) \right] - E_{q_{\theta}} \left[\log p(I_f | \phi; I_m) \right], \quad (19)$$

where D_{KL} represents KL divergence and $E_{q_{\theta}}$ represents taking the average over the distribution $q_{\theta}(\phi)$, and $p(\phi)$ represents the prior of the deformation field. Here, the prior $p(\phi)$ is usually modeled using a graph Laplacian matrix for smoothness regularization (Dalca et al., 2019b; Grzech et al., 2020, 2022), and the approximate posterior $q_{\theta}(\phi)$ is frequently modeled as a multivariate normal distribution (i.e., $\phi \sim \mathcal{N}(\mu_{\phi}, \sigma_{\phi}^2)$). A more complex prior can be designed to close the gap between the real posterior and the variational posterior (Xu et al., 2023). To reduce the dimensionality of the covariance matrix σ_{ϕ}^2 and simplify its optimization, a diagonal matirx (Dalca et al., 2019b) or a sum of a diagonal and a low rank matrices (Grzech et al., 2020, 2022) are used. Moreover, the conditional probability $p(I_f|\phi;I_m)$ typically takes the Gaussian form (i.e., $I_f \sim \mathcal{N}(I_m \circ \phi, \sigma_I^2)$) (Dalca et al., 2019b), or can be implemented as a neural network for learning a more complex form (Grzech et al., 2022). In practical applications, the mean μ_{ϕ} and the standard deviation σ_{ϕ} of the deformation field can be optimized directly as parameters using backpropagation (Grzech et al., 2020, 2022), or can be predicted by the registration network, in a similar manner to a variational autoencoder (Dalca et al., 2019b). The obtained variance σ_{ϕ}^2 represents the aleatoric uncertainty associated with the deformation field, given the input images I_f and I_m .

5.2.2. Epistemic Uncertainty

As illustrated in Fig. 10, the epistemic uncertainty in registration can be divided into two different measures (Luo et al., 2019; Xu et al., 2022; Chen et al., 2022b): transformation uncertainty and appearance uncertainty. These measures refer to

the uncertainty in generating the transformation and the plausibility of the transformation, respectively (Bierbrier et al., 2022). The former quantifies the uncertainty in the deformation space and tends to be large when the model is uncertain about establishing specific correspondences, such as when registering regions with piecewise constant intensity. In contrast, the latter is often based on the assumption that high image similarity indicates correct alignment. Consequently, this uncertainty would be large when the appearance differences between the warped and fixed images are significant.

Transformation uncertainty can be described as the variance of the sampled deformation fields, which derives from Eqn. 15 by stochastic sampling:

$$u_{e,trans} = \frac{1}{N} \sum_{i=1}^{N} (\phi_i - \frac{1}{N} \sum_{i=1}^{N} \phi_j)^2,$$
 (20)

where ϕ_i is generated by using the model weight W_i sampled from the estimated variational distribution $q_{\hat{\theta}}(W)$ with the parameter $\hat{\theta}$ optimized by Eqn. 17, and N is the total sampling number. Appearance uncertainty is expressed as the variance of the warped images, which are created using the sampled deformation fields (Luo et al., 2019; Xu et al., 2022):

$$u_{e,appea} = \frac{1}{N} \sum_{i=1}^{N} (I_m \circ \phi_i - \frac{1}{N} \sum_{i=1}^{N} I_m \circ \phi_j)^2,$$
 (21)

where ϕ_i is generated by using the sampled W_i as the model, N is the total sampling number and I_m is the moving image. However, it should be noted that the uncertainty estimated using this equation for appearance uncertainty can be biased due to overfitting, as shown in Chen et al. (2022b). To correct this, the authors suggest using the following formulation instead:

$$u_{e,appea} = \frac{1}{N} \sum_{i=1}^{N} (I_m \circ \phi_i - I_f)^2,$$
 (22)

where the predictive mean is replaced by the fixed image I_f .

It is important to note that while the presence of aleatoric and epistemic uncertainties in the image registration process, they may not provide useful insights for label propagation, where image registration is applied to warp between label maps. In such scenarios, segmentation uncertainty estimates could be more relevant. In (Chen et al., 2024), the authors demonstrated that registration uncertainty estimates, which are primarily based on image intensity information rather than the underlying labels, do not correlate well with errors in label propagation. They proposed a plug-in-and-play DNN method that estimates both aleatoric and epistemic uncertainties in segmentation, in addition to registration uncertainties, to more effectively identify potential errors in using image registration for segmentation.

5.3. Uncertainty Evaluation in Registration

One significant challenge in uncertainty estimation lies in its evaluation due to the absence of ground truth, especially in unsupervised learning-based registration. To access the quality of uncertainty, sparsification plots are usually used for voxel-wise uncertainty evaluation (Mac Aodha et al., 2012; Wannenwetsch et al., 2017; Ilg et al., 2018).

Sparsification plots demonstrate how the registration error changes by gradually removing voxels ranked by the uncertainty measure. It is anticipated that removing a voxel with higher uncertainty will result in a greater reduction in registration error, and the opposite holds true for voxels with lower uncertainty. If all voxels are arranged in descending order of uncertainty, and the uncertainty ranking matches the actual registration error ranking, the accumulated registration error under the sparsification plot will be small. Therefore, the area under sparsification plots is also used as an evaluation metric to gauge the quality of the uncertainty estimation.

6. Registration Evaluation Metrics

Manual correspondences are usually regarded as the gold standard for evaluating the performance of a registration algorithm (Peter et al., 2021). Landmark correspondences are the most frequently used type, although surfaces or lines may also serve as manual correspondences. The evaluation of registration performance using landmark correspondences is relatively simple for rigid and affine transformations, since these transformations can be expressed as matrix multiplication and the ground truth transformation can be determined through several pairs of manual landmark correspondences. In contrast, determining the parameters of deformable transformations requires dense manual landmark correspondences, which are typically not obtainable. Even in cases where manual landmark correspondences are available, they are often restricted to highly selective intensity features (Castillo et al., 2009b) and neglect regions with homogeneous intensities. Therefore, validating deformable registration algorithms is still considered a non-trivial task (Viergever et al., 2016). In current literature, the performance of deformable registration algorithms is most commonly evaluated in terms of accuracy and regularity.

6.1. Accuracy Measures

When the manual landmark correspondences are available, the accuracy of the transformation can be evaluated by target registration error (TRE),

$$TRE_{forward} = \sum_{i=1}^{N} ||T_{forward}(l_m^i) - l_f^i||_k,$$
 (23)

where T_{forward} is the estimated forward transformation that takes the moving image to the fixed image; l_m^i and l_f^i are the i^{th} pair of landmarks in the moving and fixed image, and $k \in \{1,2\}$ denoting either the ℓ^1 -norm or ℓ^2 -norm. Both l_m^i and l_f^i as well as the warped moving landmark $T(l_m^i)$ can be non-integer locations. Note that we used the forward transformation T_{forward} in Eqn. 23, but it is more common in practice to estimate the transformation T_{backward} that maps the fixed image to the moving image. In order to generate the warped image, T_{backward}^{-1} can be

applied in place of $T_{\rm forward}$. Both $T_{\rm forward}$ and $T_{\rm backward}$ are mappings from integer locations to non-integer locations. The difference between these two schemes is manifested when rendering the warped image. When $T_{\rm forward}$ is applied to I_m , integer locations are mapped to non-integer locations, which necessitates interpolating scattered data (Crum et al., 2007; Zhuang et al., 2008). On the other hand, $T_{\rm backward}^{-1}$ maps non-integer locations back to integer locations. Thus, rendering the warped image only requires interpolating the moving image, which is defined on a regular grid. For algorithms that only output $T_{\rm backward}$, TRE can be computed as

$$TRE_{backward} = \sum_{i=1}^{N} ||l_m^i - T_{backward}(l_f^i)||_k.$$
 (24)

Landmark correspondences can also be generated using artificial deformations (Bauer et al., 2021; Sdika, 2008; Ger et al., 2017). Different from manual landmark correspondences, artificial deformation can produce dense correspondences that are not limited to regions with highly selective intensity features. However, the performance of algorithms on artificial deformation may not accurately reflect their actual performance due to the discrepancy between the artificial and real deformations (Obeidat et al., 2016; Pluim et al., 2016). To overcome this issue, many works have been focused on generating deformations that are more akin to those observed in practical applications. For instance, Lobachev et al. (2021) proposed a pipeline for simulating sectioning-induced deformation fields. Vlachopoulos et al. (2015) used a thin-plate kernel spline model to simulate lung deformations arising from respiration. Biomechanical simulation (Fu et al., 2021; Teske et al., 2017) and phantoms (Wu et al., 2019; Ayyalusamy et al., 2021) are other techniques used to generate artificial deformations.

In situations where manual landmark correspondences are not available, surrogate measures are used to evaluate accuracy. The most straightforward measures of this kind include absolute intensity differences and the root-mean-square intensity difference between the warped image and the fixed image. Other similarity measures such as mutual information, structural similarity index (SSIM) can also be used. When anatomic labels are available, evaluating the overlaps between the warped and fixed label images is a popular technique. The Dice coefficient and Jaccard Index are examples of such measures. However, Rohlfing (2011) demonstrated that by simply reordering the voxels from the moving image based on the intensity values ranking without any geometrical constraints, one can achieve significantly better performance compared with the state-ofthe-art registration algorithms in most of the surrogate measures. They concluded that surrogate measures might still be useful to detect inaccurate registrations but many times they do not provide sufficient positive evidence for accurate registrations. Only the overlap of sufficiently local labels among the surrogate measures was found to distinguish between reasonable and poor registrations in their experiments.

Label surface distances from segmentation maps offers an alternative to overlap measures. Dalca et al. (2019b) converted segmentation maps into signed distance functions to approximate the distance between the fixed and warped surfaces.

They also showed that incorporating a similar surface distance loss during network training enhanced the surface alignment of anatomical structures. Cheng et al. (2020a) used the mean minimum distance (MMD), computed as the average Euclidean distance between manually defined surface points of anatomical structures and their corresponding nearest points on the warped surface, to measure the discrepancy between the surfaces. Additionally, the Hausdorff distance has been extensively used (Hering et al., 2022).

Previous studies (Lotfi et al., 2013; Sokooti et al., 2016) have explored the use of machine learning algorithms for quantifying registration errors. Compared to manual landmark correspondences, those methods provide dense error estimations that can be easily visualized. More recently, several deep learning techniques have been employed, offering a speed advantage over traditional machine learning algorithms, especially when a graphical processing unit (GPU) is available (Sokooti et al., 2021). Most of these methods were trained to predict the registration errors between a fixed and a warped image inputs. During training, artificial deformations are used to produce the warped image and the accuracy of these methods were validated using manual landmark correspondences (Eppenhof and Pluim. 2018a; Sokooti et al., 2021). Additionally, these techniques can also be applied to inter-modality registration tasks by incorporating an extra image synthesis step (Bierbrier et al., 2023).

6.2. Regularity Measures

Given the challenge of acquiring dense manual landmark correspondences and the aforementioned limitation of surrogate measures, the regularity of the transformations is often used alongside accuracy measures to obtain a more comprehensive understanding of the transformations. The underlying assumption is that accurate transformations should be spatially smooth. Particularly, transformations that fold the space result in physically un-realistic anatomy structures, which usually indicate errors. For continuous transformations, their Jacobian determinant |J| must be positive everywhere to avoid folding of space. This concept is extended to digital transformations where the number or the percentage of voxels with non-positive Jacobian determinant $|J| \le 0$ are reported to measure the irregularity (Meng et al., 2022a; Liu et al., 2022c; Mok and Chung, 2022c; Dey et al., 2022; Chen et al., 2022c; Mok and Chung, 2020a; Jia et al., 2021; Wu et al., 2022b). For a 3D transformation $T(x, y, z) = [T_x, T_y, T_z]$, the Jacobian is defined as

$$J = \begin{vmatrix} \frac{\partial T_x}{\partial x} & \frac{\partial T_x}{\partial y} & \frac{\partial T_x}{\partial z} \\ \frac{\partial T_y}{\partial x} & \frac{\partial T_y}{\partial y} & \frac{\partial T_y}{\partial z} \\ \frac{\partial T_z}{\partial x} & \frac{\partial T_z}{\partial y} & \frac{\partial T_z}{\partial z} \end{vmatrix}. \tag{25}$$

Ashburner et al. (1999) considered the transformations to be locally affine, and the Jacobian determinant could be computed using singular value decomposition. More generally, the Jacobian of a dense nonlinear transformation is estimated through numerical approximation using finite difference methods. In a recent study, Liu et al. (2022b) showed that when approximating the Jacobian using forward or backward difference, it is implicitly assumed that the digital transformations are linearly interpolated on a tetrahedra mesh grid. They

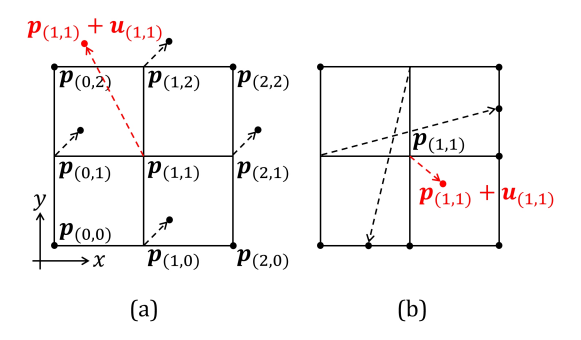


Fig. 11. Examples of the checkerboard problem (a) and the self-intersection problem (b) for the central difference approximated Jacobian determinant |J| on a 3×3 grid. The transformations are visualized as a displacement field and the displacement of the center pixel is highlighted in red. In (a), the central difference approximated |J| for the center pixel equals one but the displacement of the center pixel is *not* involved in the computation. Even if the center pixel moves outside the field of view, the central difference approximated |J| still equals one. In (b), the transformation around the center pixel already introduced folding in space regardless of the displacement of the center pixel but the central difference approximated |J| is positive.

found that the Jacobian determinant, when approximated using central difference, exhibits checkerboard and self-intersection problems. Consequently, it consistently underestimates nondiffeomorphic spaces in a transformation. In Fig. 4 of Liu et al. (2022b), the authors show examples of the checkerboard problem and the self-intersection problem in 2D. In both cases, the central difference approximated Jacobian determinants are positive, but the underlying transformations introduce folding of space (under the assumption that the digital transformations are piecewise linear). To address these issues. Liu et al. (2022b) proposed the non-diffeomorphic volume measurement, which uses a combination of forward and backward differences to measure the folding implied by a displacement field based on the volume of folded tetrahedra in the mesh grid. Importantly, Liu et al. (2022b) showed that the Jacobian determinant, when approximated using central difference, results in the checkerboard and self-intersection problems. Consequently, it consistently underestimates non-diffeomorphic spaces. Figure 11 shows examples of the checkerboard problem and the self-intersection problem in 2D. In both cases, the central difference approximated Jacobian determinants are positive, but the underlying transformations introduce folding of space (under the assumption that the digital transformations are piecewise linear). They conclude that for a 2D transformation, four unique finite difference approximations of |J|'s must be positive to ensure the entire domain is invertible and free of folding; in 3D, ten unique finite differences approximations of |J|'s are required to be positive. Note that their method is closely related to simplex counting (Holland et al., 2011) used in deformation-based volumetric change estimation. Because of the issues associated with central difference approximation of |J|'s, Liu et al. (2022b) recommend using non-diffeomorphic volume to accurately reflect the non-diffeomorphism introduced by transformations.

The logarithm of the Jacobian determinant is also an important measure, especially for applications where it requires the volume of the underlying anatomy to be preserved (Rohlfing et al., 2003a; Jian et al., 2022). The logarithm is used to symmetrically weight local expansion and compression (Rohlfing et al., 2003a; Lange et al., 2020). In recent works such as (Hering et al., 2022; Chen et al., 2022b; Dey et al., 2022; Chen et al., 2022c; Song et al., 2022), the standard deviation of the logarithm of the Jacobian determinant has been used to quantify the smoothness of the displacement field. Additionally, the statistical distribution of the logarithm of the Jacobian determinant can be used as a visualization tool to reveal differences between registration algorithms (Leow et al., 2007; Lange et al., 2020).

Similar to many surrogate measures, the regularity of the transformations can detect inaccurate transformations, but by itself, it is insufficient to provide adequate positive evidence for accurate transformations. For example, the identity transformation would be deemed a perfectly regularized transformation, but it would not provide a meaningful registration.

7. Benchmark Datasets for Medical Image Registration

Due to the inherent black-box nature of DL, developing DL models often relies on empirical studies and author-reported evaluations. The reproducibility and replicability of these experiments have been central focuses since the rise of DL, and DL-based registration is no exception. A key method to promote reproducibility is evaluating models on publicly available datasets. To support this effort, we provide a list of benchmark datasets in Table 3 to serve as a reference for the medical image registration community. While segmentation label maps are frequently used as a surrogate measure for registration accuracy, theoretically, any dataset containing segmentation label maps for the same anatomical structures across patients or within the same patient could be used to evaluate registration performance. However, our focus here is specifically on datasets designed for, or have been widely used in, registration tasks. These datasets span anatomies such as the brain, lung, heart, abdomen, and pathological images, each presenting unique challenges.

For brain imaging, the challenge arises from the need for precise alignment of small structures such as the hippocampus, ventricles, and cortical sulci. Additionally, conditions like Alzheimer's disease lead to cortical thinning and atrophy, while tumors cause local and global distortions, making registration complex and requiring both fine and large-scale alignment across and within subjects.

In lung registration, one of the primary challenges is managing the large deformations caused by respiratory motion while also accounting for finer structural changes, such as those in vessels and airways. Evaluation is typically landmark-based, as anatomical label maps of lung structures are often too coarse to precisely measure registration accuracy. However, obtaining high-quality landmarks is both time-consuming and laborintensive.

Cardiac image registration similarly faces the challenge of complex deformations due to both respiratory and cardiac motion. However, a unique difficulty is the limited availability of anatomical landmarks (Makela et al., 2002), as the heart presents fewer distinct features compared to the lungs, complicating both alignment and evaluation.

Part of Learn2Reg 2024 (Dorent et al., 2024), featuring 3 pre-processed

Microscopy

Mitochondria, nuclei

Cell

COMULISglobe 3D-CLEM (Dorent et al., 2024)

nicroscopy datasets with manually annotated landmarks. narmonic generation and bright field pathology images.

101 MRIs affine-aligned to an atlas with 106 manually delineated brain Part of Learn2Reg 2020, 22 subjects with pre-op MRI, and intra-op 3D Part of Learn2Reg 2020, 394 MR scans of the hippocampus region with 50 subjects with manual LV, RV, and Myo segmentations at ED and ES 375 subjects from multiple centers with LV, RV, and Myo segmentations Part of Learn2Reg 2021 (Hering et al., 2022), containing 16 CT/MR Vearly 600 MRI images with cortical and subcortical label maps from prior studies (Liu et al., 2024; Chen et al., 2022b; Hoopes et al., 2022c). art of Learn2Reg 2024 (Dorent et al., 2024), using the OpenBHB dataset (Dufumier et al., 2022); 4,014 MRIs from ten public datasets 40 MRI scans affine-transformed to a common atlas with 50 manually ated using FreeSurfer and SAMSEG, used in Learn2Reg 2021 (Hering 40 training, 20 validation, and 50 testing cases with manual landmarks US with annotated landmarks from EASY-RESECT (Xiao et al., 2017). Part of Learn2Reg 2024 (Dorent et al., 2024), 104 intra-operative US, 20 CTs (COPDgene and 4DCT subsets) with 7,000+ manually paired 100 paired inhale-exhale CTs with lung masks and keypoints; 10 test ual landmarks from vessels and airways for Learn2Reg 2021 (Hering 30 lung CT pairs with 100 manual landmarks for each, covering different lineations for interventional registration in Learn2Reg 2023 (Heinrich 248 paired CTs from seven datasets with 4 billion voxels and 250M 20 cardiac scans (CT and MRI) from 60 subjects with 7 key heart struc-Part of Learn2Reg 2020 (Hering et al., 2022), featuring 50 CT images 355 images with 18 different stains, resulting in 481 valid image regis-416 MRIs from OASIS-1 (Marcus et al., 2007) with label maps gener-18 paired CTs from TCIA-4D-Lung with manual organ and target dekeypoints, providing ground truth displacements and nnUNet segmenta-Part of Learn2Reg 2024 (Dorent et al., 2024), featuring paired secondimages with manual landmarks for Learn2Reg 2022 (Heinrich et al., 30 paired lung CTs with lung masks and keypoints; evaluation with man-38 T1ce, and 67 T2 MRIs from 104 patients, with manual landmarks. ures manually annotated for mono- and multi-modal registration. 4,212 whole-slide-images from 1,152 breast cancer patients. with 13 manually labeled structures from (Xu et al., 2016). landmarks for evaluating deformable registration. at ED and ES phases for intra-patient registration. scan types to evaluate registration methods. across baseline and follow-up scans. phases for intra-patient registration. manually tracings for evaluation. with label maps and landmarks. pairs with 4 labeled structures. delineated brain structures. Table 3. A summary of the publicly available benchmark dataset for medical image registration. Highlights T1w, T2-FLAIR MRI, 3D US T1w, T1ce, T2w, FLAIR MRI Inspiratory, expiratory CT Inspiratory, expiratory CT T1w, T2w MRI, 3D US Breath-hold and 4DCT T1w, T2w, PDw MRI Pathological images Pathological images Pathological images 4D cine-MRI 4D cine-MR CT, CBCT T1w MRI T1w MRI T1w MRI T1w MRI Spiral CT T1w MRI Modality CT, MRI CT, MR CJ CJ Non-affective psychosis Cancer tissue samples Cancer tissue samples Alzheimer's disease Healthy Controls Healthy Controls Healthy Controls Healthy Controls Healthy Controls Healthy Controls **Cumor** resection Cardiac diseases Cardiac diseases Cardiac diseases Cancer Patients Cancer Patients Cancer Patients COPD, cancer Breast Cancer Cohort Type Smokers Glioma Glioma Mixed Breast / Pancreas Body-wide Abdomen Abdomen Anatomy Lung Breast Brain Brain Brain Brain Brain Brain Lung Brain Brain Brain Lung Lung Lung Heart Heart Heart Lung OASIS (Marcus et al., 2007; Hoopes et al., 2022b) COMULISglobe SHG-BF (Dorent et al., 2024) Mindboggle (Klein and Tourville, 2012) Hippocampus-MR (Hering et al., 2022) Abdomen-MR-CT (Hering et al., 2022) Abdomen-CT-CT (Hering et al., 2022) DIR-Lab (Castillo et al., 2013, 2009a) ReMIND2Reg (Juvekar et al., 2024) EMPIRE10 (Murphy et al., 2011) Thorax-CBCT (Hugo et al., 2016) Lung250M-4B (Falta et al., 2024) MM-WHS (Zhuang et al., 2019) BraTS-Reg (Baheti et al., 2021) ACROBAT (Weitz et al., 2024) LPBA40 (Shattuck et al., 2008) CuRIOUS (Hering et al., 2022) M&Ms (Campello et al., 2021) ANHIR (Borovec et al., 2020) Lung-CT (Hering et al., 2022) ACDC (Bernard et al., 2018) LUMIR (Dorent et al., 2024) NLST (Team, 2011) Dataset IXIa

a https://brain-development.org/ixi-dataset/

Abdominal registration faces significant challenges due to substantial inter-subject variability in organ size, shape, and appearance, driven by factors such as age, gender, and disease. Soft tissue deformation adds another layer of complexity, constantly altering inter-organ relationships within the same subject (Xu et al., 2016). Compounding these issues, factors like body pose, respiratory cycle, and digestive status cause dynamic shifts in organ positioning. The multimodal nature of abdominal imaging, where anatomical (e.g., CT or MRI) and functional (e.g., PET or SPECT) data are often combined, further intensifies the complexity. Despite the advancements in modern hybrid scanners that perform co-registration, persistent errors remain (Livieratos, 2015; Roy et al., 2015), underscoring the need for continued research in this area.

Pathological image registration also presents distinct challenges. Thin tissue sections, only a few micrometers thick, can deform easily during sample preparation, and parts of the tissue in whole-slide images (WSIs) of the same sample may be absent in other WSIs, particularly if sections are non-consecutive (Weitz et al., 2024). Additionally, tissue appearance can vary significantly depending on the staining method. The complexity of pathological features, combined with the gigapixel resolution of WSIs, demands robust registration methods that provide multi-resolution alignment while accommodating potential topological changes for accurate registration.

While Table 3 lists datasets commonly used for benchmarking registration methods, the advent of automated segmentation tools (e.g., FreeSurfer (Fischl, 2012), SynthSeg (Billot et al., 2023), SLANT (Huo et al., 2019), TotalSegmentator (Wasserthal et al., 2023)) enables researchers to convert raw medical images from open-source platforms such as OpenNeuro (Markiewicz et al., 2021) and the Cancer Imaging Archive (Clark et al., 2013), as well as from large-scale publicly available datasets such as ADNI (Jack Jr et al., 2008), ABIDE (Heinsfeld et al., 2018), and autoPET (Gatidis et al., 2023) into benchmark datasets for image registration methods.

8. Applications of Medical Image Registration

8.1. Atlas Construction

In computational anatomy, atlases have been an essential tool for investigating the variability of human organs across populations and facilitating the segmentation of organs in individual patients. Typically, atlases are constructed through an iterative averaging process (i.e., procrustean averaging (Ma et al., 2008)) using a population of patient images (Allassonnière et al., 2007; Davis et al., 2004; Guimond et al., 2000; Joshi et al., 2004; Ma et al., 2008; Avants et al., 2010). This procedure commences with the registration of images to a common frame of reference, followed by the computation of an average based on the registered images, which serves as the atlas for the current iteration. The iteration cycle continues until convergence has been achieved, resulting in the final atlas. However, these traditional methods tend to blur regions exhibiting high-frequency deformations (Dey et al., 2021). This shortcoming arises from the averaging of intensities when constructing the atlas, which invariably results in the loss of high-frequency

information essential for capturing anatomical details. Note that the sharpness of the atlas directly affects its ability to depict structural details, which then impacts the precision with which structures are aligned within the atlas space. An atlas that is blurry and lacks detail can result in the poor alignment of anatomical structures, particularly the smaller ones, across different subjects.

Recent advancements in learning-based registration have demonstrated significant improvements in the quality of constructed atlases while concurrently expediting the atlas construction process. Dalca et al. (2019a) pioneered the development of a brain atlas within a deep learning framework, in which an initial approximation of the atlas is derived from the mean of the brain images under study. This atlas is then jointly optimized with a registration network, employing the Voxel-Morph architecture to align the atlas with individual patient images. Throughout the training process, both the atlas and the registration network weights are updated. To promote an unbiased atlas and enhance spatial smoothness in the resulting deformation fields, the authors introduce a Gaussian-inspired prior. This prior serves to penalize sharp deformation changes while simultaneously encouraging minimal average deformation across the entire dataset. This strategy resembles the maximum likelihood methods traditionally used in atlas construction, where the atlas is derived from the data by considering it as the mean within a Gaussian model, with the data samples being the deformed images (Glasbey and Mardia, 2001; Joshi et al., 2004; Allassonnière et al., 2007; Ma et al., 2008). Moreover, for an atlas to be considered unbiased, the total/mean deformations from the atlas to all images must sum to zero. This principle applies both in the context of small deformations (Allassonnière et al., 2007; Guimond et al., 2000; Bhatia et al., 2004), where linear averaging is applicable, and in large deformation settings (Joshi et al., 2004; Avants and Gee, 2004; Ma et al., 2008), where averaging extends to more general metric spaces, such as geodesics. In essence, the problem of constructing an unbiased atlas is to estimate an image that requires the least deformation to closely match each of the input images. The prior introduced by (Dalca et al., 2019a) is therefore specifically designed to ensure that the mean deformation approaches an identity, with the mean deformation being calculated through a moving average in their implementation. Moreover, patient demographic information is conditioned into the network architecture, facilitating the generation of conditional atlases that vary according to the specific attributes of different individuals. This work has inspired a variety of applications. For instance, Cheng et al. (2020b) establish continuous spatio-temporal cortical surface atlases for neonatal brains. Similarly, both Zhao et al. (2021b) and Bastiaansen et al. (2022b) construct continuous spatio-temporal atlases for fetal and infant brains. Zhao et al. developed a multiscale spherical registration network featuring group-wise registration, while Bastiaansen et al. applied group-wise registration to volumetric ultrasound images. Alternatively, Yu et al. (2020a) constructed an unconditional and universal atlas while incorporating demographic information into the displacement field generation. This approach explicitly models morphological changes related to attributes as a diffeomorphic deformation, which captures variations in shape and size. Recognizing that the necessity for images to be affinely aligned in a preprocessing step as suggested in (Dalca et al., 2019a) could not adequately capture the dynamic size and shape development of fetal brain structures, Chen et al. (2021c) proposed incorporating an affine network, conditioned on patient demographic data, to register the constructed atlas to individual patient images. This approach preserves the dynamic size and shape variations of patients at different ages. Li et al. (2021) proposed integrating the segmentation produced by a segmentation network into the atlas construction method proposed in (Dalca et al., 2019a). This method enables the joint training of segmentation and registration networks while simultaneously constructing both image and segmentation atlases. Similarly, Sinclair et al. (2022) embraced the concept of jointly training segmentation and registration networks. They were motivated by the observation that segmentation networks often yield spurious voxel-wise predictions. By warping the label map of the constructed atlas to match the segmentation prediction through learning-based diffeomorphic registration, the topology of the original anatomical structure can be preserved, thus avoiding the potential segmentation errors produced by the segmentation network. Drawing inspiration from Dalca et al. (2019a) and Shu et al. (2018), Siebert et al. (2021c) proposed using a shared encoder to extract features from input images, followed by two decoders. One decoder generates an unconditional atlas, while the other produces deformation fields that warp the atlas to individual images. To improve registration performance and enforce unbiased atlas construction, they introduced an inverse consistency and a bias reduction loss, in addition to the commonly seen similarity measure and deformation regularizer. In a related study, Wu et al. (2022a) proposed a closed-form update for constructing the atlas by leveraging pre-trained registration networks as a priori knowledge of the deformation field. Their approach involves an alternating update process for both the deformation field, which warps the atlas, and the atlas itself. This method results in an atlas construction framework that is independent of the registration model choice, offering flexibility in its application.

Researchers have explored various strategies to enhance the quality of the constructed atlases. Dey et al. (2021) improved the constructed atlas by incorporating adversarial learning, which improved both the sharpness and centrality of the resulting atlas. In a similar vein, He and Chung (2021) aimed to improve the atlas' sharpness through adversarial learning and by integrating edge information derived from anatomical label maps. Additionally, Pei et al. (2021) leveraged anatomical label maps to improve the quality of the constructed atlas by applying anatomical consistency supervision. However, Ding and Niethammer (2022) contended that the importance of atlas sharpness is secondary to the registration model's ability to align corresponding points between images in the atlas space. Therefore, they focused on the registration model upon which the atlas construction is based and proposed using the constructed atlas as a bridge. In their method, an image is first warped to align with an atlas and then further warped to match the target image using the registration network. This process facilitates a direct comparison between the warped image and the target image while enabling the construction and evaluation of the atlas without requiring segmentation of the atlas itself. Inspired by implicit neural shape representations (Mescheder et al., 2019), Yang et al. (2022a) proposed constructing atlases of anatomical shapes using a continuous occupancy grid instead of representing them in a voxel-based manner. Given the latent representation of the shape, this alternative approach constructs an atlas based on the linear combination of a learned template matrix. Their method offers a novel perspective on atlas representation, diverging from traditional voxel-based representations.

The aforementioned methods for constructing atlases through deep learning predominantly adopt a Bayesian framework (Allassonnière et al., 2007; Ma et al., 2008), in which the atlases are derived as an outcome of the training process using the training dataset. Consequently, these methods do not allow for atlas construction during test-time. To navigate this limitation, group-wise registration methods come into play, allowing for the simultaneous alignment of multiple images to an implicit template. An illustrative example is found in the work of Zhang et al. (2021b), where they introduced a DNN-based group-wise registration framework. This DNN takes in a group of images, aligning them to an implicit template that is represented by the intensity average of the warped images in the group. He et al. (2023) proposed a similar group-wise registration method where the atlas is built using principal component analysis (PCA) rather than an arithmetic mean. Furthermore, constructing an atlas at test-time is not feasible with this method, as the DNN needs the atlas as an input, which undergoes updates throughout the training phase. Other group-wise registration strategies have been introduced for atlas construction during test-time, leveraging variational autoencoders (VAEs) to produce latent vectors from a collection of images. These vectors facilitate the decoupling of the atlas from the images themselves. One technique (Siebert et al., 2021c; Gupta et al., 2021), inspired by deforming autoencoders, uses these latent representations to create the atlas. Another approach proposed in He et al. (2023) constructs the atlas by averaging these latent vectors arithmetically, then employing a registration network to enhance the atlas. This is achieved by adjusting it to more closely align with the images in the group throughout the training process. However, it is important to recognize that these methods are limited by their reliance on the small deformation assumption, where deformations are modeled as the addition between the identity and a dense displacement field, or by adopting a time-stationary velocity framework. Such assumptions can lead to inaccuracies in representing the shape average of the group through intensity averages, which may not align with the geodesic mean in the curved shape space, as highlighted in Joshi et al. (2004) and Avants and Gee (2004).

Advancements in learning-based atlas construction methods have facilitated the fast construction of high-quality atlases. The following subsection explores the application of the atlases and learning-based image registration in achieving the goal of image segmentation.

8.2. Multi-atlas Segmentation

Multi-atlas segmentation is a well-established registrationbased segmentation technique in existence for several decades (Rohlfing et al., 2003b; Iglesias and Sabuncu, 2015). The typical approach involves registering atlas images or their patches to a target image and fusing the propagated atlas labels. For deformable registration-based multi-atlas methods, the process of pairwise registration between atlas images and the target image can be computationally expensive and timeconsuming. However, recent advancements in deep learningbased deformable registration algorithms provide a promising solution to address the speed issue and potentially improve the accuracy of registration, which can subsequently improve the accuracy of multi-atlas segmentation. While many works have explored the use of deep networks to improve the fusion of multiple registered atlas images (Zhu et al., 2020; Fang et al., 2019; Xie et al., 2019, 2023; Yang et al., 2018), there are relatively few studies that incorporate deep learning-based deformable registration algorithms into their pipeline.

Ding et al. (Ding et al., 2019, 2020) proposed VoteNet, which predicts a voxel probability of the agreement between registered atlas images and the segmentation target image. They adopted Quicksilver (Yang et al., 2017) as their registration algorithm to speed up the pairwise registration process. Their followup work (Ding and Niethammer, 2021) experimented with improving the initial registration results from Quicksilver by incorporating a registration refinement step. The results showed that registration accuracy is a critical factor in achieving accurate multi-atlas segmentation. In Ding et al. (2022a), the authors addressed the challenging problem of cross-modality multi-atlas segmentation. They proposed a deep network that learns the bi-directional registration between atlas images and the target image, as well as a second network that estimates the weights for label fusion. To account for the modality differences between the atlas and target images, they used Dice loss as a similarity measure to train their registration network and conditional entropy to train the fusion network. For registering 3D first-trimester ultrasound images, Bastiaansen et al. (2022a) proposed a two-stage network for learning an affine transformation. They then applied the VoxelMorph architecture to perform deformable registration on the affinely aligned images. The segmentation of the target images was achieved by propagating the labels of the atlas images and combining them using majority voting.

The good performance of supervised training in image segmentation could be a reason for the relative lack of research on deep learning-based registration in multi-atlas segmentation. Deep neural networks have demonstrated impressive results in supervised image segmentation tasks, making them a popular choice for many researchers. However, the performance of single atlas segmentation is often used to evaluate the accuracy of a registration algorithm, as discussed in Section 3.5. Due to the close relationship between registration and segmentation, there is an increasing interest in exploring the possibility of integrating the learning of segmentation and registration (Sinclair et al., 2022; Khor et al., 2023; Xu and Niethammer, 2019). Overall, the use of deep learning-based registration in multi-atlas seg-

mentation is still in its early stages, and there is a significant opportunity for further research.

8.3. Uncertainty

Accurate registration is critical for many medical image analysis applications, such as image-guided surgery, radiation therapy, and longitudinal studies. However, registration uncertainty can arise due to factors such as training data artifacts or predictive model variances. To address this issue, incorporating registration uncertainty into medical image analysis can help guide the interpretation of the registration results and improve the reliability of various analysis tasks.

In clinical decision-making, understanding registration uncertainty is critical for image-guided surgery and radiation therapy. The absence of proper registration uncertainty awareness may lead surgeons to presume a substantial registration error throughout the entire region based on a large error in a single location, resulting in the total disregard of registration. Furthermore, the lack of registration uncertainty may also cause surgeons to place unwarranted confidence in regions with inaccurate registration, resulting in potentially severe consequences.

For image-guided surgery, Risholm et al. (2013) showed that the registration uncertainty increased at the site of resection using clinical data from neurosurgery for resection of brain tumors, which demonstrated the potential utility of registration uncertainty in recognizing the surgical regions and guiding surgery. For radiation therapy, Risholm et al. (2011) had previously presented a probabilistic framework to estimate the accumulated radiation dose and corresponding dose uncertainty delivered to significant anatomical structures during radiation therapy, such as the primary tumor and healthy surrounding organs. The uncertainty in the estimated dose directly results from registration uncertainty in the deformation used to align daily cone-beam CT images with planning CT. The accumulated radiation dose is an important metric to monitor during treatment, potentially requiring treatment plan adaptation to conform to the current patient anatomy.

A study by Nenoff et al. (2020) employed six different deformable registration algorithms to analyze dose uncertainty in proton therapy and investigate their impact on dose accumulation for non-small cell lung cancer patients with inter-fractional anatomy variations. The results show that dose degradation caused by anatomical changes was more pronounced than the uncertainty arising from using different deformable image registration algorithms for dose accumulation. However, accumulated dose variations between these algorithms can still be substantial, leading to additional dose uncertainty.

In longitudinal medical image analysis, registration is an essential step because it enables the comparison of measurements taken at different time points, which is necessary for correcting anatomical variability and tracking changes over time. Registration uncertainty estimation can be beneficial for longitudinal image processing tasks, such as image smoothing, segmentation prior propagation, joint label fusion, and others. Simpson et al. (2011) proposed an approach to calculate the deformable registration uncertainty using a probabilistic registration framework, integrating the uncertainty into spatially normalized statistics for adaptive image smoothing. This method

showed improved classification results in longitudinal MR brain images acquired from Alzheimer's Disease Neuroimaging Initiative compared to not smoothing or using a straightforward Gaussian filter kernel.

In summary, incorporating registration uncertainty into medical image registration can facilitate interpreting registration results and improve the reliability of various medical image analysis tasks. It is crucial for clinicians to understand registration uncertainty and its potential applications in clinical decision-making. Further research is needed to explore other potential applications of registration uncertainty.

8.4. Motion Estimation

In the context of medical images, deep learning-based motion estimation has been closely associated with the unsupervised optical flow (Jonschkowski et al., 2020; Stone et al., 2021; Bian et al., 2022) and point tracking (Lai and Xie, 2019; Harley et al., 2022; Ranjan et al., 2019; Bian et al., 2022) techniques within the computer vision domain. However, the application of motion estimation in medical imaging presents unique challenges, including limited training data, heterogeneous patient data for testing, and special desired properties on the motion field, such as diffeomorphism (to preserve anatomical relationships) and incompressibility (to preserve anatomical integrity). Deep learning-based registration has demonstrated successful outcomes in estimating motion for various organs, such as the human heart, brain, lungs, and tongue. Registration-based motion estimation plays a significant role in enabling the assessment of changes in the position, shape, and size of organs over time. Multiple dynamic imaging modalities are used for motion estimation in medical imaging, including but not limited to cine images, tagged-MRI (Axel and Dougherty, 1989a,b), and echocardiography.

Cine images are a temporal sequence of MR images captured in quick succession, allowing for the monitoring of organ movement and deformation over time. Recent research (Qin et al., 2018; Morales et al., 2019; Meng et al., 2022b; Yu et al., 2020c; Qin et al., 2023; López et al., 2023; Yu et al., 2020b) has successfully applied deep learning-based registration techniques to cine images. For example, FOAL (Yu et al., 2020c) proposed online optimization to mitigate distribution mismatch between the training and testing datasets for motion estimation, using meta-learning techniques to enable more efficient online optimization with fewer gradient descent steps and smaller data samples, which differs from instance-specific optimization (Balakrishnan et al., 2019). Yu et al. (2020b) applied similarity and smoothness loss to multiple scales of motion fields (pyramid) using a deep supervision strategy.

The relatively uniform signal within tissues from cine images and the lack of reliable, identifiable landmarks have motivated the exploration of additional regularization methods for estimating motion that is biologically plausible and clinically reliable. For example, Qin *et al.* (Qin et al., 2023) trained a variational autoencoder-based generative model to capture the prior of biomechanically plausible deformations by reconstructing simulated deformations using finite element models. This prior is then used as regularization during the training of the

registration network. Lopez *et al.* (López *et al.*, 2023) incorporated hyperelastic regularization terms into the framework of physics-informed neural networks (Raissi *et al.*, 2019) to estimate incompressible motion fields.

Tagged-MRI, on the other hand, employs a spatially modulated periodic pattern to magnetize tissue temporarily, producing transient tags in the image sequence that move with the tissue and capture motion information. It allows for tracking the motion of inner tissue where the region does not have contrast on cine images. DeepTag (Ye et al., 2021) takes raw 2D tagged images as input and estimates the incremental motion between two consecutive frames using a bi-directional registration network. Then it composes the incremental motion field to estimate motion between any two time frames. Harmonic phase images (Osman et al., 1999) have been found to be more robust to tag fading and imaging artifacts during motion tracking than raw tagged images. DRIMET (Bian et al., 2024b) proposed a simple sinusoidal transformation on the harmonic phase images, enabling end-to-end training for estimating a 3D dense motion field from tagged-MRI. It also incorporates a Jacobian determinant-based loss that penalizes symmetrically for contraction and expansion to estimate a biologically-plaussible incompressible motion field. DRIMET shows promising results in terms of superior registration accuracy, a comparable degree of incompressibility, and faster speed over its traditional iterative-based counterparts (Xing et al., 2017; Mansi et al., 2011). MomentaMorph (Bian et al., 2023) proposed a framework of momenta, shooting, and correction to overcome motion estimation issues in presence of large motion for time-series tagged-MRI. MomentaMorph first accumulates momenta in the tangent space, and then uses exponential mapping for shooting momenta to the group of diffeomorphism to avoid local optima, and finally finds the true optima with a correction step. The resutls show that MomentaMorph produces accuarate, dense, and diffeomorphic motion fields in presence of large motion.

Numerous deep learning-based techniques have been devised to estimate 2D motion, and although this may be adequate for certain applications, tracking dense 3D motion is typically necessary or highly desirable when estimating the motion of biological structures. To address this issue, Meng et al. (Meng et al., 2022b) integrate features extracted from multi-view 2D cine CMR images captured in both short-axis and long-axis planes to learn a 3D motion field of the heart. The edge map of myocardial wall is used as a shape regularization of the estimated motion field. Alternatively, DRIMET (Bian et al., 2024b) uses sparsely acquired tagged images and interpolates them onto an isotropic grid with a resolution based on the inplane resolution. This approach is based on the observation that the tag pattern changes slowly in the through-plane direction and therefore will not cause aliasing issues during sampling. By doing so, DRIMET is capable of tracking dense 3D motion.

Recent studies have shown that joint learning of segmentation and motion estimation can be mutually beneficial (Qin et al., 2018; Ta et al., 2020; Ahn et al., 2020). For instance, Qin et al. (Qin et al., 2018) employ a dual-branch framework consisting of a segmentation branch and a motion estimation branch to simultaneously estimate motion and segmentation

from a sequence of cardiac cine images. During training, a *shared* feature encoder is learned under the premise that joint features can complement both tasks. In contrast, Ta *et al.* (Ta et al., 2020) and Ahn (Ahn et al., 2020) adopt a task-level approach to jointly tackle motion estimation and segmentation in the context of estimating cardiac motion from echocardiography. Specifically, they warp the segmentation (of one time frame) using the estimated motion field and regularize the motion field by incorporating shape information obtained from the segmentation. This approach differs from previous studies which couple motion estimation and segmentation at the feature-level, and may offer a novel perspective on joint learning of these tasks.

In addition to MRIs and echocardiography, numerous deep learning-based algorithms have been developed for motion estimation with 4D-CT (Fu et al., 2020b; Ho et al., 2023; Wolterink et al., 2022; Fechter and Baltas, 2020; Hering et al., 2021; Ji et al., 2022; Liang et al., 2023). 4D-CT imaging captures images at different phases of respiratory or cardiac cycles, providing valuable insights for lung imaging applications, including radiation therapy planning and lung function assessment. DIR-LAB (Castillo et al., 2009b) is a widely-used dataset, containing 4D CT images of ten patients, to evaluate 4D-CT registration techniques, with the aim of registering inspiration images to expiration images. This task is challenging due to the superimposed motion of the heart and lungs, which is larger in scale than the small lung structures being studied.

LungRegNet (Fu et al., 2020b) trains two separate networks to handle large lung motion. One network predicts large motion on a coarse scale, and the other network takes the coarsely warped image and fixed image as input to predict fine motion. In addition to similarity and smoothness losses, an adversarial loss is applied as extra regularization to prevent unrealistic deformed images. Hering et al., (Hering et al., 2021) employs a coarse-to-fine multi-level optimization strategy. The deformations of coarse levels provide an initial guess for subsequent finer levels. Networks are trained progressively, with each handling one level and initialized with parameters from the previous level. It incorporates a penalty for volume change and utilizes an 12 loss function to match corresponding keypoints that are automatically detected. Ho et al., (Ho et al., 2023) applied cycle-consistent training (Kuang, 2019) to reduce foldings using two networks. After the first network's forward pass, the warped and moving images are sent to the second network to predict inverse deformation, with a similarity loss applied to maximize the similarity between the moving images and inversely-deformed moving images. IDIR (Wolterink et al., 2022) use a multi-layer perceptron to represent the transformation function of coordinates and demonstrate the ability to incorporate the Jacobian regularizer, hyperelastic regularizer (Burger et al., 2013), and bending energy (Rueckert et al., 1999) into the framework. The resulting deformation is void of foldings and achieves a mean target registration error (TRE) of 1.07 mm on DIR-LAB datasets. However, this method requires more time compared to CNN-based approaches, prompting researchers to consider acceleration as a potential future direction.

In order to accurately register previously unseen images out-

side of training datasets, the application of one-shot learning has been employed for the estimation of lung motion (Fechter and Baltas, 2020; Ji et al., 2022). Fechter *et al.* (Fechter and Baltas, 2020) concatenated images captured at different phases in the channel dimension in order to leverage temporal information. To minimize memory requirements, they partitioned images into non-overlapping patches and applied a boundary smoothness constraint on the transitions between patches. Additionally, they utilized a coarse-to-fine approach by constructing an image pyramid, where the estimated vector fields of finer scales were added to the upsampled vector fields of coarser scales. The proposed method showed a competitive performance without the need for training in advance.

Despite advancements, current motion estimation techniques in medical imaging face several key challenges. A primary challenge is accurately modeling large organ movement and deformation, such as lung expansion during respiration, tongue deformation during speech, or cardiac motions during the heart-beat cycle. These deformations are nonlinear and complex, making it difficult for algorithms to capture both coarse and fine-scale motions without introducing artifacts or unrealistic distortions.

The second key challenge is the high computational cost associated with capturing dense 3D motion over time, which is essential for a comprehensive understanding of organ dynamics. Transitioning from 2D to 3D significantly increases computational and memory requirements, especially when temporal information (more than two frames) needs to be considered. Incorporating biomechanical constraints like diffeomorphism and incompressibility into models further adds to the computational complexity, as these require sophisticated regularization and may involve iterative optimization processes, limiting their applicability in time-sensitive clinical settings. Approaches like integrating multi-view 2D data to infer 3D motion (Meng et al., 2022b) and incrementally accumulating neighboring motions (Bian et al., 2023) have been explored, but efficient and accurate 3D motion estimation over time remains an open problem. Accelerating these algorithms without sacrificing accuracy is an ongoing research endeavor.

The third challenge arises when image intensity or contrast changes over time, which disrupt traditional photometric consistency assumptions. For example, in tagged MRI, the contrast diminishes due to the process reaching steady-state and T1 relaxation, which makes widely-used image similarity losses, such as MSE, NCC, NGF, MI, and MIND, less effective at accurately tracking deforming tissue throughout the entire sequence (Bian et al., 2024a). Similarly, intraoperative imaging faces challenges due to the application of dyes and changes in lighting conditions (Alam et al., 2018), and the alignment in imaging-guided radiation therapy is complicated by tissue responses to radiation that can alter image intensity (Jaffray, 2012). Addressing this challenge may involve a better understanding of the underlying physics to model and compensate for intensity variations. Additionally, borrowing experiences from inter-modality image similarity learning—which are robust to contrast differences—could provide valuable insights.

8.5. 2D-3D Registration

Recent progress in the field of interventional procedures for invasive treatment protocols has been associated with high precision in surgeries performed at a reasonable cost (Pfandler et al., 2019; Dlouhy et al., 2014). In these procedures, 2D-3D registration plays a significant role in determining the spatial relationship between the 3D anatomical structures and 2D images, such as X-Ray fluoroscopic images, ultrasound image frames, or endoscopic images. 2D-3D medical image registration primarily involves registering 2D interventional images to 3D pre-operative CT/MR images, i.e., to obtain the 3D geometric transformation that aligns with the 2D view available. Conventional 2D-3D registration methods involve iterative optimization methods with similarity metrics (Maes et al., 1997) based on image intensity as the objective function. Due to the sparsity of spatial information derived from 2D images, the problem is non-convex, which may lead to convergence at a local minimum if the initial estimate is not sufficiently close to the correct one. 2D-3D registration is a problem with a minimum of six degrees of freedom which may also lead to registration ambiguity as the spatial information along each projection line is compressed to a single point in the 2D plane. This high-dimensional optimization problem increases the difficulty of determining the parameters associated with the depth of anatomical features in the 3D volume. Alternatively, deeplearning-based methods have gained popularity for this application as they do not require explicit functional mappings (Unberath et al., 2021). In this discussion, we briefly highlight recent advancements in 2D-3D registration, while directing interested readers to (Unberath et al., 2021) for a comprehensive review of the influence of various learning-based methods in this area.

Common 2D-3D registration applications and examples include registration of 2D fluoroscopic/angiography images to 3D CT/MR images of pelvic, lung, or brain region (Gu et al., 2020; Liao et al., 2019; Gao et al., 2020b,a; Jaganathan et al., 2023; Huang et al., 2022; Shrestha et al., 2023), registering endoscopy images to CT/MR images (Liu et al., 2020; Bobrow et al., 2023), registering histopathological image to CT (Leroy et al., 2023), and registering 2D ultrasound (US) frames to 3D MR images to facilitate interventional procedures, such as liver tumor ablation (Wei et al., 2021b; Wang et al., 2023c) or prostate cancer biopsy (Guo et al., 2022).

In (Gu et al., 2020; Wei et al., 2021b; Huang et al., 2022), the 2D-3D registration problem was modeled as a regression learning problem where the network is trained to directly predict the desired geometric parameters. These models are trained by completely relying on the data, *i.e.*, it has little to no tie to the actual image formation physics involved. Specifically, in (Gu et al., 2020) a 2D X-Ray image is registered to a 3D CT volume using a ConvNet, which takes the X-Ray image and a digitally reconstructed radiograph (DRR) from the CT volume at some known pose as input. The ConvNet regresses a geodesic loss function over the geometric parameter space to estimate the relative pose between the fixed X-ray image and the DRR from the CT volume without the need for accurate pose initialization. A similar approach is employed in Zhang et al. (2023a), which

enhances the model by simulating patient-specific X-ray images from CT scans for self-supervised learning of X-ray to CT registration. In contrast, Aubert et al. (2022) adopts a GAN-based image-to-image translation method to synthesize X-ray images into DRRs for the registration of spine X-ray images to 3D vertebra models. The registration employs a non-DL-based regression technique to estimate the rigid transformation of the 3D model that produces a DRR most closely resembling the synthesized DRR, as determined by a specific similarity measure.

In (Wei et al., 2021b), Wei et al. propose a two-step registration process to determine the position and orientation of the ultrasound plane in the 3D MR volume data. In the first step, a ResNet-18 network is employed to determine the US probe orientation. Following this, a U-Net is used to regress a weighted dice loss function, which facilitates the determination of the orientation and position of the corresponding XY plane in the resampled 3D MR volume associated with the US frame. In (Huang et al., 2022), Huang et al. also implemented a twostep registration process for aligning 3D MR vessel wall images (VWI) with 2D Digital Subtraction Angiography (DSA) images. This approach encompasses a ConvNet regressor (Miao et al., 2016) that estimates the initial pose, followed by an instance-based centroid alignment, which serves to further minimize parameter estimation errors between the images. Adopting a different two-step method, Haouchine et al. (2023) addresses the registration of preoperative MRI scans to intraoperative RGB images by initially simulating the expected appearances of intraoperative images from various 3D poses of the MRI scan using an image synthesis network. This is followed by employing a regression network to determine the optimal 3D pose that best aligns the simulated 2D image with the intraoperative image. In addition to these two-step methods, Leroy et al. (2023) proposed StructuRegNet for multi-model 2D-3D registration, which used generative model for style transfer between different imaging modalities prior to registration, and used deformable registration after cascaded plane selection for refining the final alignment, especially the out-of-plane distortions.

In Shrestha et al. (2023), Shrestha et al. proposed to regress the scene coordinate with respect to the CT volume directly from the X-ray image using a fully convolutional neural network. The authors applied the camera intrinsic matrix and extrinsic matrix to calculate the back-projection from a pixel on the X-ray to the CT volume, and used that as gound truth in the loss funciton for training the network. The results show that the proposed method performs well under partially visible structure and extreme view points.

As an alternative to formulating registration as a regression problem that necessitates ground truth transformation parameters, several recent studies (Liao et al., 2019; Gao et al., 2020b,a; Jaganathan et al., 2023; Guo et al., 2022) have explored framing it as an unsupervised optimization problem. In such a formulation, the cost function is determined by a similarity metric measured between the transformed and fixed images. Liao *et al.* (Liao et al., 2019) trained a network to track a set of points of interest (POIs) derived from the 3D CT volume in the 2D DRR and in the multi-view fluoroscopic 2D images (used

as fixed images), enabling the network to learn the spatial correspondences between the POIs. In this method, a Siamese U-Net architecture is employed to extract features from the DRRs and fixed images, subsequently tracking the POIs within the extracted features. A triangulation layer is incorporated to pinpoint the locations of the tracked POIs within the fixed image in 3D space. Finally, the geometric transformation between the estimated locations of POIs derived from the fixed image and their true positions is determined analytically. In (Gao et al., 2020b), Gao et al. proposed a novel differential volume rendering transformer network combined with a feature extraction encoder to approximate the image similarity metric in a manner that renders the geometric parameter estimation as a convex problem with respect to the pose parameters.

The examples and applications discussed thus far have primarily focused on rigid 2D-3D registration. However, non-rigid 2D-3D registration is essential in certain applications, such as cephalometry (Li et al., 2020) and lung tumor tracking in radiation therapy (Foote et al., 2019; Dong et al., 2023). Cephalometry, for instance, involves formulating the problem as deformed 2D-3D registration with the objective of generating a 3D volumetric image from a 2D X-ray image using a 3D skull atlas. Li et al. (Li et al., 2020) developed a convolutional encoder that uniquely codes the cephalogram image into a volumetric image. The network is trained by minimizing the NCC between the synthesized DRR originating from the volumetric image and the 2D cephalogram.

Numerous deep learning-based models and metrics have been developed to improve the performance of 2D-3D registration in specific applications, although these methods are specialized and not as versatile as traditional optimization methods. Nonetheless, Machine Learning/Deep Learning has been instrumental in tackling the persistent challenges associated with algorithmic approaches. These techniques have tackled a narrow optimal range of parameters, while also decreasing registration ambiguity. CNN-based approaches are also comparably fast. These factors encourage users to further improve learning-based 2D-3D registration pipeline.

9. Challenges and Future Perspectives

Over the past decade, learning-based registration models have been attracting increasing research interest. As illustrated in the left panel of Fig. 12, there has been a growing trend in developing and applying these models since 2013. Unlike other medical image analysis tasks, such as segmentation or classification, which typically necessitate labor-intensive and timeconsuming manual annotations to develop high-performing models, registration is inherently a self-supervised task. Traditional registration models have predominantly been unsupervised, requiring only moving and fixed images to execute registration. While traditional registration models are typically unsupervised, learning-based registration models initially began as a supervised process, generating ground truth deformation fields using traditional registration methods. However, these supervised models often could not surpass the performance of traditional methods. Instead, they often served

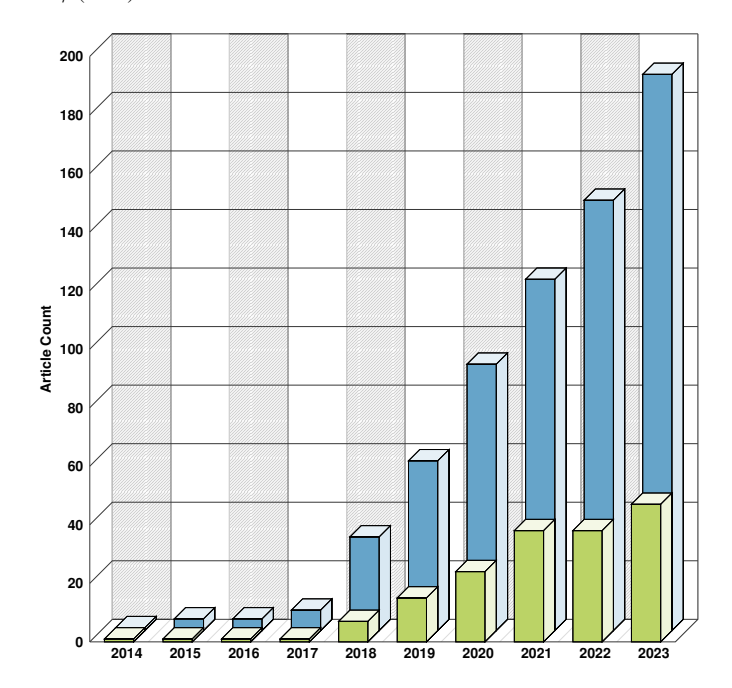


Fig. 12. The figure shows the paper count statistics from PubMed for the years 2014 to 2023. The blue bars represent the count of papers that include keywords related to learning-based image registration in their title or abstract, while the green bars display the count of papers specifically related to unsupervised learning-based image registration.

as an intermediate step to expedite conventional approaches like geodetic shooting (Shen et al., 2019), FLASH (Wang and Zhang, 2020), etc. Despite traditional methods providing appealing deformation properties such as time-dependent diffeomorphic transformations, researchers have recently begun exploring the unsupervised nature of learning-based registration (as seen in the left panel of Fig. 12). By training DNNs using loss functions adapted from traditional methods' objective functions, these methods aim to improve both registration accuracy and speed. Incorporating segmentation and landmark correspondences during training can further enhance registration accuracy, providing capabilities not achievable with traditional methods. Moreover, with a powerful pretrained feature extractor such as self-supervised anatomical embedding (Yan et al., 2022), registration performance can be further improved (Liu et al., 2021a; Li et al., 2023b). Given the rapid progress of deep learning and its growing adoption in medical applications, we anticipate an increasing focus on learning-based medical image registration.

In this section, we provide future perspectives and discuss potential avenues for advancing learning-based medical image registration. Our discussion will focus on the development of registration models, assessment of registration uncertainty, and prospective applications.

9.1. Deep Learning-based Registration Models

9.1.1. Network Architecture

Network architectures employed in image registration occasionally draw inspiration from other image analysis tasks, such as segmentation. For instance, VoxelMorph (Balakrishnan et al., 2019), CycleMorph (Kim et al., 2021), SYMNet (Mok

and Chung, 2020a), and DiffuseMorph (Kim et al., 2022) all borrow U-Net-like architectures, originally developed for image segmentation. In such cases, they often generate deformation fields at a single resolution. In contrast, traditional registration algorithms have demonstrated the benefits of adopting a multi-resolution registration strategy, which decomposes deformations across multiple scales. This method not only improves registration performance but also imparts beneficial deformation properties, such as the ability to enforce larger deformations. This aspect can be particularly beneficial for lung or abdominal organ registration, where organ displacement between scans can be significant. As discussed in section 4.10, there has been a growing interest in integrating multi-resolution strategies into network architecture, and these methods have consistently demonstrated notable performance improvements compared to using a single resolution alone. It is worth noting that this finding has parallels with observations in other image analysis fields, where adopting deep supervision can significantly boost performance (Zhou et al., 2019; Isensee et al., 2021).

The task of image registration is fundamentally distinct from other image processing tasks, as its primary objective is to capture the correspondences between images, with less emphasis on semantic information. In this context, SynthMorph (Hoffmann et al., 2021) demonstrated that training an effective medical image registration network does not necessarily require actual medical images. Instead, random shapes or synthetic images can also be used as training datasets for registration networks. Similarly, Bigalke et al. (2023) introduced a teacherstudent model for unsupervised deformable registration. They also found that at the initial training stage, matching random features can produce reasonable deformation. Given the objective of establishing correspondences, network architectures that incorporate inductive biases focused on this capability may offer significant advantages. Architectures such as Transformers (particularly cross-attention Transformers), contrastive learning, Siamese networks, and correlation layers, which leverage comparisons between moving and fixed images, are of special interest for image registration. We expect to see an increasing number of studies incorporating these designs in the future, along with other advancements in deep learning applied to image registration.

Optical flow estimation, a field closely related to image registration, shares significant conceptual and methodological overlap that has greatly influenced the development of medical image registration methods. Notable examples include the classic Demons algorithm (Thirion, 1998), where the displacementdriven force is derived from an optical flow equation inspired by (Horn and Schunck, 1981; Aggarwal and Nandhakumar, 1988). Another example is the transformation of the variational optical flow energy function into a convex optimization problem through quadratic relaxation (Steinbrücker et al., 2009), which has inspired various medical image registration methods (Heinrich et al., 2013a; Ha et al., 2018) and even recent learning-based approaches (Jia et al., 2021; Li et al., 2023b; Siebert et al., 2021b). The development of FlowNet (Dosovitskiy et al., 2015; Ilg et al., 2017) for learning-based optical flow estimation, which integrates a correlation layer for explicit feature matching, has also influenced various learning-based medical image registration methods (Heinrich, 2019; Siebert and Heinrich, 2022; Siebert et al., 2021b). Moreover, many motion estimation techniques designed for dynamic medical imaging draw from by optical flow methods, as discussed in Section 7.4. As the field of optical flow estimation continues to rapidly evolve, with its distinct perspectives on handling challenges such as large displacements (Weinzaepfel et al., 2013; Ilg et al., 2017) and pretraining strategies (Shi et al., 2023), it is poised to further inspire innovative learning-based registration methods for medical imaging. For readers interested in this intersection, we recommend a recent review article on optical flow by Zhai et al. (2021) for further reading.

9.1.2. Loss Function

In unsupervised models, the image similarity measures predominantly used for mono-modal registration are MSE and NCC, as shown in Table 1. NCC is generally considered a better choice than MSE, as it is locally adaptive and less sensitive to local intensity variations (Avants et al., 2008). For multi-modal registration, MI has historically been the preferred choice (Maes et al., 1997; Wells III et al., 1996). However, to auto-differentiate MI using modern deep learning frameworks for end-to-end training, joint and marginal probabilities are often approximated using the Parzen window. A notable drawback of this approximation is the increased computational burden. In actual implementation, each voxel location expands to include a vector, with the elements in the vector representing the probability of the voxel belonging to each intensity bin. Increasing the number of intensity bins effectively results in an increased channel dimension, ultimately leading to a higher computational burden. Conversely, using a small number of bins often limits the registration performance. Recent learningbased methods have explored surrogates to tackle multi-modal registration problems. For instance, given the advantage of learning, anatomical loss functions like Dice can serve as a modality-independent loss function for training the registration network (Hoffmann et al., 2021). The trained network can then be applied to images without requiring anatomical segmentation, offering an advantage that traditional methods cannot provide. Multi-modal registration can also be addressed using advanced learning methods, such as contrastive learning and adversarial learning, as discussed in sections 4.2 and 4.1. These methods guide the neural network in understanding similarities and dissimilarities between images across different modalities using paired data without requiring explicit multi-modal similarity measures. We expect future research to continue to develop more efficient and innovative approaches to tackle multimodal registration.

Regarding the use of regularization in learning-based deformable registration, there is currently an inadequate emphasis on the development and application of spatially-varying regularization. Despite being a significant area of research historically (Schnabel et al., 2016; Schmah et al., 2013; Vialard and Risser, 2014; Stefanescu et al., 2004; Tang et al., 2010; Pitiot and Guimond, 2008; Gerig et al., 2014; Simpson et al., 2015; Pace et al., 2013; Myronenko and Song, 2010; Papież

et al., 2014; Fu et al., 2018; Risser et al., 2013; Papież et al., 2015), spatially-varying regularization has been largely overshadowed by the rise of learning-based registration, with only a few studies addressing it within a deep learning framework framework (Niethammer et al., 2019; Shen et al., 2019; Chen et al., 2023b, 2021f). As illustrated in Table 1, most methods opt for a simple spatially-invariant regularization, predominantly employing the diffusion regularizer. However, as outlined in section 3.4, spatially-varying regularization provides the advantage of accommodating spatially-varying deformations, preserving discontinuities, and facilitating sliding motion, all of which are essential for a variety of applications. Advancements in modeling spatially-varying regularization within or through deep learning frameworks are eagerly anticipated in the future.

9.2. Registration Uncertainty

Registration uncertainty in medical image analysis is an ongoing challenge and opportunity. On the one hand, advancements in deep learning have the potential to improve registration accuracy and reduce registration uncertainty by extracting features that are robust to noise and other artifacts. On the other hand, uncertainty can be estimated for use in interpreting the registration results and providing valuable information for clinical decision-making.

However, there are several limitations that restrict the further usage of uncertainty estimation in various applications. One significant limitation is the lack of ground truth for evaluating the quality of uncertainty estimation. Without ground truth, it is challenging to validate the accuracy of uncertainty estimation directly. Instead, most existing evaluation methods rely on indirect proofs such as sparsification analysis. This not only affects the reliability of uncertainty estimation, but also limits further developments for better uncertainty estimations. Another limitation is the computational complexity of estimating uncertainty, which can be time-consuming and may limit its usage in real-time clinical applications. Additionally, interpreting uncertainty estimates can be challenging for clinicians, as some statistical measures are not always straightforward. This can limit the adoption of uncertainty estimation in clinical decisionmaking, where clear and concise information is essential for making informed decisions.

To overcome these limitations, it may be helpful to develop improved evaluation methods that rely on direct validation rather than indirect proofs, such as the creation of synthetic data or the use of simulation frameworks where the ground truth is known. This could enhance the accuracy and reliability of uncertainty estimation. Moreover, new computational techniques and algorithms such as incorporating Markov Chain Monte Carlo into a multilevel framework (Schultz et al., 2018) and quantifying image registration uncertainty based on a low dimensional representation of geometric deformations (Wang et al., 2019b) can reduce the computational workload. Last, efforts should be made to provide clinicians with more accessible and intuitive ways to interpret uncertainty estimates, such as visual aids or simpler statistic measures.

In addition to the limitations of uncertainty estimation in

medical image analysis, there are also many potential applications of registration uncertainty that remain unexplored. One promising area of application is atlas-based segmentation, where registration is often used to align an atlas image to a target image for the purpose of segmenting anatomical structures. In this context, registration uncertainty can be used as a criterion for generating a soft segmentation mask, where the probability of each voxel belonging to a particular anatomical structure is weighted by the uncertainty estimate. Another potential application of registration uncertainty is multi-atlas-based segmentation, where multiple atlases are registered to a target image and combined to produce a final segmentation result. In this context, registration uncertainty can be used to weight different segmentation results, producing a more reliable segmentation. This approach could be particularly useful in cases where some atlases are more appropriate for a particular image than others.

Overall, these limitations and potential applications of registration uncertainty in medical image analysis offer an exciting range of opportunities for future research, and it is likely that continued progress in this area will have a substantial impact on the field of medical image analysis and beyond.

9.3. Towards Zero-shot Registration

Classical registration algorithms, while potentially slower, are usually available for immediate use and provide end-users with the flexibility to choose the similarity measure and weighting of regularization terms that best meet their needs. In contrast, deep learning algorithms are susceptible to the domain shift problem, which arises when a trained network struggles to perform well when presented with input images from a different distribution than the training data. Several sources of domain shift can arise in learning-based registration algorithms, such as changes in the input image modality, different populations of subjects, or variations in the direction of registration. To address this challenge, researchers have explored several methods to improve the generalizability of registration networks. For instance, SynthMorph (Hoffmann et al., 2021) uses synthetic images to force the network to learn contrast-invariant features, while HyperMorph (Hoopes et al., 2021) uses a hypernetwork to enable the adjustment of the regularization term during test time. Although these approaches have shown promising results, they have not yet been widely adopted, and further studies and validations are necessary to verify their generalizability and practical usability, particularly with clinical-quality data.

Recent developments in zero-shot learning offer a promising avenue for further improving the generalizability of learning-based registration algorithms. In particular, Foundation models that are pretrained on a broad range of data have shown competitive or even superior zero-shot performance compared to prior supervised models in various tasks (Kirillov et al., 2023; Brown et al., 2020), without requiring specific training data for each new task. Leveraging these techniques can potentially reduce the time and resource requirements for developing deep learning registration algorithms in clinical pipelines, making the existing registration algorithms more accessible and useful to a wider range of users.

9.4. Metamorphic Image Registration

As outlined in Section 2.3, diffeomorphic registration is a bijective mapping that preserves topology. In clinical scenarios, however, registration often involves the deformation of a healthy control or an atlas to fit patient images that may contain tumors or other anomalies. For example, longitudinal scans of the same patient with a tumor may need to be mapped to one another to facilitate the study of the tumor progression or response. Such situations violate the one-to-one mapping assumption of diffeomorphisms due to topological changes between scans. To address this challenge, alternative registration methods such as metamorphic registration models (Brett et al., 2001; Sdika and Pelletier, 2009; Niethammer et al., 2011; Hong et al., 2012; François et al., 2022) have been proposed, which can accommodate changes in topology and appearance. For a mathematical definition of metamorphosis, readers can refer to (Trouvé and Younes, 2005; Younes, 2010). However, these methods often require manual segmentation of the anomalies and are optimization-based, which can be time-consuming and computationally expensive, thereby limiting their practical adoption.

Recently proposed learning-based metamorphic registration methods (Wang et al., 2023b; Liu and Gu, 2023; Han et al., 2020; Bône et al., 2020; Maillard et al., 2022) have been built upon a metamorphic framework (Trouvé and Younes, 2005; Younes, 2010), which adds time-varying intensity variations on top of the diffeomorphic flow, thereby enabling topological changes over time. The registration networks learn to disentangle geometric and appearance changes and sometimes leverage available segmentation to constrain changes within a desired location (e.g., a tumor). With the success of learning-based image segmentation, the time-consuming manual segmentation previously required by classical methods to guide the metamorphosis can now be addressed using segmentation networks. Several recent approaches take advantage of segmentation networks through joint training or by integrating segmentation capabilities directly into the registration network (Han et al., 2020; Liu and Gu, 2023). Alternatively, some studies learn to disentangle appearance and shape changes directly from data without requiring to explicitly define a region (Bône et al., 2020; Maillard et al., 2022). Despite these recent advancements, learningbased metamorphic registration is still in its infancy. Successfully capturing topological changes still greatly depends on the accuracy of the segmentation network. Meanwhile, the effective modeling of time-varying diffeomorphic flow using DNNs continues to be an area of ongoing research. Considering the practical potential of metamorphic registration, metamorphic registration represents an appealing direction for future investigation in learning-based registration research.

9.4.1. Spatial-temporal Image Registration

Learning-based image registration methods have primarily been centered around aligning just one pair of images. Yet, there is a crucial but underexplored need in medical imaging applications: tracking tissue motion across multiple frames. This is particularly relevant in modalities such as tagged/cine MRIs, 4D-CT, and echocardiography.

Addressing the challenge of motion tracking involves overcoming several challenges and taking into account key questions that require careful consideration. For instance, how can one ensure the preservation of desired properties, such as smoothness, diffeomorphism, and incompressibility, throughout temporally long-range tracking? Achieving accurate 4D tracking while maintaining a reasonable computational burden in terms of both temporal and spatial complexity poses another challenge. Moreover, how can varying input frame lengths be effectively managed? These questions demand further exploration and investigation in order to advance our understanding and capability in motion tracking. Encouragingly, recent advancements in computer vision, particularly in the context of natural video, have demonstrated promising results. Methods such as correspondence learning (Jabri et al., 2020; Bian et al., 2022; Zhang et al., 2023b; Araslanov et al., 2021) and spatialtemporal representation learning (Kim et al., 2019; Yao et al., 2020; Wang et al., 2019a; Qian et al., 2021; Dave et al., 2022) may offer valuable insights to tackle these challenges we face. By building upon these recent advancements, we may pave the way for more effective and efficient motion-tracking methods for medical imaging applications.

9.4.2. Spatial Normalization

Spatial normalization is the process of aligning medical images to a common atlas to reduce anatomical variations (Ashburner and Friston, 1999; Friston et al., 1995). This process facilitates voxel-based analysis, allowing for comparisons between individual patients as well as between a patient and a larger population. Additionally, it is useful for mitigating anatomical differences that arise due to factors like motion across various image modalities from the same patient. However, a primary challenge of this approach is achieving accurate registration, often hindered by significant anatomical differences among patients. Moreover, traditionally constructed atlases tend to be of subpar quality, primarily because conventional atlas construction methods usually involve averaging, leading to significant blurring of anatomical features. However, as discussed in section 8.1, deep learning is currently playing a transformative role. It is not only accelerating the atlas construction process but also significantly enhancing the quality of the atlases in aspects like contrast and sharpness. Historically, atlases have been largely used in brain research owing to the comparatively smaller anatomical differences among patients. But with the advancements introduced by deep learning, combined with learning-based registration models, there is potential to broaden their application beyond just the brain to include other body parts. Such an expansion can be invaluable in various medical imaging applications, from cancer treatment planning and monitoring tumor progression or therapy response, to the creation of patient-specific digital twins.

10. Conclusion

In this survey, we presented a thorough examination of deep learning for medical image registration. In contrast to existing review papers, which might not fully capture the most recent advancements and tend to be systematic in nature with a limited focus on technical aspects, our comprehensive survey analyzed over 250 papers with an emphasis on the most recent technological advancements. Beginning with a review of the fundamentals of learning-based image registration, our investigation incorporated widely-used and novel loss functions, as well as network architectures for image registration. We also thoroughly investigated the estimation methods of registration uncertainty and appropriate metrics of registration accuracy and regularity. Furthermore, we provided insights into potential clinical applications, future perspectives, and challenges, aiming to guide future research in this rapidly evolving field.

Acknowledgments

Junyu Chen and Yong Du were supported by grants from the National Institutes of Health (NIH), United States, U01-CA140204 (PI: Y. Du), R01-EB031023 (PI: Y. Du), and U01-EB031798 (PI: G. Sgouros). Yihao Liu, Shuwen Wei, Zhangxing Bian, Aaron Carass, and Jerry L. Prince were supported by the NIH from National Eye Institute grants R01-EY024655 (PI: J.L. Prince) and R01-EY032284 (PI: J.L. Prince), as well as the National Science Foundation grant 1819326 (Co-PI: S. Scott, Co-PI: A. Carass). This work was also made possible by a 2023 Johns Hopkins Discovery grant (Co-PI: J. Chen, Co-PI: A. Carass). The authors thank Lianrui Zuo for valuable discussions and insights.

The views expressed in written conference materials or publications and by speakers and moderators do not necessarily reflect the official policies of the NIH; nor does mention by trade names, commercial practices, or organizations imply endorsement by the U.S. Government.

References

- Aggarwal, J., Nandhakumar, N., 1988. On the computation of motion from sequences of images-a review. Proceedings of the IEEE 76, 917–935.
- Ahn, S.S., Ta, K., Lu, A., Stendahl, J.C., Sinusas, A.J., Duncan, J.S., 2020. Unsupervised motion tracking of left ventricle in echocardiography, in: Medical imaging 2020: Ultrasonic imaging and tomography, SPIE. pp. 196–202.
- Alam, F., Rahman, S.U., Ullah, S., Gulati, K., 2018. Medical image registration in image guided surgery: Issues, challenges and research opportunities. Biocybernetics and Biomedical Engineering 38, 71–89.
- Aljabar, P., Heckemann, R.A., Hammers, A., Hajnal, J.V., Rueckert, D., 2009. Multi-atlas based segmentation of brain images: atlas selection and its effect on accuracy. NeuroImage 46, 726–738.
- Allassonnière, S., Amit, Y., Trouvé, A., 2007. Towards a coherent statistical framework for dense deformable template estimation. Journal of the Royal Statistical Society: Series B (Statistical Methodology) 69, 3–29.
- Araslanov, N., Schaub-Meyer, S., Roth, S., 2021. Dense unsupervised learning for video segmentation. Advances in Neural Information Processing Systems 34, 25308–25319.
- Arsigny, V., Commowick, O., Pennec, X., Ayache, N., 2006. A log-euclidean framework for statistics on diffeomorphisms, in: 9th International Conference on Medical Image Computing and Computer Assisted Intervention (MICCAI 2006), Springer. pp. 924–931.
- Ashburner, J., 2007. A fast diffeomorphic image registration algorithm. NeuroImage 38, 95–113.
- Ashburner, J., Andersson, J.L., Friston, K.J., 1999. High-dimensional image registration using symmetric priors. NeuroImage 9, 619–628.
- Ashburner, J., Friston, K.J., 1999. Nonlinear spatial normalization using basis functions. Human Brain Mapping 7, 254–266.

- Aubert, B., Cresson, T., de Guise, J.A., Vazquez, C., 2022. X-ray to drr images translation for efficient multiple objects similarity measures in deformable model 3d/2d registration. IEEE Trans. Med. Imag. 42, 897–909.
- Avants, B., Gee, J.C., 2004. Geodesic estimation for large deformation anatomical shape averaging and interpolation. Neuroimage 23, S139–S150.
- Avants, B.B., Epstein, C.L., Grossman, M., Gee, J.C., 2008. Symmetric diffeomorphic image registration with cross-correlation: Evaluating automated labeling of elderly and neurodegenerative brain. Medical Image Analysis 12, 26–41.
- Avants, B.B., Yushkevich, P., Pluta, J., Minkoff, D., Korczykowski, M., Detre, J., Gee, J.C., 2010. The optimal template effect in hippocampus studies of diseased populations. NeuroImage 49, 2457–2466.
- Axel, L., Dougherty, L., 1989a. Heart wall motion: Improved method of spatial modulation of magnetization for MR imaging. Radiology 172, 349–350.
- Axel, L., Dougherty, L., 1989b. MR imaging of motion with spatial modulation of magnetization. Radiology 171, 841–845.
- Ayyalusamy, A., Vellaiyan, S., Subramanian, S., Satpathy, S., 2021. Performance of a deformable image registration algorithm for CT and cone beam CT using physical multi-density geometric and digital anatomic phantoms. La Radiologia Medica 126, 106–116.
- Baheti, B., Waldmannstetter, D., Chakrabarty, S., Akbari, H., Bilello, M., Wiestler, B., Schwarting, J., Calabrese, E., Rudie, J., Abidi, S., et al., 2021. The brain tumor sequence registration challenge: establishing correspondence between pre-operative and follow-up mri scans of diffuse glioma patients. arXiv preprint arXiv:2112.06979.
- Balakrishnan, G., Zhao, A., Sabuncu, M.R., Guttag, J., Dalca, A.V., 2019. VoxelMorph: A learning framework for deformable medical image registration. IEEE Trans. Med. Imag. 38, 1788–1800.
- Bastiaansen, W.A., Rousian, M., Steegers-Theunissen, R.P., Niessen, W.J., Koning, A.H., Klein, S., 2022a. Multi-atlas segmentation and spatial alignment of the human embryo in first trimester 3D ultrasound. Machine Learning for Biomedical Imaging 1, 1–31. URL: https://melba-journal.org/2022:020, doi:https://doi.org/10.59275/j.melba.2022-cb15.
- Bastiaansen, W.A., Rousian, M., Steegers-Theunissen, R.P., Niessen, W.J., Koning, A.H., Klein, S., 2022b. Towards a 4D Spatio-Temporal Atlas of the Embryonic and Fetal Brain Using a Deep Learning Approach for Groupwise Image Registration, in: Biomedical Image Registration: 10th International Workshop, WBIR 2022, Munich, Germany, July 10–12, 2022, Proceedings, Springer. pp. 29–34.
- Bauer, D.F., Russ, T., Waldkirch, B.I., Tönnes, C., Segars, W.P., Schad, L.R., Zöllner, F.G., Golla, A.K., 2021. Generation of annotated multimodal ground truth datasets for abdominal medical image registration. International journal of computer assisted radiology and surgery 16, 1277–1285.
- Baum, Z.M., Hu, Y., Barratt, D.C., 2022. Meta-learning initializations for interactive medical image registration. IEEE Trans. Med. Imag. 42, 823–833.
- Beg, M.F., Miller, M.I., Trouvé, A., Younes, L., 2005. Computing large deformation metric mappings via geodesic flows of diffeomorphisms. International Journal of Computer Vision 61, 139–157.
- Berg, A., Vandersmissen, E., Wimmer, M., Major, D., Neubauer, T., Lenis, D., Cant, J., Snoeckx, A., Bühler, K., 2023. Employing similarity to highlight differences: On the impact of anatomical assumptions in chest x-ray registration methods. Computers in Biology and Medicine 154, 106543.
- Bernard, O., Lalande, A., Zotti, C., Cervenansky, F., Yang, X., Heng, P.A., Cetin, I., Lekadir, K., Camara, O., Ballester, M.A.G., et al., 2018. Deep learning techniques for automatic mri cardiac multi-structures segmentation and diagnosis: is the problem solved? IEEE transactions on medical imaging 37, 2514–2525.
- Bhatia, K.K., Hajnal, J.V., Puri, B.K., Edwards, A.D., Rueckert, D., 2004. Consistent groupwise non-rigid registration for atlas construction, in: 2004 2nd IEEE International Symposium on Biomedical Imaging: Nano to Macro (IEEE Cat No. 04EX821), IEEE. pp. 908–911.
- Bian, Z., Alshareef, A., Wei, S., Chen, J., Wang, Y., Woo, J., Pham, D.L., Zhuo, J., Carass, A., Prince, J.L., 2024a. Is registering raw tagged-mr enough for strain estimation in the era of deep learning?, in: Medical Imaging 2024: Image Processing, SPIE. pp. 79–85.
- Bian, Z., Jabri, A., Efros, A.A., Owens, A., 2022. Learning pixel trajectories with multiscale contrastive random walks, in: Proceedings of the IEEE/CVF Conference on Computer Vision and Pattern Recognition, pp. 6508–6519.
- Bian, Z., Wei, S., Liu, Y., Chen, J., Zhuo, J., Xing, F., Woo, J., Carass, A., Prince, J.L., 2023. Momentamorph: Unsupervised spatial-temporal registration with momenta, shooting, and correction, in: 26th International Con-

- ference on Medical Image Computing and Computer Assisted Intervention (MICCAI 2023), Springer. pp. 24–34.
- Bian, Z., Xing, F., Yu, J., Shao, M., Liu, Y., Carass, A., Woo, J., Prince, J.L., 2024b. DRIMET: Deep registration-based 3D incompressible motion estimation in Tagged-MRI with application to the tongue, in: Medical Imaging with Deep Learning, pp. 134–150.
- Bierbrier, J., Eskandari, M., Di Giovanni, D.A., Collins, D.L., 2023. Towards Estimating MRI-Ultrasound Registration Error in Image-Guided Neurosurgery. IEEE Transactions on Ultrasonics, Ferroelectrics, and Frequency Control.
- Bierbrier, J., Gueziri, H.E., Collins, D.L., 2022. Estimating medical image registration error and confidence: A taxonomy and scoping review. Medical Image Analysis, 102531.
- Bigalke, A., Hansen, L., Mok, T.C., Heinrich, M.P., 2023. Unsupervised 3D registration through optimization-guided cyclical self-training, in: 26th International Conference on Medical Image Computing and Computer Assisted Intervention (MICCAI 2023), Springer. pp. 677–687.
- Billot, B., Greve, D.N., Puonti, O., Thielscher, A., Van Leemput, K., Fischl, B., Dalca, A.V., Iglesias, J.E., et al., 2023. Synthseg: Segmentation of brain mri scans of any contrast and resolution without retraining. Medical image analysis 86, 102789.
- Blendowski, M., Bouteldja, N., Heinrich, M.P., 2020. Multimodal 3D medical image registration guided by shape encoder–decoder networks. International journal of computer assisted radiology and surgery 15, 269–276.
- Blendowski, M., Hansen, L., Heinrich, M.P., 2021. Weakly-supervised learning of multi-modal features for regularised iterative descent in 3D image registration. Medical Image Analysis 67, 101822.
- Bobrow, T.L., Golhar, M., Vijayan, R., Akshintala, V.S., Garcia, J.R., Durr, N.J., 2023. Colonoscopy 3D Video Dataset with Paired Depth from 2D-3D Registration. Medical Image Analysis 90, 102956.
- Bône, A., Vernhet, P., Colliot, O., Durrleman, S., 2020. Learning joint shape and appearance representations with metamorphic auto-encoders, in: 23rd International Conference on Medical Image Computing and Computer Assisted Intervention (MICCAI 2020), Springer. pp. 202–211.
- Borovec, J., Kybic, J., Arganda-Carreras, I., Sorokin, D.V., Bueno, G., Khvostikov, A.V., Bakas, S., Chang, E.I.C., Heldmann, S., Kartasalo, K., Latonen, L., Lotz, J., et al., 2020. ANHIR: Automatic Non-Rigid Histological Image Registration Challenge. IEEE Trans. Med. Imag. 39, 3042–3052.
- Brett, M., Leff, A.P., Rorden, C., Ashburner, J., 2001. Spatial normalization of brain images with focal lesions using cost function masking. NeuroImage 14, 486–500.
- Brown, T., Mann, B., Ryder, N., Subbiah, M., Kaplan, J.D., Dhariwal, P., Nee-lakantan, A., Shyam, P., Sastry, G., Askell, A., et al., 2020. Language models are few-shot learners. Advances in Neural Information Processing Systems 33, 1877–1901.
- Burger, M., Modersitzki, J., Ruthotto, L., 2013. A hyperelastic regularization energy for image registration. SIAM Journal on Scientific Computing 35, B132–B148.
- Byra, M., Poon, C., Shimogori, T., Skibbe, H., 2023. Implicit neural representations for joint decomposition and registration of gene expression images in the marmoset brain, in: 26th International Conference on Medical Image Computing and Computer Assisted Intervention (MICCAI 2023), Springer. pp. 645–654.
- Cabezas, M., Oliver, A., Lladó, X., Freixenet, J., Cuadra, M.B., 2011. A review of atlas-based segmentation for magnetic resonance brain images. Computer Methods and Programs in Biomedicine 104, e158–e177.
- Cachier, P., Pennec, X., 2000. 3D non-rigid registration by gradient descent on a Gaussian-windowed similarity measure using convolutions, in: Proceedings IEEE Workshop on Mathematical Methods in Biomedical Image Analysis. MMBIA-2000 (Cat. No.PR00737), pp. 182–189.
- Campello, V.M., Gkontra, P., Izquierdo, C., Martin-Isla, C., Sojoudi, A., Full, P.M., Maier-Hein, K., Zhang, Y., He, Z., Ma, J., et al., 2021. Multi-centre, multi-vendor and multi-disease cardiac segmentation: the m&ms challenge. IEEE Transactions on Medical Imaging 40, 3543–3554.
- Cao, X., Yang, J., Zhang, J., Nie, D., Kim, M., Wang, Q., Shen, D., 2017. Deformable image registration based on similarity-steered cnn regression, in: 20th International Conference on Medical Image Computing and Computer Assisted Intervention (MICCAI 2017), Springer. pp. 300–308.
- Carion, N., Massa, F., Synnaeve, G., Usunier, N., Kirillov, A., Zagoruyko, S., 2020. End-to-end object detection with transformers, in: Computer Vision–ECCV 2020: 16th European Conference, Glasgow, UK, August 23–28, 2020, Proceedings, Part I 16, Springer. pp. 213–229.

- Casamitjana, A., Mancini, M., Iglesias, J.E., 2021. Synth-by-reg (sbr): Contrastive learning for synthesis-based registration of paired images, in: Simulation and Synthesis in Medical Imaging: 6th International Workshop, SASHIMI 2021, Held in Conjunction with MICCAI 2021, Strasbourg, France, September 27, 2021, Proceedings 6, Springer. pp. 44–54.
- Castillo, E., Castillo, R., Martinez, J., Shenoy, M., Guerrero, T., 2009a. Four-dimensional deformable image registration using trajectory modeling. Physics in Medicine & Biology 55, 305.
- Castillo, R., Castillo, E., Fuentes, D., Ahmad, M., Wood, A.M., Ludwig, M.S., Guerrero, T., 2013. A reference dataset for deformable image registration spatial accuracy evaluation using the copdgene study archive. Physics in Medicine & Biology 58, 2861.
- Castillo, R., Castillo, E., Guerra, R., Johnson, V.E., McPhail, T., Garg, A.K., Guerrero, T., 2009b. A framework for evaluation of deformable image registration spatial accuracy using large landmark point sets. Physics in Medicine & Biology 54, 1849.
- Chambolle, A., 2004. An algorithm for total variation minimization and applications. Journal of Mathematical imaging and vision 20, 89–97.
- Che, T., Wang, X., Zhao, K., Zhao, Y., Zeng, D., Li, Q., Zheng, Y., Yang, N., Wang, J., Li, S., 2023. AMNet: Adaptive multi-level network for deformable registration of 3D brain MR images. Medical Image Analysis 85, 102740.
- Chen, C.F.R., Fan, Q., Panda, R., 2021a. Crossvit: Cross-attention multi-scale vision transformer for image classification, in: Proceedings of the IEEE/CVF Conference on Computer Vision and Pattern Recognition, pp. 357–366.
- Chen, J., Frey, E.C., Du, Y., 2022a. Unsupervised Learning of Diffeomorphic Image Registration via TransMorph, in: Biomedical Image Registration: 10th International Workshop, WBIR 2022, Munich, Germany, July 10–12, 2022, Proceedings, Springer. pp. 96–102.
- Chen, J., Frey, E.C., He, Y., Segars, W.P., Li, Y., Du, Y., 2022b. Transmorph: Transformer for unsupervised medical image registration. Medical Image Analysis 82, 102615.
- Chen, J., He, Y., Frey, E., Li, Y., Du, Y., 2021b. Vit-v-net: Vision transformer for unsupervised volumetric medical image registration, in: Medical Imaging with Deep Learning.
- Chen, J., Li, Y., Du, Y., Frey, E.C., 2020. Generating anthropomorphic phantoms using fully unsupervised deformable image registration with convolutional neural networks. Med. Phys. 47, 6366–6380.
- Chen, J., Liu, Y., He, Y., Du, Y., 2023a. Deformable cross-attention transformer for medical image registration, in: International Workshop on Machine Learning in Medical Imaging, pp. 115–125.
- Chen, J., Liu, Y., He, Y., Du, Y., 2023b. Spatially-varying Regularization with Conditional Transformer for Unsupervised Image Registration. arXiv preprint arXiv:2303.06168.
- Chen, J., Liu, Y., Wei, S., Bian, Z., Carass, A., Du, Y., 2024. From registration uncertainty to segmentation uncertainty, in: 21th International Symposium on Biomedical Imaging (ISBI 2024).
- Chen, J., Lu, D., Zhang, Y., Wei, D., Ning, M., Shi, X., Xu, Z., Zheng, Y., 2022c. Deformer: Towards displacement field learning for unsupervised medical image registration, in: 25th International Conference on Medical Image Computing and Computer Assisted Intervention (MICCAI 2022), Springer. pp. 141–151.
- Chen, L., Wu, Z., Hu, D., Pei, Y., Zhao, F., Sun, Y., Wang, Y., Lin, W., Wang, L., Li, G., et al., 2021c. Construction of longitudinally consistent 4D infant cerebellum atlases based on deep learning, in: 24th International Conference on Medical Image Computing and Computer Assisted Intervention (MIC-CAI 2021), Springer. pp. 139–149.
- Chen, R.T., Rubanova, Y., Bettencourt, J., Duvenaud, D.K., 2018. Neural ordinary differential equations. Advances in Neural Information Processing Systems 31.
- Chen, X., Diaz-Pinto, A., Ravikumar, N., Frangi, A.F., 2021d. Deep learning in medical image registration. Progress in Biomedical Engineering 3, 012003.
- Chen, X., Meng, Y., Zhao, Y., Williams, R., Vallabhaneni, S.R., Zheng, Y., 2021e. Learning unsupervised parameter-specific affine transformation for medical images registration, in: 24th International Conference on Medical Image Computing and Computer Assisted Intervention (MICCAI 2021), Springer. pp. 24–34.
- Chen, X., Xia, Y., Ravikumar, N., Frangi, A.F., 2021f. A deep discontinuity-preserving image registration network, in: 24th International Conference on Medical Image Computing and Computer Assisted Intervention (MIC-CAI 2021), Springer. pp. 46–55.
- Chen, Z., Zheng, Y., Gee, J.C., 2023c. Transmatch: a transformer-based mul-

- tilevel dual-stream feature matching network for unsupervised deformable image registration. IEEE Trans. Med. Imag. .
- Cheng, J., Dalca, A.V., Fischl, B., Zöllei, L., Alzheimer's Disease Neuroimaging Initiative, et al., 2020a. Cortical surface registration using unsupervised learning. NeuroImage 221, 117161.
- Cheng, J., Dalca, A.V., Zöllei, L., 2020b. Unbiased atlas construction for neonatal cortical surfaces via unsupervised learning, in: Medical Ultrasound, and Preterm, Perinatal and Paediatric Image Analysis: First International Workshop, ASMUS 2020, and 5th International Workshop, PIPPI 2020, Held in Conjunction with MICCAI 2020, Lima, Peru, October 4-8, 2020, Proceedings 1, Springer. pp. 334–342.
- Christensen, G.E., Joshi, S.C., Miller, M.I., 1997. Volumetric transformation of brain anatomy. IEEE Trans. Med. Imag. 16, 864–877.
- Christensen, G.E., Rabbitt, R.D., Miller, M.I., 1996. Deformable templates using large deformation kinematics. IEEE Trans. Imag. Proc. 5, 1435–1447.
- Clark, K., Vendt, B., Smith, K., Freymann, J., Kirby, J., Koppel, P., Moore, S., Phillips, S., Maffitt, D., Pringle, M., et al., 2013. The cancer imaging archive (tcia): maintaining and operating a public information repository. Journal of digital imaging 26, 1045–1057.
- Croquet, B., Christiaens, D., Weinberg, S.M., Bronstein, M., Vandermeulen, D., Claes, P., 2021. Unsupervised diffeomorphic surface registration and non-linear modelling, in: Medical Image Computing and Computer Assisted Intervention–MICCAI 2021: 24th International Conference, Strasbourg, France, September 27–October 1, 2021, Proceedings, Part IV 24, Springer. pp. 118–128.
- Crum, W.R., Camara, O., Hawkes, D.J., 2007. Methods for inverting dense displacement fields: Evaluation in brain image registration, in: 10th International Conference on Medical Image Computing and Computer Assisted Intervention (MICCAI 2007), Springer. pp. 900–907.
- Czolbe, S., Krause, O., Feragen, A., 2021. Semantic similarity metrics for learned image registration, in: Medical Imaging with Deep Learning, PMLR. pp. 105–118.
- Czolbe, S., Pegios, P., Krause, O., Feragen, A., 2023. Semantic similarity metrics for image registration. Medical Image Analysis 87, 102830.
- Dalca, A., Rakic, M., Guttag, J., Sabuncu, M., 2019a. Learning conditional deformable templates with convolutional networks. Advances in Neural Information Processing Systems 32.
- Dalca, A.V., Balakrishnan, G., Guttag, J., Sabuncu, M.R., 2019b. Unsupervised learning of probabilistic diffeomorphic registration for images and surfaces. Medical Image Analysis 57, 226–236.
- Dave, I., Gupta, R., Rizve, M.N., Shah, M., 2022. Tclr: Temporal contrastive learning for video representation. Computer Vision and Image Understanding 219, 103406.
- Davis, B., Lorenzen, P., Joshi, S.C., 2004. Large deformation minimum mean squared error template estimation for computational anatomy., in: 2nd International Symposium on Biomedical Imaging (ISBI 2004), pp. 173–176.
- De Vos, B.D., Berendsen, F.F., Viergever, M.A., Sokooti, H., Staring, M., Išgum, I., 2019. A deep learning framework for unsupervised affine and deformable image registration. Medical Image Analysis 52, 128–143.
- De Vos, B.D., Berendsen, F.F., Viergever, M.A., Staring, M., Išgum, I., 2017. End-to-end unsupervised deformable image registration with a convolutional neural network, in: Deep Learning in Medical Image Analysis and Multimodal Learning for Clinical Decision Support: Third International Workshop, DLMIA 2017, and 7th International Workshop, ML-CDS 2017, Held in Conjunction with MICCAI 2017, Québec City, QC, Canada, September 14, Proceedings 3, Springer. pp. 204–212.
- De Vos, B.D., van der Velden, B.H., Sander, J., Gilhuijs, K.G., Staring, M., Išgum, I., 2020. Mutual information for unsupervised deep learning image registration, in: Medical Imaging 2020: Image Processing, SPIE. pp. 155– 161.
- Dey, N., Ren, M., Dalca, A.V., Gerig, G., 2021. Generative adversarial registration for improved conditional deformable templates, in: Proceedings of the IEEE/CVF Conference on Computer Vision and Pattern Recognition, pp. 3929–3941.
- Dey, N., Schlemper, J., Salehi, S.S.M., Zhou, B., Gerig, G., Sofka, M., 2022. ContraReg: Contrastive Learning of Multi-modality Unsupervised Deformable Image Registration, in: 25th International Conference on Medical Image Computing and Computer Assisted Intervention (MICCAI 2022), Springer. pp. 66–77.
- Ding, W., Li, L., Zhuang, X., Huang, L., 2022a. Cross-modality multi-atlas segmentation via deep registration and label fusion. IEEE Journal of Biomedical and Health Informatics 26, 3104–3115.

- Ding, X., Zhang, X., Han, J., Ding, G., 2022b. Scaling up your kernels to 31x31: Revisiting large kernel design in cnns, in: Proceedings of the IEEE/CVF Conference on Computer Vision and Pattern Recognition, pp. 11963–11975
- Ding, Z., Han, X., Niethammer, M., 2019. Votenet: A deep learning label fusion method for multi-atlas segmentation, in: 22nd International Conference on Medical Image Computing and Computer Assisted Intervention (MIC-CAI 2019), Springer. pp. 202–210.
- Ding, Z., Han, X., Niethammer, M., 2020. Votenet+: An improved deep learning label fusion method for multi-atlas segmentation, in: 17th International Symposium on Biomedical Imaging (ISBI 2020), IEEE. pp. 363–367.
- Ding, Z., Niethammer, M., 2021. Votenet++: Registration refinement for multiatlas segmentation, in: 18th International Symposium on Biomedical Imaging (ISBI 2021), IEEE. pp. 275–279.
- Ding, Z., Niethammer, M., 2022. Aladdin: Joint atlas building and diffeomorphic registration learning with pairwise alignment, in: Proceedings of the IEEE/CVF Conference on Computer Vision and Pattern Recognition, pp. 20784–20793.
- Dlouhy, B.J., Rao, R.C., Page, P., Julià, D., Gómez, N., Codina-Cazador, A., 2014. Surgical skill and complication rates after bariatric surgery. The New England journal of medicine 370, 285–285.
- Dong, G., Dai, J., Li, N., Zhang, C., He, W., Liu, L., Chan, Y., Li, Y., Xie, Y., Liang, X., 2023. 2D/3D Non-Rigid Image Registration via Two Orthogonal X-ray Projection Images for Lung Tumor Tracking. Bioengineering 10, 144.
- Dong, X., Bao, J., Chen, D., Zhang, W., Yu, N., Yuan, L., Chen, D., Guo, B., 2022. Cswin transformer: A general vision transformer backbone with cross-shaped windows, in: Proceedings of the IEEE/CVF Conference on Computer Vision and Pattern Recognition, pp. 12124–12134.
- Dorent, R., Kapur, T., Wells, S., Golby, A., Heyer, W., Chen, J., Liu, Y., Heinrich, M., Walter, A., Lindblad, J., 2024. Learn2reg 2024. doi:10.5281/zenodo.10991879.
- Dosovitskiy, A., Beyer, L., Kolesnikov, A., Weissenborn, D., Zhai, X., Unterthiner, T., Dehghani, M., Minderer, M., Heigold, G., Gelly, S., Uszkoreit, J., Houlsby, N., 2021a. An image is worth 16x16 words: Transformers for image recognition at scale, in: International Conference on Learning Representations.
- Dosovitskiy, A., Beyer, L., Kolesnikov, A., Weissenborn, D., Zhai, X., Unterthiner, T., Dehghani, M., Minderer, M., Heigold, G., Gelly, S., et al., 2021b. An image is worth 16×16 words: Transformers for image recognition at scale, in: International Conference on Learning Representations.
- Dosovitskiy, A., Fischer, P., Ilg, E., Hausser, P., Hazirbas, C., Golkov, V., Van Der Smagt, P., Cremers, D., Brox, T., 2015. Flownet: Learning optical flow with convolutional networks, in: Proceedings of the IEEE/CVF Conference on Computer Vision and Pattern Recognition, pp. 2758–2766.
- Dou, H., Bi, N., Han, L., Huang, Y., Mann, R., Yang, X., Ni, D., Ravikumar, N., Frangi, A.F., Huang, Y., 2023. GSMorph: Gradient surgery for cine-MRI cardiac deformable registration, in: 26th International Conference on Medical Image Computing and Computer Assisted Intervention (MICCAI 2023), Springer. pp. 613–622.
- Duan, L., Yuan, G., Gong, L., Fu, T., Yang, X., Chen, X., Zheng, J., 2019.
 Adversarial learning for deformable registration of brain MR image using a multi-scale fully convolutional network. Biomedical Signal Processing and Control 53, 101562.
- Dufumier, B., Grigis, A., Victor, J., Ambroise, C., Frouin, V., Duchesnay, E., 2022. Openbhb: a large-scale multi-site brain mri data-set for age prediction and debiasing. NeuroImage 263, 119637.
- Dumoulin, V., Shlens, J., Kudlur, M., 2017. A learned representation for artistic style, in: International Conference on Learning Representations.
- Ehrhardt, J., Werner, R., Schmidt-Richberg, A., Handels, H., 2010. Automatic landmark detection and non-linear landmark-and surface-based registration of lung CT images. Medical Image Analysis for the Clinic-A Grand Challenge, MICCAI 2010, 165–174.
- Elmahdy, M.S., Wolterink, J.M., Sokooti, H., Išgum, I., Staring, M., 2019. Adversarial optimization for joint registration and segmentation in prostate CT radiotherapy, in: 22nd International Conference on Medical Image Computing and Computer Assisted Intervention (MICCAI 2019), Springer. pp. 366–374
- Eppenhof, K.A., Lafarge, M.W., Moeskops, P., Veta, M., Pluim, J.P., 2018. Deformable image registration using convolutional neural networks, in: Medical Imaging 2018: Image Processing, SPIE. pp. 192–197.
- Eppenhof, K.A., Lafarge, M.W., Veta, M., Pluim, J.P., 2019. Progressively trained convolutional neural networks for deformable image registration.

- IEEE Trans. Med. Imag. 39, 1594-1604.
- Eppenhof, K.A., Pluim, J.P., 2018a. Error estimation of deformable image registration of pulmonary CT scans using convolutional neural networks. Journal of Medical Imaging 5, 024003–024003.
- Eppenhof, K.A., Pluim, J.P., 2018b. Pulmonary CT registration through supervised learning with convolutional neural networks. IEEE Trans. Med. Imag. 38, 1097–1105.
- Esser, J.E., 2010. Primal dual algorithms for convex models and applications to image restoration, registration and nonlocal inpainting. University of California, Los Angeles.
- Estienne, T., Vakalopoulou, M., Christodoulidis, S., Battistela, E., Lerousseau, M., Carre, A., Klausner, G., Sun, R., Robert, C., Mougiakakou, S., et al., 2019. U-ReSNet: Ultimate coupling of registration and segmentation with deep nets, in: 22nd International Conference on Medical Image Computing and Computer Assisted Intervention (MICCAI 2019), Springer. pp. 310–319.
- Falta, F., Großbröhmer, C., Hering, A., Bigalke, A., Heinrich, M., 2024. Lung250m-4b: a combined 3d dataset for ct-and point cloud-based intrapatient lung registration. Advances in Neural Information Processing Systems 36.
- Fan, J., Cao, X., Wang, Q., Yap, P.T., Shen, D., 2019a. Adversarial learning for mono-or multi-modal registration. Medical Image Analysis 58, 101545.
- Fan, J., Cao, X., Xue, Z., Yap, P.T., Shen, D., 2018. Adversarial similarity network for evaluating image alignment in deep learning based registration, in: 21st International Conference on Medical Image Computing and Computer Assisted Intervention (MICCAI 2018), Springer. pp. 739–746.
- Fan, J., Cao, X., Yap, P.T., Shen, D., 2019b. Birnet: Brain image registration using dual-supervised fully convolutional networks. Medical Image Analysis 54, 193–206.
- Fang, L., Zhang, L., Nie, D., Cao, X., Rekik, I., Lee, S.W., He, H., Shen, D., 2019. Automatic brain labeling via multi-atlas guided fully convolutional networks. Medical Image Analysis 51, 157–168.
- Fechter, T., Baltas, D., 2020. One-shot learning for deformable medical image registration and periodic motion tracking. IEEE Trans. Med. Imag. 39, 2506–2517.
- Fischer, B., Modersitzki, J., 2003a. Combination of automatic non-rigid and landmark-based registration: the best of both worlds, in: Medical Imaging 2003: Image Processing, SPIE. pp. 1037–1048.
- Fischer, B., Modersitzki, J., 2003b. Curvature based image registration. Journal of Mathematical Imaging and Vision 18, 81–85.
- Fischl, B., 2012. Freesurfer. Neuroimage 62, 774-781.
- Fluck, O., Vetter, C., Wein, W., Kamen, A., Preim, B., Westermann, R., 2011.
 A survey of medical image registration on graphics hardware. Computer Methods and Programs in Biomedicine 104, e45–e57.
- Foote, M.D., Zimmerman, B.E., Sawant, A., Joshi, S.C., 2019. Real-time 2D-3D deformable registration with deep learning and application to lung radiotherapy targeting, in: Information Processing in Medical Imaging: 26th International Conference, IPMI 2019, Hong Kong, China, June 2–7, 2019, Proceedings 26, Springer. pp. 265–276.
- Franceschi, L., Frasconi, P., Salzo, S., Grazzi, R., Pontil, M., 2018. Bilevel programming for hyperparameter optimization and meta-learning, in: 35th International Conference on Machine Learning (ICML 2016), PMLR. pp. 1568–1577.
- François, A., Maillard, M., Oppenheim, C., Pallud, J., Bloch, I., Gori, P., Glaunès, J., 2022. Weighted metamorphosis for registration of images with different topologies, in: Biomedical Image Registration: 10th International Workshop, WBIR 2022, Munich, Germany, July 10–12, 2022, Proceedings, Springer. pp. 8–17.
- Friston, K.J., Ashburner, J., Frith, C.D., Poline, J.B., Heather, J.D., Frackowiak, R.S., 1995. Spatial registration and normalization of images. Human Brain Mapping 3, 165–189.
- Fu, Y., Lei, Y., Wang, T., Curran, W.J., Liu, T., Yang, X., 2020a. Deep learning in medical image registration: a review. Physics in Medicine & Biology 65, 20TR01
- Fu, Y., Lei, Y., Wang, T., Higgins, K., Bradley, J.D., Curran, W.J., Liu, T., Yang, X., 2020b. LungRegNet: an unsupervised deformable image registration method for 4D-CT lung. Med. Phys. 47, 1763–1774.
- Fu, Y., Liu, S., Li, H.H., Li, H., Yang, D., 2018. An adaptive motion regularization technique to support sliding motion in deformable image registration. Med. Phys. 45, 735–747.
- Fu, Y., Wang, T., Lei, Y., Patel, P., Jani, A.B., Curran, W.J., Liu, T., Yang, X., 2021. Deformable MR-CBCT prostate registration using biomechanically

- constrained deep learning networks. Med. Phys. 48, 253-263.
- Fuerst, B., Wein, W., Müller, M., Navab, N., 2014. Automatic ultrasound–mri registration for neurosurgery using the 2d and 3d lc2 metric. Medical Image Analysis 18, 1312–1319.
- Gal, Y., Ghahramani, Z., 2016. Dropout as a bayesian approximation: Representing model uncertainty in deep learning, in: 33rd International Conference on Machine Learning (ICML 2016), PMLR. pp. 1050–1059.
- Gandelsman, Y., Shocher, A., Irani, M., 2019. "double-dip": unsupervised image decomposition via coupled deep-image-priors, in: 2019 IEEE Conference on Computer Vision and Pattern Recognition (CVPR), pp. 11026– 11035.
- Ganser, K.A., Dickhaus, H., Metzner, R., Wirtz, C.R., 2004. A deformable digital brain atlas system according to Talairach and Tournoux. Medical Image Analysis 8, 3–22.
- Gao, C., Grupp, R.B., Unberath, M., Taylor, R.H., Armand, M., 2020a. Fiducial-free 2D/3D registration of the proximal femur for robot-assisted femoroplasty, in: Medical Imaging 2020: Image-Guided Procedures, Robotic Interventions, and Modeling, SPIE. pp. 350–355.
- Gao, C., Liu, X., Gu, W., Killeen, B., Armand, M., Taylor, R., Unberath, M., 2020b. Generalizing spatial transformers to projective geometry with applications to 2D/3D registration, in: 23rd International Conference on Medical Image Computing and Computer Assisted Intervention (MICCAI 2020), Springer. pp. 329–339.
- Gao, X., Zhong, W., Wang, R., Heimann, A.F., Tannast, M., Zheng, G., 2024. MAIRNet: weakly supervised anatomy-aware multimodal articulated image registration network. International Journal of Computer Assisted Radiology and Surgery, 1–11.
- Gatidis, S., Früh, M., Fabritius, M., Gu, S., Nikolaou, K., La Fougère, C., Ye, J., He, J., Peng, Y., Bi, L., et al., 2023. The autopet challenge: towards fully automated lesion segmentation in oncologic pet/ct imaging.
- Ger, R.B., Yang, J., Ding, Y., Jacobsen, M.C., Fuller, C.D., Howell, R.M., Li, H., Jason Stafford, R., Zhou, S., Court, L.E., 2017. Accuracy of deformable image registration on magnetic resonance images in digital and physical phantoms. Med. Phys. 44, 5153–5161.
- Gerig, T., Shahim, K., Reyes, M., Vetter, T., Lüthi, M., 2014. Spatially varying registration using gaussian processes, in: 17th International Conference on Medical Image Computing and Computer Assisted Intervention (MIC-CAI 2014), Springer. pp. 413–420.
- Glasbey, C., Mardia, K., 2001. A penalized likelihood approach to image warping. Journal of the Royal Statistical Society: Series B (Statistical Methodology) 63, 465–492.
- Glocker, B., Komodakis, N., Tziritas, G., Navab, N., Paragios, N., 2008. Dense image registration through MRFs and efficient linear programming. Medical Image Analysis 12, 731–741.
- Glocker, B., Sotiras, A., Komodakis, N., Paragios, N., 2011. Deformable medical image registration: setting the state of the art with discrete methods. Annual Review of Biomedical Engineering 13, 219–244.
- Gong, X., Khaidem, L., Zhu, W., Zhang, B., Doermann, D., 2022. Uncertainty learning towards unsupervised deformable medical image registration, in: Proceedings of the IEEE/CVF Winter Conference on Applications of Computer Vision, pp. 2484–2493.
- Goodfellow, I., Pouget-Abadie, J., Mirza, M., Xu, B., Warde-Farley, D., Ozair, S., Courville, A., Bengio, Y., 2020. Generative adversarial networks. Communications of the ACM 63, 139–144.
- Greer, H., Kwitt, R., Vialard, F.X., Niethammer, M., 2021. Icon: Learning regular maps through inverse consistency, in: Proceedings of the IEEE/CVF Conference on Computer Vision and Pattern Recognition, pp. 3396–3405.
- Greer, H., Tian, L., Vialard, F.X., Kwitt, R., Bouix, S., San Jose Estepar, R., Rushmore, R., Niethammer, M., 2023. Inverse consistency by construction for multistep deep registration, in: 26th International Conference on Medical Image Computing and Computer Assisted Intervention (MICCAI 2023), Springer. pp. 688–698.
- Grzech, D., Azampour, M.F., Glocker, B., Schnabel, J., Navab, N., Kainz, B., Le Folgoc, L., 2022. A variational bayesian method for similarity learning in non-rigid image registration, in: Proceedings of the IEEE/CVF Conference on Computer Vision and Pattern Recognition, pp. 119–128.
- Grzech, D., Kainz, B., Glocker, B., Le Folgoc, L., 2020. Image registration via stochastic gradient markov chain monte carlo, in: Uncertainty for Safe Utilization of Machine Learning in Medical Imaging, and Graphs in Biomedical Image Analysis: Second International Workshop, UNSURE 2020, and Third International Workshop, GRAIL 2020, Held in Conjunction with MICCAI 2020, Lima, Peru, October 8, 2020, Proceedings, Springer Nature. p. 3.

- Gu, W., Gao, C., Grupp, R., Fotouhi, J., Unberath, M., 2020. Extended Capture Range of Rigid 2D/3D Registration by Estimating Riemannian Pose Gradients. Machine learning in medical imaging. MLMI 12436, 281–291.
- Guimond, A., Meunier, J., Thirion, J.P., 2000. Average brain models: A convergence study. Computer Vision and Image Understanding 77, 192–210.
- Guo, C.K., 2019. Multi-modal image registration with unsupervised deep learning. Master's thesis. Massachusetts Institute of Technology.
- Guo, H., Xu, X., Song, X., Xu, S., Chao, H., Myers, J., Turkbey, B., Pinto, P.A., Wood, B.J., Yan, P., 2022. Ultrasound frame-to-volume registration via deep learning for interventional guidance. IEEE Transactions on Ultrasonics, Ferroelectrics, and Frequency Control.
- Gupta, P., Siebert, H., Heinrich, M.P., Rajamani, K.T., 2021. DA-AR-Net: an attentive activation based Deformable auto-encoder for group-wise registration, in: Medical Imaging 2021: Image Processing, SPIE. pp. 181–188.
- Ha, D., Dai, A.M., Le, Q.V., 2017. Hypernetworks, in: International Conference on Learning Representations.
- Ha, I.Y., Wilms, M., Handels, H., Heinrich, M.P., 2018. Model-based sparse-to-dense image registration for realtime respiratory motion estimation in image-guided interventions. IEEE Transactions on Biomedical Engineering 66, 302–310.
- Haber, E., Modersitzki, J., 2006. Intensity gradient based registration and fusion of multi-modal images, in: 9th International Conference on Medical Image Computing and Computer Assisted Intervention (MICCAI 2006), Springer. pp. 726–733.
- Han, K., Sun, S., Yan, X., You, C., Tang, H., Naushad, J., Ma, H., Kong, D., Xie, X., 2023. Diffeomorphic image registration with neural velocity field, in: Proceedings of the IEEE/CVF Winter Conference on Applications of Computer Vision, pp. 1869–1879.
- Han, R., Jones, C.K., Lee, J., Wu, P., Vagdargi, P., Uneri, A., Helm, P.A., Luciano, M., Anderson, W.S., Siewerdsen, J.H., 2022. Deformable MR-CT image registration using an unsupervised, dual-channel network for neurosurgical guidance. Medical Image Analysis 75, 102292.
- Han, X., Hong, J., Reyngold, M., Crane, C., Cuaron, J., Hajj, C., Mann, J., Zinovoy, M., Greer, H., Yorke, E., et al., 2021. Deep-learning-based image registration and automatic segmentation of organs-at-risk in cone-beam CT scans from high-dose radiation treatment of pancreatic cancer. Med. Phys. 48, 3084–3095.
- Han, X., Shen, Z., Xu, Z., Bakas, S., Akbari, H., Bilello, M., Davatzikos, C., Niethammer, M., 2020. A deep network for joint registration and reconstruction of images with pathologies, in: Machine Learning in Medical Imaging: 11th International Workshop, MLMI 2020, Held in Conjunction with MIC-CAI 2020, Lima, Peru, October 4, 2020, Proceedings 11, Springer. pp. 342– 352.
- Hansen, L., Heinrich, M.P., 2021. GraphRegNet: Deep graph regularisation networks on sparse keypoints for dense registration of 3D lung CTs. IEEE Trans. Med. Imag. 40, 2246–2257.
- Haouchine, N., Dorent, R., Juvekar, P., Torio, E., Wells III, W.M., Kapur, T., Golby, A.J., Frisken, S., 2023. Learning expected appearances for intraoperative registration during neurosurgery, in: 26th International Conference on Medical Image Computing and Computer Assisted Intervention (MIC-CAI 2023), Springer. pp. 227–237.
- Harley, A.W., Fang, Z., Fragkiadaki, K., 2022. Particle video revisited: Tracking through occlusions using point trajectories, in: Computer Vision–ECCV 2022: 17th European Conference, Tel Aviv, Israel, October 23–27, 2022, Proceedings, Part XXII, Springer. pp. 59–75.
- van Harten, L., Van Herten, R.L.M., Stoker, J., Isgum, I., 2024. Deformable image registration with geometry-informed implicit neural representations, in: Medical Imaging with Deep Learning, PMLR. pp. 730–742.
- Haskins, G., Kruecker, J., Kruger, U., Xu, S., Pinto, P.A., Wood, B.J., Yan, P., 2019. Learning deep similarity metric for 3D MR–TRUS image registration. International journal of computer assisted radiology and surgery 14, 417–425.
- He, Z., Chung, A.C., 2021. Learning-based template synthesis for groupwise image registration, in: Simulation and Synthesis in Medical Imaging: 6th International Workshop, SASHIMI 2021, Held in Conjunction with MICCAI 2021, Strasbourg, France, September 27, 2021, Proceedings 6, Springer. pp. 55–66.
- He, Z., Mok, T.C., Chung, A.C., 2023. Groupwise image registration with atlas of multiple resolutions refined at test phase, in: 26th International Conference on Medical Image Computing and Computer Assisted Intervention (MICCAI 2023), Springer. pp. 286–298.
- Heinrich, M., Hansen, L., Hering, A., Großbröhmer, C., 2022. Learn2reg the

- challenge (2022), doi:10.5281/zenodo.6361979.
- Heinrich, M., Sieren, M., Großbröhmer, C., Hering, A., 2023. Learn2reg the challenge (2023). doi:10.5281/zenodo.7844798.
- Heinrich, M.P., 2019. Closing the gap between deep and conventional image registration using probabilistic dense displacement networks, in: 22nd International Conference on Medical Image Computing and Computer Assisted Intervention (MICCAI 2019), Springer. pp. 50–58.
- Heinrich, M.P., Handels, H., Simpson, I.J., 2015. Estimating large lung motion in COPD patients by symmetric regularised correspondence fields, in: 18th International Conference on Medical Image Computing and Computer Assisted Intervention (MICCAI 2015), Springer. pp. 338–345.
- Heinrich, M.P., Hansen, L., 2020. Highly accurate and memory efficient unsupervised learning-based discrete CT registration using 2.5 D displacement search, in: 23rd International Conference on Medical Image Computing and Computer Assisted Intervention (MICCAI 2020), Springer. pp. 190–200.
- Heinrich, M.P., Hansen, L., 2022. Voxelmorph++ going beyond the cranial vault with keypoint supervision and multi-channel instance optimisation, in: Biomedical Image Registration: 10th International Workshop, WBIR 2022, Munich, Germany, July 10–12, 2022, Proceedings, Springer. pp. 85–95.
- Heinrich, M.P., Jenkinson, M., Bhushan, M., Matin, T., Gleeson, F.V., Brady, M., Schnabel, J.A., 2012a. MIND: Modality independent neighbourhood descriptor for multi-modal deformable registration. Medical Image Analysis 16, 1423–1435.
- Heinrich, M.P., Jenkinson, M., Brady, M., Schnabel, J.A., 2013a. MRF-based deformable registration and ventilation estimation of lung CT. IEEE Trans. Med. Imag. 32, 1239–1248.
- Heinrich, M.P., Jenkinson, M., Brady, S.M., Schnabel, J.A., 2012b. Globally optimal deformable registration on a minimum spanning tree using dense displacement sampling, in: Medical Image Computing and Computer-Assisted Intervention–MICCAI 2012: 15th International Conference, Nice, France, October 1-5, 2012, Proceedings, Part III 15, Springer. pp. 115–122.
- Heinrich, M.P., Jenkinson, M., Papież, B.W., Brady, S.M., Schnabel, J.A., 2013b. Towards realtime multimodal fusion for image-guided interventions using self-similarities, in: 16th International Conference on Medical Image Computing and Computer Assisted Intervention (MICCAI 2013), Springer. pp. 187–194.
- Heinrich, M.P., Oktay, O., Bouteldja, N., 2019. OBELISK-Net: Fewer layers to solve 3D multi-organ segmentation with sparse deformable convolutions. Medical Image Analysis 54, 1–9.
- Heinrich, M.P., Papież, B.W., Schnabel, J.A., Handels, H., 2014. Non-parametric discrete registration with convex optimisation, in: Biomedical Image Registration: 6th International Workshop, WBIR 2014, London, UK, July 7-8, 2014. Proceedings 6, Springer. pp. 51–61.
- Heinsfeld, A.S., Franco, A.R., Craddock, R.C., Buchweitz, A., Meneguzzi, F., 2018. Identification of autism spectrum disorder using deep learning and the abide dataset. NeuroImage: Clinical 17, 16–23.
- Hering, A., Ginneken, B.v., Heldmann, S., 2019. mlvirnet: Multilevel variational image registration network, in: 22nd International Conference on Medical Image Computing and Computer Assisted Intervention (MICCAI 2019), Springer. pp. 257–265.
- Hering, A., Häger, S., Moltz, J., Lessmann, N., Heldmann, S., van Ginneken, B., 2021. CNN-based lung CT registration with multiple anatomical constraints. Medical Image Analysis 72, 102139.
- Hering, A., Hansen, L., Mok, T.C., Chung, A.C., Siebert, H., Häger, S., Lange, A., Kuckertz, S., Heldmann, S., Shao, W., et al., 2022. Learn2reg: comprehensive multi-task medical image registration challenge, dataset and evaluation in the era of deep learning. IEEE Trans. Med. Imag. .
- Hernandez, M., Bossa, M.N., Olmos, S., 2009. Registration of anatomical images using paths of diffeomorphisms parameterized with stationary vector field flows. International Journal of Computer Vision 85, 291–306.
- Hill, D.L., Batchelor, P.G., Holden, M., Hawkes, D.J., 2001. Medical image registration. Physics in Medicine & Biology 46, R1.
- Ho, J., Jain, A., Abbeel, P., 2020. Denoising diffusion probabilistic models. Advances in Neural Information Processing Systems 33, 6840–6851.
- Ho, T.T., Kim, W.J., Lee, C.H., Jin, G.Y., Chae, K.J., Choi, S., 2023. An unsupervised image registration method employing chest computed tomography images and deep neural networks. Computers in Biology and Medicine 154, 106612.
- Hoffmann, M., Billot, B., Greve, D.N., Iglesias, J.E., Fischl, B., Dalca, A.V., 2021. Synthmorph: learning contrast-invariant registration without acquired images. IEEE Trans. Med. Imag. 41, 543–558.
- Hofmann, M., Steinke, F., Scheel, V., Charpiat, G., Farquhar, J., Aschoff, P.,

- Brady, M., Schölkopf, B., Pichler, B.J., 2008. MRI-based attenuation correction for PET/MRI: a novel approach combining pattern recognition and atlas registration. Journal of nuclear medicine 49, 1875–1883.
- Holland, D., Dale, A.M., Alzheimer's Disease Neuroimaging Initiative, et al., 2011. Nonlinear registration of longitudinal images and measurement of change in regions of interest. Medical Image Analysis 15, 489–497.
- Hong, Y., Joshi, S., Sanchez, M., Styner, M., Niethammer, M., 2012. Metamorphic geodesic regression, in: 15th International Conference on Medical Image Computing and Computer Assisted Intervention (MICCAI 2012), Springer. pp. 197–205.
- Hoopes, A., Hoffman, M., Greve, D.N., Fischl, B., Guttag, J., Dalca, A.V., 2022a. Learning the effect of registration hyperparameters with hypermorph. Machine Learning for Biomedical Imaging 1, 1–30.
- Hoopes, A., Hoffmann, M., Fischl, B., Guttag, J., Dalca, A.V., 2021. Hypermorph: Amortized hyperparameter learning for image registration, in: Information Processing in Medical Imaging: 27th International Conference, IPMI 2021, Virtual Event, June 28–June 30, 2021, Proceedings 27, Springer. pp. 3–17.
- Hoopes, A., Hoffmann, M., Greve, D.N., Fischl, B., Guttag, J., Dalca, A.V., 2022b. Learning the effect of registration hyperparameters with hypermorph. The journal of machine learning for biomedical imaging 1.
- Hoopes, A., Mora, J.S., Dalca, A.V., Fischl, B., Hoffmann, M., 2022c. Synthstrip: skull-stripping for any brain image. NeuroImage 260, 119474.
- Horn, B.K., Schunck, B.G., 1981. Determining optical flow. Artificial intelligence 17, 185–203.
- Hu, B., Zhou, S., Xiong, Z., Wu, F., 2020. Self-recursive contextual network for unsupervised 3D medical image registration, in: Machine Learning in Medical Imaging: 11th International Workshop, MLMI 2020, Held in Conjunction with MICCAI 2020, Lima, Peru, October 4, 2020, Proceedings 11, Springer. pp. 60–69.
- Hu, J., Sun, S., Yang, X., Zhou, S., Wang, X., Fu, Y., Zhou, J., Yin, Y., Cao, K., Song, Q., et al., 2019a. Towards accurate and robust multi-modal medical image registration using contrastive metric learning. IEEE Access 7, 132816–132827.
- Hu, X., Kang, M., Huang, W., Scott, M.R., Wiest, R., Reyes, M., 2019b. Dual-stream pyramid registration network, in: 22nd International Conference on Medical Image Computing and Computer Assisted Intervention (MIC-CAI 2019), Springer. pp. 382–390.
- Hu, Y., Modat, M., Gibson, E., Li, W., Ghavami, N., Bonmati, E., Wang, G., Bandula, S., Moore, C.M., Emberton, M., et al., 2018. Weakly-supervised convolutional neural networks for multimodal image registration. Medical Image Analysis 49, 1–13.
- Huang, D.X., Zhou, X.H., Xie, X.L., Liu, S.Q., Feng, Z.Q., Hao, J.L., Hou, Z.G., Ma, N., Yan, L., 2022. A Novel Two-Stage Framework for 2D/3D Registration in Neurological Interventions, in: 2022 IEEE International Conference on Robotics and Biomimetics (ROBIO), IEEE. pp. 266–271.
- Huang, G., Li, Y., Pleiss, G., Liu, Z., Hopcroft, J.E., Weinberger, K.Q., 2017. Snapshot ensembles: Train 1, get m for free, in: International Conference on Learning Representations.
- Hugo, G.D., Weiss, E., Sleeman, W.C., Balik, S., Keall, P.J., Lu, J., Williamson, J.F., 2016. Data from 4d lung imaging of nsclc patients. The Cancer Imaging Archive 10, K9.
- Huo, Y., Xu, Z., Xiong, Y., Aboud, K., Parvathaneni, P., Bao, S., Bermudez, C., Resnick, S.M., Cutting, L.E., Landman, B.A., 2019. 3d whole brain segmentation using spatially localized atlas network tiles. NeuroImage 194, 105–119.
- Iglesias, J.E., Sabuncu, M.R., 2015. Multi-atlas segmentation of biomedical images: a survey. Medical Image Analysis 24, 205–219.
- Ilg, E., Cicek, O., Galesso, S., Klein, A., Makansi, O., Hutter, F., Brox, T., 2018. Uncertainty estimates and multi-hypotheses networks for optical flow, in: Proceedings of the European Conference on Computer Vision (ECCV), pp. 652–667.
- Ilg, E., Mayer, N., Saikia, T., Keuper, M., Dosovitskiy, A., Brox, T., 2017. Flownet 2.0: Evolution of optical flow estimation with deep networks, in: Proceedings of the IEEE/CVF Conference on Computer Vision and Pattern Recognition, pp. 2462–2470.
- Isensee, F., Jaeger, P.F., Kohl, S.A., Petersen, J., Maier-Hein, K.H., 2021. nnU-Net: A self-configuring method for deep learning-based biomedical image segmentation. Nature Methods 18, 203–211.
- Jabri, A., Owens, A., Efros, A., 2020. Space-time correspondence as a contrastive random walk. Advances in Neural Information Processing Systems 33, 19545–19560.

- Jack Jr, C.R., Bernstein, M.A., Fox, N.C., Thompson, P., Alexander, G., Harvey, D., Borowski, B., Britson, P.J., L. Whitwell, J., Ward, C., et al., 2008. The alzheimer's disease neuroimaging initiative (adni): Mri methods. Journal of Magnetic Resonance Imaging: An Official Journal of the International Society for Magnetic Resonance in Medicine 27, 685–691.
- Jaderberg, M., Simonyan, K., Zisserman, A., et al., 2015. Spatial transformer networks. Advances in Neural Information Processing Systems 28.
- Jaffray, D.A., 2012. Image-guided radiotherapy: from current concept to future perspectives. Nature reviews Clinical oncology 9, 688–699.
- Jaganathan, S., Kukla, M., Wang, J., Shetty, K., Maier, A., 2023. Self-Supervised 2D/3D Registration for X-Ray to CT Image Fusion, in: Proceedings of the IEEE/CVF Winter Conference on Applications of Computer Vision, pp. 2788–2798.
- Ji, Y., Zhu, Z., Wei, Y., 2022. A One-shot Lung 4D-CT Image Registration Method with Temporal-spatial Features, in: 2022 IEEE Biomedical Circuits and Systems Conference (BioCAS), IEEE. pp. 203–207.
- Jia, X., Bartlett, J., Chen, W., Song, S., Zhang, T., Cheng, X., Lu, W., Qiu, Z., Duan, J., 2023. Fourier-Net: Fast image registration with band-limited deformation, in: Proceedings of the AAAI Conference on Artificial Intelligence, pp. 1015–1023.
- Jia, X., Bartlett, J., Zhang, T., Lu, W., Qiu, Z., Duan, J., 2022. U-net vs transformer: Is u-net outdated in medical image registration?, in: Machine Learning in Medical Imaging: 13th International Workshop, MLMI 2022, Held in Conjunction with MICCAI 2022, Singapore, September 18, 2022, Proceedings, Springer. pp. 151–160.
- Jia, X., Thorley, A., Chen, W., Qiu, H., Shen, L., Styles, I.B., Chang, H.J., Leonardis, A., De Marvao, A., O'Regan, D.P., et al., 2021. Learning a model-driven variational network for deformable image registration. IEEE Trans. Med. Imag. 41, 199–212.
- Jian, B., Azampour, M.F., De Benetti, F., Oberreuter, J., Bukas, C., Gersing, A.S., Foreman, S.C., Dietrich, A.S., Rischewski, J., Kirschke, J.S., et al., 2022. Weakly-supervised Biomechanically-constrained CT/MRI Registration of the Spine, in: 25th International Conference on Medical Image Computing and Computer Assisted Intervention (MICCAI 2022), Springer. pp. 227–236.
- Jiang, Z., Yin, F.F., Ge, Y., Ren, L., 2020. A multi-scale framework with unsupervised joint training of convolutional neural networks for pulmonary deformable image registration. Physics in Medicine & Biology 65, 015011.
- Jonschkowski, R., Stone, A., Barron, J.T., Gordon, A., Konolige, K., Angelova, A., 2020. What matters in unsupervised optical flow, in: Computer Vision–ECCV 2020: 16th European Conference, Glasgow, UK, August 23–28, 2020, Proceedings, Part II 16, Springer. pp. 557–572.
- Joshi, A., Hong, Y., 2022. Diffeomorphic image registration using lipschitz continuous residual networks, in: International Conference on Medical Imaging with Deep Learning, PMLR. pp. 605–617.
- Joshi, A., Hong, Y., 2023. R2net: Efficient and flexible diffeomorphic image registration using lipschitz continuous residual networks. Medical Image Analysis 89, 102917.
- Joshi, S., Davis, B., Jomier, M., Gerig, G., 2004. Unbiased diffeomorphic atlas construction for computational anatomy. NeuroImage 23, S151–S160.
- Juvekar, P., Dorent, R., Kögl, F., Torio, E., Barr, C., Rigolo, L., Galvin, C., Jowkar, N., Kazi, A., Haouchine, N., et al., 2024. Remind: The brain resection multimodal imaging database. Scientific Data 11, 494.
- Kang, M., Hu, X., Huang, W., Scott, M.R., Reyes, M., 2022. Dual-stream pyramid registration network. Medical Image Analysis 78, 102379.
- Kazerouni, A., Aghdam, E.K., Heidari, M., Azad, R., Fayyaz, M., Haci-haliloglu, I., Merhof, D., 2023. Diffusion models in medical image analysis: A comprehensive survey. Medical Image Analysis, 102846.
- Kendall, A., Gal, Y., 2017. What uncertainties do we need in bayesian deep learning for computer vision? Advances in Neural Information Processing Systems 30.
- Khor, H.G., Ning, G., Sun, Y., Lu, X., Zhang, X., Liao, H., 2023. Anatomically constrained and attention-guided deep feature fusion for joint segmentation and deformable medical image registration. Medical Image Analysis, 102811.
- Kim, B., Han, I., Ye, J.C., 2022. DiffuseMorph: Unsupervised Deformable Image Registration Using Diffusion Model, in: Proceedings of the European Conference on Computer Vision (ECCV), Springer. pp. 347–364.
- Kim, B., Kim, D.H., Park, S.H., Kim, J., Lee, J.G., Ye, J.C., 2021. CycleMorph: Cycle consistent unsupervised deformable image registration. Medical Image Analysis 71, 102036.
- Kim, D., Cho, D., Kweon, I.S., 2019. Self-supervised video representation

- learning with space-time cubic puzzles, in: Proceedings of the AAAI conference on artificial intelligence, pp. 8545–8552.
- Kirillov, A., Mintun, E., Ravi, N., Mao, H., Rolland, C., Gustafson, L., Xiao, T., Whitehead, S., Berg, A.C., Lo, W.Y., et al., 2023. Segment anything, in: Proceedings of the IEEE/CVF International Conference on Computer Vision, pp. 4015–4026.
- Kirkwood, J.G., Baldwin, R.L., Dunlop, P.J., Gosting, L.J., Kegeles, G., 1960.Flow equations and frames of reference for isothermal diffusion in liquids.The Journal of Chemical Physics 33, 1505–1513.
- Klein, A., Tourville, J., 2012. 101 labeled brain images and a consistent human cortical labeling protocol. Frontiers in neuroscience 6, 171.
- Klein, S., Staring, M., Murphy, K., Viergever, M.A., Pluim, J.P., 2009. Elastix: A toolbox for intensity-based medical image registration. IEEE Trans. Med. Imag. 29, 196–205.
- Krebs, J., Delingette, H., Mailhé, B., Ayache, N., Mansi, T., 2019. Learning a probabilistic model for diffeomorphic registration. IEEE Trans. Med. Imag. 38, 2165–2176.
- Krebs, J., Mansi, T., Delingette, H., Zhang, L., Ghesu, F.C., Miao, S., Maier, A.K., Ayache, N., Liao, R., Kamen, A., 2017. Robust non-rigid registration through agent-based action learning, in: 20th International Conference on Medical Image Computing and Computer Assisted Intervention (MIC-CAI 2017), Springer. pp. 344–352.
- Kuang, D., 2019. Cycle-consistent training for reducing negative jacobian determinant in deep registration networks, in: Simulation and Synthesis in Medical Imaging: 4th International Workshop, SASHIMI 2019, Held in Conjunction with MICCAI 2019, Shenzhen, China, October 13, 2019, Proceedings 4, Springer. pp. 120–129.
- Kuang, D., Schmah, T., 2019. Faim–a convnet method for unsupervised 3D medical image registration, in: International Workshop on Machine Learning in Medical Imaging, Springer. pp. 646–654.
- Kybic, J., 2009. Bootstrap resampling for image registration uncertainty estimation without ground truth. IEEE Trans. Imag. Proc. 19, 64–73.
- Lai, Z., Xie, W., 2019. Self-supervised learning for video correspondence flow, in: British Machine Vision Conference.
- Lange, F.J., Ashburner, J., Smith, S.M., Andersson, J.L., 2020. A symmetric prior for the regularisation of elastic deformations: Improved anatomical plausibility in nonlinear image registration. NeuroImage 219, 116962.
- Lara-Hernandez, A., Rienmüller, T., Juárez, I., Pérez, M., Reyna, F., Baumgartner, D., Makarenko, V.N., Bockeria, O.L., Maksudov, M., Rienmüller, R., et al., 2023. Deep learning-based image registration in dynamic myocardial perfusion ct imaging. IEEE Trans. Med. Imag. 42, 684–696.
- Laves, M.H., Ihler, S., Ortmaier, T., 2019. Deformable medical image registration using a randomly-initialized CNN as regularization prior, in: Medical Imaging with Deep Learning.
- Le-Khac, P.H., Healy, G., Smeaton, A.F., 2020. Contrastive representation learning: A framework and review. IEEE Access 8, 193907–193934.
- Lei, Y., Fu, Y., Wang, T., Liu, Y., Patel, P., Curran, W.J., Liu, T., Yang, X., 2020. 4D-CT deformable image registration using multiscale unsupervised deep learning. Physics in Medicine & Biology 65, 085003.
- Leow, A.D., Yanovsky, I., Chiang, M.C., Lee, A.D., Klunder, A.D., Lu, A., Becker, J.T., Davis, S.W., Toga, A.W., Thompson, P.M., 2007. Statistical properties of jacobian maps and the realization of unbiased large-deformation nonlinear image registration. IEEE Trans. Med. Imag. 26, 822–832.
- Leroy, A., Cafaro, A., Gessain, G., Champagnac, A., Grégoire, V., Deutsch, E., Lepetit, V., Paragios, N., 2023. Structuregnet: Structure-guided multimodal 2d-3d registration, in: 26th International Conference on Medical Image Computing and Computer Assisted Intervention (MICCAI 2023), Springer. pp. 771–780.
- Li, H., Fan, Y., 2018. Non-rigid image registration using self-supervised fully convolutional networks without training data, in: 15th International Symposium on Biomedical Imaging (ISBI 2018), IEEE. pp. 1075–1078.
- Li, J., Chen, J., Tang, Y., Wang, C., Landman, B.A., Zhou, S.K., 2023a. Transforming medical imaging with transformers? a comparative review of key properties, current progresses, and future perspectives. Medical Image Analysis, 102762.
- Li, L., Sinclair, M., Makropoulos, A., Hajnal, J.V., David Edwards, A., Kainz, B., Rueckert, D., Alansary, A., 2021. CAS-Net: conditional atlas generation and brain segmentation for fetal MRI, in: Uncertainty for Safe Utilization of Machine Learning in Medical Imaging, and Perinatal Imaging, Placental and Preterm Image Analysis: 3rd International Workshop, UNSURE 2021, and 6th International Workshop, PIPPI 2021, Held in Conjunction with MICCAI

- 2021, Strasbourg, France, October 1, 2021, Proceedings 3, Springer. pp. 221–230.
- Li, P., Pei, Y., Guo, Y., Ma, G., Xu, T., Zha, H., 2020. Non-Rigid 2D-3D Registration Using Convolutional Autoencoders, in: 17th International Symposium on Biomedical Imaging (ISBI 2020), pp. 700–704. doi:10.1109/ ISBI45749.2020.9098602.
- Li, Z., Ogino, M., 2019. Adversarial learning for deformable image registration: Application to 3D ultrasound image fusion, in: Smart Ultrasound Imaging and Perinatal, Preterm and Paediatric Image Analysis: First International Workshop, SUSI 2019, and 4th International Workshop, PIPPI 2019, Held in Conjunction with MICCAI 2019, Shenzhen, China, October 13 and 17, 2019, Proceedings 4, Springer. pp. 56–64.
- Li, Z., Tian, L., Mok, T.C., Bai, X., Wang, P., Ge, J., Zhou, J., Lu, L., Ye, X., Yan, K., et al., 2023b. Samconvex: Fast discrete optimization for ct registration using self-supervised anatomical embedding and correlation pyramid, in: 26th International Conference on Medical Image Computing and Computer Assisted Intervention (MICCAI 2023), Springer. pp. 559–569.
- Liang, X., Lin, S., Liu, F., Schreiber, D., Yip, M., 2023. Orrn: An ode-based recursive registration network for deformable respiratory motion estimation with lung 4dct images. IEEE Transactions on Biomedical Engineering.
- Liao, H., Lin, W.A., Zhang, J., Zhang, J., Luo, J., Zhou, S.K., 2019. Multiview 2D/3D rigid registration via a point-of-interest network for tracking and triangulation, in: Proceedings of the IEEE/CVF Conference on Computer Vision and Pattern Recognition, pp. 12638–12647.
- Liu, F., Yan, K., Harrison, A.P., Guo, D., Lu, L., Yuille, A.L., Huang, L., Xie, G., Xiao, J., Ye, X., et al., 2021a. Same: Deformable image registration based on self-supervised anatomical embeddings, in: 24th International Conference on Medical Image Computing and Computer Assisted Intervention (MICCAI 2021), Springer. pp. 87–97.
- Liu, L., Aviles-Rivero, A.I., Schönlieb, C.B., 2023a. Contrastive registration for unsupervised medical image segmentation. IEEE Transactions on Neural Networks and Learning Systems, 1–13.
- Liu, L., Hu, X., Zhu, L., Heng, P.A., 2019. Probabilistic multilayer regularization network for unsupervised 3D brain image registration, in: 22nd International Conference on Medical Image Computing and Computer Assisted Intervention (MICCAI 2019), Springer. pp. 346–354.
- Liu, L., Huang, Z., Liò, P., Schönlieb, C.B., Aviles-Rivero, A.I., 2022a. PC-SwinMorph: Patch representation for unsupervised medical image registration and segmentation. arXiv preprint arXiv:2203.05684.
- Liu, X., Zheng, Y., Killeen, B., Ishii, M., Hager, G.D., Taylor, R.H., Unberath, M., 2020. Extremely dense point correspondences using a learned feature descriptor, in: Proceedings of the IEEE/CVF Conference on Computer Vision and Pattern Recognition, pp. 4847–4856.
- Liu, Y., Chen, J., Wei, S., Carass, A., Prince, J., 2022b. On finite difference jacobian computation in deformable image registration. International Journal of Computer Vision.
- Liu, Y., Chen, J., Zuo, L., Carass, A., Prince, J.L., 2024. Vector field attention for deformable image registration. arXiv preprint arXiv:2407.10209.
- Liu, Y., Gu, S., 2023. Co-learning semantic-aware unsupervised segmentation for pathological image registration, in: 26th International Conference on Medical Image Computing and Computer Assisted Intervention (MIC-CAI 2023), Springer. pp. 537–547.
- Liu, Y., Wang, W., Li, Y., Lai, H., Huang, S., Yang, X., 2023b. Geometryconsistent adversarial registration model for unsupervised multi-modal medical image registration. IEEE Journal of Biomedical and Health Informatics
- Liu, Y., Zuo, L., Han, S., Xue, Y., Prince, J.L., Carass, A., 2022c. Coordinate translator for learning deformable medical image registration, in: International Workshop on Multiscale Multimodal Medical Imaging, Springer. pp. 98–109.
- Liu, Z., Lin, Y., Cao, Y., Hu, H., Wei, Y., Zhang, Z., Lin, S., Guo, B., 2021b. Swin transformer: Hierarchical vision transformer using shifted windows, in: Proceedings of the IEEE/CVF Conference on Computer Vision and Pattern Recognition, pp. 10012–10022.
- Liu, Z., Mao, H., Wu, C.Y., Feichtenhofer, C., Darrell, T., Xie, S., 2022d. A convnet for the 2020s, in: Proceedings of the IEEE/CVF Conference on Computer Vision and Pattern Recognition, pp. 11976–11986.
- Liu, Z., Ning, J., Cao, Y., Wei, Y., Zhang, Z., Lin, S., Hu, H., 2022e. Video swin transformer, in: Proceedings of the IEEE/CVF Conference on Computer Vision and Pattern Recognition, pp. 3202–3211.
- Livieratos, L., 2015. Technical pitfalls and limitations of spect/ct, in: Seminars in nuclear medicine, Elsevier. pp. 530–540.

- Lobachev, O., Funatomi, T., Pfaffenroth, A., Förster, R., Knudsen, L., Wrede, C., Guthe, M., Haberthür, D., Hlushchuk, R., Salaets, T., et al., 2021. Evaluating registrations of serial sections with distortions of the ground truths. IEEE Access 9, 152514–152535.
- López, P.A., Mella, H., Uribe, S., Hurtado, D.E., Costabal, F.S., 2023. Warp-PINN: Cine-MR image registration with physics-informed neural networks. Medical Image Analysis 89, 102925.
- Lotfi, T., Tang, L., Andrews, S., Hamarneh, G., 2013. Improving probabilistic image registration via reinforcement learning and uncertainty evaluation, in: Machine Learning in Medical Imaging: 4th International Workshop, MLMI 2013, Held in Conjunction with MICCAI 2013, Nagoya, Japan, September 22, 2013. Proceedings 4, Springer. pp. 187–194.
- Luo, J., Sedghi, A., Popuri, K., Cobzas, D., Zhang, M., Preiswerk, F., Toews, M., Golby, A., Sugiyama, M., Wells, W.M., et al., 2019. On the applicability of registration uncertainty, in: MICCAI19, Springer. pp. 410–419.
- Luo, W., Li, Y., Urtasun, R., Zemel, R., 2016. Understanding the effective receptive field in deep convolutional neural networks. Advances in Neural Information Processing Systems 29.
- Luo, Y., Cao, W., He, Z., Zou, W., He, Z., 2021. Deformable adversarial registration network with multiple loss constraints. Computerized Medical Imaging and Graphics 91, 101931.
- Lv, J., Wang, Z., Shi, H., Zhang, H., Wang, S., Wang, Y., Li, Q., 2022. Joint progressive and coarse-to-fine registration of brain MRI via deformation field integration and non-rigid feature fusion. IEEE Trans. Med. Imag. 41, 2788–2802.
- Ma, J., Chen, J., Ng, M., Huang, R., Li, Y., Li, C., Yang, X., Martel, A.L., 2021.
 Loss odyssey in medical image segmentation. Medical Image Analysis 71, 102035.
- Ma, J., Miller, M.I., Trouvé, A., Younes, L., 2008. Bayesian template estimation in computational anatomy. NeuroImage 42, 252–261.
- Ma, M., Xu, Y., Song, L., Liu, G., 2022. Symmetric transformer-based network for unsupervised image registration. Knowledge-Based Systems 257, 109959
- Ma, T., Dai, X., Zhang, S., Wen, Y., 2023. Pivit: Large deformation image registration with pyramid-iterative vision transformer, in: 26th International Conference on Medical Image Computing and Computer Assisted Intervention (MICCAI 2023), Springer, pp. 602–612.
- Mac Aodha, O., Humayun, A., Pollefeys, M., Brostow, G.J., 2012. Learning a confidence measure for optical flow. IEEE Trans. Patt. Anal. Mach. Intell. 35, 1107–1120.
- Madsen, D., Morel-Forster, A., Kahr, P., Rahbani, D., Vetter, T., Lüthi, M., 2020. A closest point proposal for mcmc-based probabilistic surface registration, in: Computer Vision–ECCV 2020: 16th European Conference, Glasgow, UK, August 23–28, 2020, Proceedings, Part XVII 16, Springer. pp. 281–296.
- Maes, F., Collignon, A., Vandermeulen, D., Marchal, G., Suetens, P., 1997.Multimodality image registration by maximization of mutual information.IEEE Trans. Med. Imag. 16, 187–198.
- Mahapatra, D., Antony, B., Sedai, S., Garnavi, R., 2018a. Deformable medical image registration using generative adversarial networks, in: 15th International Symposium on Biomedical Imaging (ISBI 2018), IEEE. pp. 1449– 1453
- Mahapatra, D., Ge, Z., 2020. Training data independent image registration using generative adversarial networks and domain adaptation. Pattern Recognition 100, 107109.
- Mahapatra, D., Ge, Z., Sedai, S., Chakravorty, R., 2018b. Joint registration and segmentation of xray images using generative adversarial networks, in: Machine Learning in Medical Imaging: 9th International Workshop, MLMI 2018, Held in Conjunction with MICCAI 2018, Granada, Spain, September 16, 2018, Proceedings 9, Springer. pp. 73–80.
- Maillard, M., François, A., Glaunès, J., Bloch, I., Gori, P., 2022. A deep residual learning implementation of metamorphosis, in: 19th International Symposium on Biomedical Imaging (ISBI 2022), IEEE. pp. 1–4.
- Maintz, J.A., Viergever, M.A., 1998. A survey of medical image registration. Medical Image Analysis 2, 1–36.
- Makela, T., Clarysse, P., Sipila, O., Pauna, N., Pham, Q.C., Katila, T., Magnin, I.E., 2002. A review of cardiac image registration methods. IEEE Transactions on medical imaging 21, 1011–1021.
- Makhzani, A., Shlens, J., Jaitly, N., Goodfellow, I., Frey, B., 2015. Adversarial autoencoders. arXiv preprint arXiv:1511.05644.
- Mansi, T., Pennec, X., Sermesant, M., Delingette, H., Ayache, N., 2011. iLogDemons: A demons-based registration algorithm for tracking incom-

- pressible elastic biological tissues. International Journal of Computer Vision 92, 92–111.
- Marcus, D.S., Wang, T.H., Parker, J., Csernansky, J.G., Morris, J.C., Buckner, R.L., 2007. Open access series of imaging studies (oasis): cross-sectional mri data in young, middle aged, nondemented, and demented older adults. Journal of cognitive neuroscience 19, 1498–1507.
- Markiewicz, C.J., Gorgolewski, K.J., Feingold, F., Blair, R., Halchenko, Y.O., Miller, E., Hardcastle, N., Wexler, J., Esteban, O., Goncavles, M., et al., 2021. The openneuro resource for sharing of neuroscience data. Elife 10, e71774.
- Meng, M., Bi, L., Fulham, M., Feng, D., Kim, J., 2023. Non-iterative coarse-tofine transformer networks for joint affine and deformable image registration, in: 26th International Conference on Medical Image Computing and Computer Assisted Intervention (MICCAI 2023), Springer. pp. 750–760.
- Meng, M., Bi, L., Fulham, M., Feng, D.D., Kim, J., 2022a. Enhancing medical image registration via appearance adjustment networks. NeuroImage 259, 119444.
- Meng, Q., Qin, C., Bai, W., Liu, T., de Marvao, A., O'Regan, D.P., Rueckert, D., 2022b. MulViMotion: Shape-aware 3D Myocardial Motion Tracking from Multi-View Cardiac MRI. IEEE Trans. Med. Imag. 41, 1961–1974.
- Mescheder, L., Oechsle, M., Niemeyer, M., Nowozin, S., Geiger, A., 2019. Occupancy networks: Learning 3D reconstruction in function space, in: Proceedings of the IEEE/CVF Conference on Computer Vision and Pattern Recognition, pp. 4460–4470.
- Miao, S., Wang, Z.J., Liao, R., 2016. A CNN regression approach for real-time 2D/3D registration. IEEE Trans. Med. Imag. 35, 1352–1363.
- Mildenhall, B., Srinivasan, P.P., Tancik, M., Barron, J.T., Ramamoorthi, R., Ng, R., 2021. Nerf: Representing scenes as neural radiance fields for view synthesis. Communications of the ACM 65, 99–106.
- Miller, M.I., Trouvé, A., Younes, L., 2006. Geodesic shooting for computational anatomy. Journal of Mathematical Imaging and Vision 24, 209–228.
- Mok, T.C., Chung, A., 2020a. Fast symmetric diffeomorphic image registration with convolutional neural networks, in: Proceedings of the IEEE/CVF Conference on Computer Vision and Pattern Recognition, pp. 4644–4653.
- Mok, T.C., Chung, A., 2020b. Large deformation diffeomorphic image registration with laplacian pyramid networks, in: 23rd International Conference on Medical Image Computing and Computer Assisted Intervention (MIC-CAI 2020), Springer. pp. 211–221.
- Mok, T.C., Chung, A., 2021a. Conditional deep laplacian pyramid image registration network in learn2reg challenge, in: 24th International Conference on Medical Image Computing and Computer Assisted Intervention (MIC-CAI 2021), Springer. pp. 161–167.
- Mok, T.C., Chung, A., 2021b. Conditional deformable image registration with convolutional neural network, in: 24th International Conference on Medical Image Computing and Computer Assisted Intervention (MICCAI 2021), Springer. pp. 35–45.
- Mok, T.C., Chung, A., 2022a. Affine medical image registration with coarse-to-fine vision transformer, in: Proceedings of the IEEE/CVF Conference on Computer Vision and Pattern Recognition, pp. 20835–20844.
- Mok, T.C., Chung, A., 2022b. Robust Image Registration with Absent Correspondences in Pre-operative and Follow-up Brain MRI Scans of Diffuse Glioma Patients, in: International MICCAI Brainlesion Workshop, pp. 231–240
- Mok, T.C., Chung, A.C., 2022c. Unsupervised Deformable Image Registration with Absent Correspondences in Pre-operative and Post-recurrence Brain Tumor MRI Scans, in: 25th International Conference on Medical Image Computing and Computer Assisted Intervention (MICCAI 2022), Springer. pp. 25–35.
- Morales, M.A., Izquierdo-Garcia, D., Aganj, I., Kalpathy-Cramer, J., Rosen, B.R., Catana, C., 2019. Implementation and validation of a three-dimensional cardiac motion estimation network. Radiology: Artificial Intelligence 1, e180080.
- Murphy, K., Van Ginneken, B., Reinhardt, J.M., Kabus, S., Ding, K., Deng, X., Cao, K., Du, K., Christensen, G.E., Garcia, V., et al., 2011. Evaluation of registration methods on thoracic ct: the empire10 challenge. IEEE transactions on medical imaging 30, 1901–1920.
- Myronenko, A., Song, X., 2010. Intensity-based image registration by minimizing residual complexity. IEEE Trans. Med. Imag. 29, 1882–1891.
- Nan, A., Tennant, M., Rubin, U., Ray, N., 2020. Drmime: Differentiable mutual information and matrix exponential for multi-resolution image registration, in: Medical Imaging with Deep Learning, PMLR. pp. 527–543.
- Nenoff, L., Ribeiro, C.O., Matter, M., Hafner, L., Josipovic, M., Langendijk,

- J.A., Persson, G.F., Walser, M., Weber, D.C., Lomax, A.J., et al., 2020. Deformable image registration uncertainty for inter-fractional dose accumulation of lung cancer proton therapy. Radiotherapy and Oncology 147, 178–185.
- Niemeyer, M., Mescheder, L., Oechsle, M., Geiger, A., 2019. Occupancy flow: 4D reconstruction by learning particle dynamics, in: Proceedings of the IEEE/CVF Conference on Computer Vision and Pattern Recognition, pp. 5379–5389.
- Niethammer, M., Hart, G.L., Pace, D.F., Vespa, P.M., Irimia, A., Van Horn, J.D., Aylward, S.R., 2011. Geometric metamorphosis, in: 14th International Conference on Medical Image Computing and Computer Assisted Intervention (MICCAI 2011), NIH Public Access. p. 639.
- Niethammer, M., Kwitt, R., Vialard, F.X., 2019. Metric learning for image registration, in: Proceedings of the IEEE/CVF Conference on Computer Vision and Pattern Recognition, pp. 8463–8472.
- Obeidat, M., Narayanasamy, G., Cline, K., Stathakis, S., Pouliot, J., Kim, H., Kirby, N., 2016. Comparison of different qa methods for deformable image registration to the known errors for prostate and head-and-neck virtual phantoms. Biomedical Physics & Engineering Express 2, 067002.
- Oishi, K., Faria, A., Jiang, H., Li, X., Akhter, K., Zhang, J., Hsu, J.T., Miller, M.I., van Zijl, P.C., Albert, M., et al., 2009. Atlas-based whole brain white matter analysis using large deformation diffeomorphic metric mapping: application to normal elderly and Alzheimer's disease participants. NeuroImage 46, 486–499.
- Oliveira, F.P., Tavares, J.M.R., 2014. Medical image registration: A review. Computer Methods in Biomechanics and Biomedical Engineering 17, 73–93.
- Oord, A.v.d., Li, Y., Vinyals, O., 2018. Representation learning with contrastive predictive coding. arXiv preprint arXiv:1807.03748.
- Osman, N.F., Kerwin, W.S., McVeigh, E.R., Prince, J.L., 1999. Cardiac motion tracking using CINE harmonic phase (HARP) magnetic resonance imaging. Mag. Reson. Med. 42, 1048–1060.
- Pace, D.F., Aylward, S.R., Niethammer, M., 2013. A locally adaptive regularization based on anisotropic diffusion for deformable image registration of sliding organs. IEEE Trans. Med. Imag. 32, 2114–2126.
- Papież, B.W., Franklin, J., Heinrich, M.P., Gleeson, F.V., Schnabel, J.A., 2015. Liver motion estimation via locally adaptive over-segmentation regularization, in: 18th International Conference on Medical Image Computing and Computer Assisted Intervention (MICCAI 2015), Springer. pp. 427–434.
- Papież, B.W., Heinrich, M.P., Fehrenbach, J., Risser, L., Schnabel, J.A., 2014. An implicit sliding-motion preserving regularisation via bilateral filtering for deformable image registration. Medical Image Analysis 18, 1299–1311.
- Park, J.J., Florence, P., Straub, J., Newcombe, R., Lovegrove, S., 2019. Deepsdf: Learning continuous signed distance functions for shape representation, in: Proceedings of the IEEE/CVF Conference on Computer Vision and Pattern Recognition, pp. 165–174.
- Park, T., Efros, A.A., Zhang, R., Zhu, J.Y., 2020. Contrastive learning for unpaired image-to-image translation, in: Computer Vision–ECCV 2020: 16th European Conference, Glasgow, UK, August 23–28, 2020, Proceedings, Part IX 16, Springer. pp. 319–345.
- Pathan, S., Hong, Y., 2018. Predictive image regression for longitudinal studies with missing data, in: Medical Imaging with Deep Learning.
- Pei, Y., Chen, L., Zhao, F., Wu, Z., Zhong, T., Wang, Y., Chen, C., Wang, L., Zhang, H., Wang, L., et al., 2021. Learning spatiotemporal probabilistic atlas of fetal brains with anatomically constrained registration network, in: 24th International Conference on Medical Image Computing and Computer Assisted Intervention (MICCAI 2021), Springer. pp. 239–248.
- Peter, L., Alexander, D.C., Magnain, C., Iglesias, J.E., 2021. Uncertainty-aware annotation protocol to evaluate deformable registration algorithms. IEEE Trans. Med. Imag. 40, 2053–2065.
- Pfandler, M., Stefan, P., Mehren, C., Lazarovici, M., Weigl, M., 2019. Technical and nontechnical skills in surgery: A simulated operating room environment study. Spine 44, E1396–E1400.
- Pielawski, N., Wetzer, E., Öfverstedt, J., Lu, J., Wählby, C., Lindblad, J., Sladoje, N., 2020. CoMIR: Contrastive multimodal image representation for registration. Advances in Neural Information Processing Systems 33, 18433–18444.
- Pitiot, A., Guimond, A., 2008. Geometrical regularization of displacement fields for histological image registration. Medical Image Analysis 12, 16– 25.
- Pluim, J., Maintz, J., Viergever, M., 2000. Image registration by maximization of combined mutual information and gradient information. IEEE Trans.

- Med. Imag. 19, 809-814.
- Pluim, J.P., Muenzing, S.E., Eppenhof, K.A., Murphy, K., 2016. The truth is hard to make: Validation of medical image registration, in: 2016 23rd International Conference on Pattern Recognition (ICPR), IEEE. pp. 2294– 2300.
- Polzin, T., Rühaak, J., Werner, R., Strehlow, J., Heldmann, S., Handels, H., Modersitzki, J., 2013. Combining automatic landmark detection and variational methods for lung CT registration, in: Fifth international workshop on pulmonary image analysis, pp. 85–96.
- Qian, R., Meng, T., Gong, B., Yang, M.H., Wang, H., Belongie, S., Cui, Y., 2021. Spatiotemporal contrastive video representation learning, in: Proceedings of the IEEE/CVF Conference on Computer Vision and Pattern Recognition, pp. 6964–6974.
- Qin, C., Bai, W., Schlemper, J., Petersen, S.E., Piechnik, S.K., Neubauer, S., Rueckert, D., 2018. Joint learning of motion estimation and segmentation for cardiac MR image sequences, in: 21st International Conference on Medical Image Computing and Computer Assisted Intervention (MICCAI 2018), Springer. pp. 472–480.
- Qin, C., Shi, B., Liao, R., Mansi, T., Rueckert, D., Kamen, A., 2019. Unsupervised deformable registration for multi-modal images via disentangled representations, in: Information Processing in Medical Imaging: 26th International Conference, IPMI 2019, Hong Kong, China, June 2–7, 2019, Proceedings 26, Springer. pp. 249–261.
- Qin, C., Wang, S., Chen, C., Bai, W., Rueckert, D., 2023. Generative myocardial motion tracking via latent space exploration with biomechanicsinformed prior. Medical Image Analysis 83, 102682.
- Qin, Y., Li, X., 2023. FSDiffReg: Feature-Wise and Score-Wise Diffusion-Guided Unsupervised Deformable Image Registration for Cardiac Images, in: 26th International Conference on Medical Image Computing and Computer Assisted Intervention (MICCAI 2023), Springer. pp. 655–665.
- Qiu, H., Qin, C., Schuh, A., Hammernik, K., Rueckert, D., 2021. Learning diffeomorphic and modality-invariant registration using b-splines, in: Medical Imaging with Deep Learning.
- Raissi, M., Perdikaris, P., Karniadakis, G.E., 2019. Physics-informed neural networks: A deep learning framework for solving forward and inverse problems involving nonlinear partial differential equations. Journal of Computational physics 378, 686–707.
- Rajchl, M., Baxter, J.S., Qiu, W., Khan, A.R., Fenster, A., Peters, T.M., Rueckert, D., Yuan, J., 2016. Fast deformable image registration with non-smooth dual optimization, in: Proceedings of the IEEE Conference on Computer Vision and Pattern Recognition Workshops, pp. 25–32.
- Ramon, U., Hernandez, M., Mayordomo, E., 2022. LDDMM meets GANs: Generative Adversarial Networks for diffeomorphic registration, in: Biomedical Image Registration: 10th International Workshop, WBIR 2022, Munich, Germany, July 10–12, 2022, Proceedings, Springer. pp. 18–28.
- Ranjan, A., Jampani, V., Balles, L., Kim, K., Sun, D., Wulff, J., Black, M.J., 2019. Competitive collaboration: Joint unsupervised learning of depth, camera motion, optical flow and motion segmentation, in: Proceedings of the IEEE/CVF Conference on Computer Vision and Pattern Recognition, pp. 12240–12249.
- Reed, V.K., Woodward, W.A., Zhang, L., Strom, E.A., Perkins, G.H., Tereffe, W., Oh, J.L., Yu, T.K., Bedrosian, I., Whitman, G.J., et al., 2009. Automatic segmentation of whole breast using atlas approach and deformable image registration. International Journal of Radiation Oncology* Biology* Physics 73, 1493–1500.
- Risholm, P., Balter, J., Wells, W.M., 2011. Estimation of delivered dose in radiotherapy: the influence of registration uncertainty, in: 14th International Conference on Medical Image Computing and Computer Assisted Intervention (MICCAI 2011), Springer. pp. 548–555.
- Risholm, P., Janoos, F., Norton, I., Golby, A.J., Wells III, W.M., 2013. Bayesian characterization of uncertainty in intra-subject non-rigid registration. Medical Image Analysis 17, 538–555.
- Risser, L., Vialard, F.X., Baluwala, H.Y., Schnabel, J.A., 2013. Piecewise-diffeomorphic image registration: Application to the motion estimation between 3D CT lung images with sliding conditions. Medical Image Analysis 17, 182–193.
- Roche, A., Malandain, G., Pennec, X., Ayache, N., 1998. The correlation ratio as a new similarity measure for multimodal image registration, in: 1st International Conference on Medical Image Computing and Computer Assisted Intervention (MICCAI 1998), Springer. pp. 1115–1124.
- Rohé, M.M., Datar, M., Heimann, T., Sermesant, M., Pennec, X., 2017. SVF-Net: Learning deformable image registration using shape matching, in: 20th

- International Conference on Medical Image Computing and Computer Assisted Intervention (MICCAI 2017), Springer. pp. 266–274.
- Rohlfing, T., 2011. Image similarity and tissue overlaps as surrogates for image registration accuracy: Widely used but unreliable. IEEE Trans. Med. Imag. 31, 153–163.
- Rohlfing, T., Maurer, C.R., Bluemke, D.A., Jacobs, M.A., 2003a. Volume-preserving nonrigid registration of MR breast images using free-form deformation with an incompressibility constraint. IEEE Trans. Med. Imag. 22, 730–741.
- Rohlfing, T., Russakoff, D.B., Maurer, C.R., 2003b. Expectation maximization strategies for multi-atlas multi-label segmentation, in: 18th Inf. Proc. in Med. Imaging (IPMI 2003), Springer. pp. 210–221.
- Ronchetti, M., Wein, W., Navab, N., Zettinig, O., Prevost, R., 2023. DISA: Differentiable similarity approximation for universal multimodal registration, in: 26th International Conference on Medical Image Computing and Computer Assisted Intervention (MICCAI 2023), Springer. pp. 761–770.
- Ronneberger, O., Fischer, P., Brox, T., 2015. U-net: Convolutional networks for biomedical image segmentation, in: 18th International Conference on Medical Image Computing and Computer Assisted Intervention (MICCAI 2015), Springer. pp. 234–241.
- Roy, P., Lee, J.K., Sheikh, A., Lin, W., 2015. Quantitative comparison of misregistration in abdominal and pelvic organs between pet/mri and pet/ct: effect of mode of acquisition and type of sequence on different organs. American Journal of Roentgenology 205, 1295–1305.
- Rueckert, D., Sonoda, L.I., Hayes, C., Hill, D.L., Leach, M.O., Hawkes, D.J., 1999. Nonrigid registration using free-form deformations: Application to breast MR images. IEEE Trans. Med. Imag. 18, 712–721.
- Rühaak, J., Polzin, T., Heldmann, S., Simpson, I.J., Handels, H., Modersitzki, J., Heinrich, M.P., 2017. Estimation of large motion in lung CT by integrating regularized keypoint correspondences into dense deformable registration. IEEE Trans. Med. Imag. 36, 1746–1757.
- Sandkühler, R., Jud, C., Andermatt, S., Cattin, P.C., 2018. AIRLab: autograd image registration laboratory. arXiv preprint arXiv:1806.09907.
- Santini, S., Jain, R., 1999. Similarity measures. IEEE Trans. Patt. Anal. Mach. Intell. 21, 871–883
- Schmah, T., Risser, L., Vialard, F.X., 2013. Left-invariant metrics for diffeomorphic image registration with spatially-varying regularisation, in: 16th International Conference on Medical Image Computing and Computer Assisted Intervention (MICCAI 2013), Springer. pp. 203–210.
- Schnabel, J.A., Heinrich, M.P., Papież, B.W., Brady, J.M., 2016. Advances and challenges in deformable image registration: from image fusion to complex motion modelling. Medical Image Analysis 33, 145–148.
- Schultz, S., Handels, H., Ehrhardt, J., 2018. A multilevel markov chain monte carlo approach for uncertainty quantification in deformable registration, in: Medical Imaging 2018: Image Processing, SPIE. pp. 162–169.
- Sdika, M., 2008. A fast nonrigid image registration with constraints on the jacobian using large scale constrained optimization. IEEE Trans. Med. Imag. 27, 271–281.
- Sdika, M., Pelletier, D., 2009. Nonrigid registration of multiple sclerosis brain images using lesion inpainting for morphometry or lesion mapping. Technical Report. Wiley Online Library.
- Shams, R., Sadeghi, P., Kennedy, R.A., Hartley, R.I., 2010. A survey of medical image registration on multicore and the gpu. IEEE signal processing magazine 27, 50–60.
- Shao, S., Pei, Z., Chen, W., Zhu, W., Wu, X., Zhang, B., 2022. A multi-scale unsupervised learning for deformable image registration. International Journal of Computer Assisted Radiology and Surgery, 1–10.
- Shattuck, D.W., Mirza, M., Adisetiyo, V., Hojatkashani, C., Salamon, G., Narr, K.L., Poldrack, R.A., Bilder, R.M., Toga, A.W., 2008. Construction of a 3d probabilistic atlas of human cortical structures. Neuroimage 39, 1064–1080.
- Shen, Z., Vialard, F.X., Niethammer, M., 2019. Region-specific diffeomorphic metric mapping. Advances in Neural Information Processing Systems 32.
- Shi, J., He, Y., Kong, Y., Coatrieux, J.L., Shu, H., Yang, G., Li, S., 2022. Xmorpher: Full transformer for deformable medical image registration via cross attention, in: 25th International Conference on Medical Image Computing and Computer Assisted Intervention (MICCAI 2022), Springer. pp. 217–226.
- Shi, X., Huang, Z., Li, D., Zhang, M., Cheung, K.C., See, S., Qin, H., Dai, J., Li, H., 2023. Flowformer++: Masked cost volume autoencoding for pretraining optical flow estimation, in: Proceedings of the IEEE/CVF Conference on Computer Vision and Pattern Recognition, pp. 1599–1610.
- Shrestha, P., Xie, C., Shishido, H., Yoshii, Y., Kitahara, I., 2023. X-ray to ct

- rigid registration using scene coordinate regression, in: 26th International Conference on Medical Image Computing and Computer Assisted Intervention (MICCAI 2023), Springer. pp. 781–790.
- Shu, Z., Sahasrabudhe, M., Guler, R.A., Samaras, D., Paragios, N., Kokkinos, I., 2018. Deforming autoencoders: Unsupervised disentangling of shape and appearance, in: Proceedings of the European Conference on Computer Vision (ECCV), pp. 650–665.
- Siebert, H., Hansen, L., Heinrich, M.P., 2021a. Fast 3D registration with accurate optimisation and little learning for Learn2Reg 2021, in: Biomedical Image Registration, Domain Generalisation and Out-of-Distribution Analysis: MICCAI 2021 Challenges: MIDOG 2021, MOOD 2021, and Learn2Reg 2021, Held in Conjunction with MICCAI 2021, Strasbourg, France, September 27–October 1, 2021, Proceedings. Springer, pp. 174–179.
- Siebert, H., Hansen, L., Heinrich, M.P., 2021b. Fast 3d registration with accurate optimisation and little learning for learn2reg 2021, in: 24th International Conference on Medical Image Computing and Computer Assisted Intervention (MICCAI 2021), Springer. pp. 174–179.
- Siebert, H., Heinrich, M.P., 2022. Learn to fuse input features for large-deformation registration with differentiable convex-discrete optimisation, in: Biomedical Image Registration: 10th International Workshop, WBIR 2022, Munich, Germany, July 10–12, 2022, Proceedings, Springer, pp. 119–123.
- Siebert, H., Rajamani, K.T., Heinrich, M.P., 2021c. Learning inverse consistent 3D groupwise registration with deforming autoencoders, in: Medical Imaging 2021: Image Processing, SPIE. pp. 89–95.
- Simpson, I.J., Cardoso, M.J., Modat, M., Cash, D.M., Woolrich, M.W., Andersson, J.L., Schnabel, J.A., Ourselin, S., Initiative, A.D.N., et al., 2015. Probabilistic non-linear registration with spatially adaptive regularisation. Medical Image Analysis 26, 203–216.
- Simpson, I.J., Woolrich, M., Groves, A.R., Schnabel, J.A., 2011. Longitudinal brain MRI analysis with uncertain registration, in: 14th International Conference on Medical Image Computing and Computer Assisted Intervention (MICCAI 2011), Springer. pp. 647–654.
- Sinclair, M., Schuh, A., Hahn, K., Petersen, K., Bai, Y., Batten, J., Schaap, M., Glocker, B., 2022. Atlas-ISTN: joint segmentation, registration and atlas construction with image-and-spatial transformer networks. Medical Image Analysis 78, 102383.
- Sitzmann, V., Martel, J., Bergman, A., Lindell, D., Wetzstein, G., 2020. Implicit neural representations with periodic activation functions. Advances in Neural Information Processing Systems 33, 7462–7473.
- Smolders, A., Lomax, T., Weber, D., Albertini, F., 2022. Deformable image registration uncertainty quantification using deep learning for dose accumulation in adaptive proton therapy, in: Biomedical Image Registration: 10th International Workshop, WBIR 2022, Munich, Germany, July 10–12, 2022, Proceedings, Springer. pp. 57–66.
- Sohl-Dickstein, J., Weiss, E., Maheswaranathan, N., Ganguli, S., 2015. Deep unsupervised learning using nonequilibrium thermodynamics, in: 32nd International Conference on Machine Learning (ICML 2016), PMLR. pp. 2256– 2265.
- Sokooti, H., Saygili, G., Glocker, B., Lelieveldt, B.P., Staring, M., 2016. Accuracy estimation for medical image registration using regression forests, in: 19th International Conference on Medical Image Computing and Computer Assisted Intervention (MICCAI 2016), Springer. pp. 107–115.
- Sokooti, H., Vos, B.d., Berendsen, F., Lelieveldt, B.P., Išgum, I., Staring, M., 2017. Nonrigid image registration using multi-scale 3D convolutional neural networks, in: 20th International Conference on Medical Image Computing and Computer Assisted Intervention (MICCAI 2017), Springer. pp. 232– 239.
- Sokooti, H., Yousefi, S., Elmahdy, M.S., Lelieveldt, B.P., Staring, M., 2021. Hierarchical prediction of registration misalignment using a convolutional LSTM: Application to chest CT scans. IEEE Access 9, 62008–62020.
- Song, X., Chao, H., Xu, X., Guo, H., Xu, S., Turkbey, B., Wood, B.J., Sanford, T., Wang, G., Yan, P., 2022. Cross-modal attention for multi-modal image registration. Medical Image Analysis 82, 102612.
- Sotiras, A., Davatzikos, C., Paragios, N., 2013. Deformable medical image registration: A survey. IEEE Trans. Med. Imag. 32, 1153–1190.
- Stefanescu, R., Pennec, X., Ayache, N., 2004. Grid powered nonlinear image registration with locally adaptive regularization. Medical Image Analysis 8, 325–342.
- Steinbrücker, F., Pock, T., Cremers, D., 2009. Large displacement optical flow computation withoutwarping, in: 1995 IEEE International Conference on Computer Vision (ICCV), IEEE. pp. 1609–1614.
- Stone, A., Maurer, D., Ayvaci, A., Angelova, A., Jonschkowski, R., 2021.

- SMURF: Self-teaching multi-frame unsupervised RAFT with full-image warping, in: Proceedings of the IEEE/CVF Conference on Computer Vision and Pattern Recognition, pp. 3887–3896.
- Studholme, C., Constable, R.T., Duncan, J.S., 2000. Accurate alignment of functional EPI data to anatomical MRI using a physics-based distortion model. IEEE Trans. Med. Imag. 19, 1115–1127.
- Su, H., Yang, X., 2023. Nonuniformly spaced control points based on variational cardiac image registration, in: 26th International Conference on Medical Image Computing and Computer Assisted Intervention (MICCAI 2023), Springer. pp. 634–644.
- Sun, S., Han, K., Kong, D., Tang, H., Yan, X., Xie, X., 2022. Topology-preserving shape reconstruction and registration via neural diffeomorphic flow, in: Proceedings of the IEEE/CVF Conference on Computer Vision and Pattern Recognition, pp. 20845–20855.
- Sun, Y., Yuan, J., Rajchl, M., Qiu, W., Romagnoli, C., Fenster, A., 2013. Efficient convex optimization approach to 3D non-rigid MR-TRUS registration, in: Medical Image Computing and Computer-Assisted Intervention—MICCAI 2013: 16th International Conference, Nagoya, Japan, September 22-26, 2013, Proceedings, Part I 16, Springer. pp. 195–202.
- Ta, K., Ahn, S.S., Stendahl, J.C., Sinusas, A.J., Duncan, J.S., 2020. A semi-supervised joint network for simultaneous left ventricular motion tracking and segmentation in 4D echocardiography, in: 23rd International Conference on Medical Image Computing and Computer Assisted Intervention (MIC-CAI 2020), Springer. pp. 468–477.
- Tan, Z., Zhang, H., Tian, F., Zhang, L., Sun, W., Lu, H., 2023. Progressively Coupling Network for Brain MRI Registration in Few-Shot Situation, in: 26th International Conference on Medical Image Computing and Computer Assisted Intervention (MICCAI 2023), Springer. pp. 623–633.
- Tang, K., Li, Z., Tian, L., Wang, L., Zhu, Y., 2020. ADMIR–affine and deformable medical image registration for drug-addicted brain images. IEEE Access 8, 70960–70968.
- Tang, L., Hamarneh, G., Abugharbieh, R., 2010. Reliability-driven, spatially-adaptive regularization for deformable registration, in: Biomedical Image Registration: 4th International Workshop, WBIR 2010, Lübeck, Germany, July 11-13, 2010. Proceedings 4, Springer. pp. 173–185.
- Team, N.L.S.T.R., 2011. Reduced lung-cancer mortality with low-dose computed tomographic screening. New England Journal of Medicine 365, 395–409.
- Terpstra, M.L., Maspero, M., Sbrizzi, A., van den Berg, C.A., 2022. ⊥-loss: A symmetric loss function for magnetic resonance imaging reconstruction and image registration with deep learning. Medical Image Analysis, 102509.
- Teske, H., Bartelheimer, K., Meis, J., Bendl, R., Stoiber, E.M., Giske, K., 2017.
 Construction of a biomechanical head and neck motion model as a guide to evaluation of deformable image registration. Physics in Medicine & Biology 62, N271.
- Thévenaz, P., Unser, M., 2000. Optimization of mutual information for multiresolution image registration. IEEE Trans. Imag. Proc. 9, 2083–2099.
- Thirion, J.P., 1998. Image matching as a diffusion process: an analogy with maxwell's demons. Medical Image Analysis 2, 243–260.
- Tian, L., Greer, H., Vialard, F.X., Kwitt, R., Estépar, R.S.J., Niethammer, M., 2022. GradICON: Approximate diffeomorphisms via gradient inverse consistency, in: Proceedings of the IEEE/CVF Conference on Computer Vision and Pattern Recognition, pp. 18084–18094.
- Tran, M.Q., Do, T., Tran, H., Tjiputra, E., Tran, Q.D., Nguyen, A., 2022. Light-weight deformable registration using adversarial learning with distilling knowledge. IEEE Trans. Med. Imag. 41, 1443–1453.
- Trouvé, A., Younes, L., 2005. Metamorphoses through lie group action. Foundations of computational mathematics 5, 173–198.
- Ulyanov, D., Vedaldi, A., Lempitsky, V., 2018. Deep image prior, in: Proceedings of the IEEE/CVF Conference on Computer Vision and Pattern Recognition, pp. 9446–9454.
- Unberath, M., Gao, C., Hu, Y., Judish, M., Taylor, R.H., Armand, M., Grupp, R., 2021. The impact of machine learning on 2D/3D registration for imageguided interventions: A systematic review and perspective. Frontiers in Robotics and AI 8, 716007.
- Unnikrishnan, R., Hebert, M., 2005. Measures of similarity, in: 2005 Seventh IEEE Workshops on Applications of Computer Vision (WACV/MOTION'05)-Volume 1, IEEE. pp. 394–394.
- Uzunova, H., Wilms, M., Handels, H., Ehrhardt, J., 2017. Training cnns for image registration from few samples with model-based data augmentation, in: Medical Image Computing and Computer Assisted Intervention- MICCAI 2017: 20th International Conference, Quebec City, QC, Canada, September

- 11-13, 2017, Proceedings, Part I 20, Springer. pp. 223-231.
- Vaswani, A., Shazeer, N., Parmar, N., Uszkoreit, J., Jones, L., Gomez, A.N., Kaiser, Ł., Polosukhin, I., 2017. Attention is all you need. Advances in Neural Information Processing Systems 30.
- Vercauteren, T., Pennec, X., Perchant, A., Ayache, N., 2009. Diffeomorphic demons: Efficient non-parametric image registration. NeuroImage 45, S61– S72
- Vialard, F.X., Risser, L., 2014. Spatially-varying metric learning for diffeomorphic image registration: A variational framework, in: 17th International Conference on Medical Image Computing and Computer Assisted Intervention (MICCAI 2014), Springer. pp. 227–234.
- Viergever, M.A., Maintz, J.A., Klein, S., Murphy, K., Staring, M., Pluim, J.P., 2016. A survey of medical image registration—under review. Medical Image Analysis 33, 140–144.
- Viola, P., Wells III, W.M., 1997. Alignment by maximization of mutual information. International Journal of Computer Vision 24, 137–154.
- Vishnevskiy, V., Gass, T., Szekely, G., Tanner, C., Goksel, O., 2016. Isotropic total variation regularization of displacements in parametric image registration. IEEE Trans. Med. Imag. 36, 385–395.
- Vlachopoulos, G., Korfiatis, P., Skiadopoulos, S., Kazantzi, A., Kalogeropoulou, C., Pratikakis, I., Costaridou, L., 2015. Selecting registration schemes in case of interstitial lung disease follow-up in CT. Med. Phys. 42, 4511–4525.
- Vos, B.D.d., Berendsen, F.F., Viergever, M.A., Staring, M., Išgum, I., 2017. End-to-end unsupervised deformable image registration with a convolutional neural network, in: Deep learning in medical image analysis and multimodal learning for clinical decision support. Springer, pp. 204–212.
- Wang, H., Ni, D., Wang, Y., 2023a. Modet: Learning deformable image registration via motion decomposition transformer, in: 26th International Conference on Medical Image Computing and Computer Assisted Intervention (MICCAI 2023), Springer. pp. 740–749.
- Wang, J., Jiao, J., Bao, L., He, S., Liu, Y., Liu, W., 2019a. Self-supervised spatio-temporal representation learning for videos by predicting motion and appearance statistics, in: Proceedings of the IEEE/CVF Conference on Computer Vision and Pattern Recognition, pp. 4006–4015.
- Wang, J., Wells III, W.M., Golland, P., Zhang, M., 2019b. Registration uncertainty quantification via low-dimensional characterization of geometric deformations. Magnetic resonance imaging 64, 122–131.
- Wang, J., Xing, J., Druzgal, J., Wells III, W.M., Zhang, M., 2023b. MetaMorph: Learning Metamorphic Image Transformation With Appearance Changes, in: 28th Inf. Proc. in Med. Imaging (IPMI 2023), pp. 576–587.
- Wang, J., Zhang, M., 2020. Deepflash: An efficient network for learning-based medical image registration, in: Proceedings of the IEEE/CVF Conference on Computer Vision and Pattern Recognition, pp. 4444–4452.
- Wang, J., Zhang, M., 2022. Geo-SIC: Learning deformable geometric shapes in deep image classifiers. Advances in Neural Information Processing Systems 35, 27994–28007.
- Wang, J., Zhang, M., et al., 2022. Deep learning for regularization prediction in diffeomorphic image registration. Machine Learning for Biomedical Imaging 1, 1–10.
- Wang, Y., Fu, T., Wu, C., Xiao, J., Fan, J., Song, H., Liang, P., Yang, J., 2023c. Multimodal registration of ultrasound and mr images using weighted self-similarity structure vector. Computers in Biology and Medicine 155, 106661.
- Wang, Z., Bovik, A.C., Sheikh, H.R., Simoncelli, E.P., 2004. Image quality assessment: from error visibility to structural similarity. IEEE Trans. Imag. Proc. 13, 600–612.
- Wannenwetsch, A.S., Keuper, M., Roth, S., 2017. ProbFlow: Joint optical flow and uncertainty estimation, in: Proceedings of the IEEE/CVF Conference on Computer Vision and Pattern Recognition, pp. 1173–1182.
- Wasserthal, J., Breit, H.C., Meyer, M.T., Pradella, M., Hinck, D., Sauter, A.W., Heye, T., Boll, D.T., Cyriac, J., Yang, S., et al., 2023. Totalsegmentator: robust segmentation of 104 anatomic structures in ct images. Radiology: Artificial Intelligence 5.
- Wei, D., Ahmad, S., Guo, Y., Chen, L., Huang, Y., Ma, L., Wu, Z., Li, G., Wang, L., Lin, W., et al., 2021a. Recurrent tissue-aware network for deformable registration of infant brain MR images. IEEE Trans. Med. Imag. 41, 1219– 1229.
- Wei, D., Ahmad, S., Huo, J., Peng, W., Ge, Y., Xue, Z., Yap, P.T., Li, W., Shen, D., Wang, Q., 2019. Synthesis and inpainting-based MR-CT registration for image-guided thermal ablation of liver tumors, in: 22nd International Conference on Medical Image Computing and Computer Assisted Interven-

- tion (MICCAI 2019), Springer. pp. 512-520.
- Wei, W., Haishan, X., Alpers, J., Rak, M., Hansen, C., 2021b. A deep learning approach for 2D ultrasound and 3D CT/MR image registration in liver tumor ablation. Computer Methods and Programs in Biomedicine 206, 106117. doi:10.1016/j.cmpb.2021.106117.
- Weinzaepfel, P., Revaud, J., Harchaoui, Z., Schmid, C., 2013. Deepflow: Large displacement optical flow with deep matching, in: 2013 IEEE International Conference on Computer Vision (ICCV), pp. 1385–1392.
- Weitz, P., Valkonen, M., Solorzano, L., Carr, C., Kartasalo, K., Boissin, C., Koivukoski, S., Kuusela, A., Rasic, D., Feng, Y., et al., 2024. The ACRO-BAT 2022 challenge: Automatic registration of breast cancer tissue. Medical Image Analysis 97, 103257.
- Wells III, W.M., Viola, P., Atsumi, H., Nakajima, S., Kikinis, R., 1996. Multi-modal volume registration by maximization of mutual information. Medical Image Analysis 1, 35–51.
- Wetzer, E., Lindblad, J., Sladoje, N., 2023. Can representation learning for multimodal image registration be improved by supervision of intermediate layers?, in: Iberian Conference on Pattern Recognition and Image Analysis, pp. 261–275.
- Wolterink, J.M., Zwienenberg, J.C., Brune, C., 2022. Implicit neural representations for deformable image registration, in: International Conference on Medical Imaging with Deep Learning, PMLR. pp. 1349–1359.
- Wu, G., Kim, M., Wang, Q., Gao, Y., Liao, S., Shen, D., 2013. Unsupervised deep feature learning for deformable registration of MR brain images, in: 16th International Conference on Medical Image Computing and Computer Assisted Intervention (MICCAI 2013), Springer. pp. 649–656.
- Wu, N., Wang, J., Zhang, M., Zhang, G., Peng, Y., Shen, C., 2022a. Hybrid atlas building with deep registration priors, in: 19th International Symposium on Biomedical Imaging (ISBI 2022), IEEE. pp. 1–5.
- Wu, R.Y., Liu, A.Y., Wisdom, P., Zhu, X.R., Frank, S.J., Fuller, C.D., Gunn, G.B., Palmer, M.B., Wages, C.A., Gillin, M.T., et al., 2019. Characterization of a new physical phantom for testing rigid and deformable image registration. Journal of Applied Clinical Medical Physics 20, 145–153.
- Wu, Y., Jiahao, T.Z., Wang, J., Yushkevich, P.A., Hsieh, M.A., Gee, J.C., 2022b. NODEO: A Neural Ordinary Differential Equation Based Optimization Framework for Deformable Image Registration, in: Proceedings of the IEEE/CVF Conference on Computer Vision and Pattern Recognition, pp. 20804–20813.
- Xiao, H., Teng, X., Liu, C., Li, T., Ren, G., Yang, R., Shen, D., Cai, J., 2021. A review of deep learning-based three-dimensional medical image registration methods. Quantitative Imaging in Medicine and Surgery 11, 4895.
- Xiao, Y., Fortin, M., Unsgård, G., Rivaz, H., Reinertsen, I., 2017. Re trospective evaluation of cerebral tumors (resect): A clinical database of pre-operative mri and intra-operative ultrasound in low-grade glioma surgeries. Medical physics 44, 3875–3882.
- Xie, L., Wang, J., Dong, M., Wolk, D.A., Yushkevich, P.A., 2019. Improving multi-atlas segmentation by convolutional neural network based patch error estimation, in: 22nd International Conference on Medical Image Computing and Computer Assisted Intervention (MICCAI 2019), Springer. pp. 347– 355.
- Xie, L., Wisse, L.E., Wang, J., Ravikumar, S., Khandelwal, P., Glenn, T., Luther, A., Lim, S., Wolk, D.A., Yushkevich, P.A., 2023. Deep label fusion: A generalizable hybrid multi-atlas and deep convolutional neural network for medical image segmentation. Medical Image Analysis 83, 102683.
- Xing, F., Woo, J., Gomez, A.D., Pham, D.L., Bayly, P.V., Stone, M., Prince, J.L., 2017. Phase vector incompressible registration algorithm for motion estimation from tagged magnetic resonance images. IEEE Trans. Med. Imag. 36, 2116–2128.
- Xu, J., Chen, E.Z., Chen, X., Chen, T., Sun, S., 2021. Multi-scale neural ODES for 3D medical image registration, in: 24th International Conference on Medical Image Computing and Computer Assisted Intervention (MICCAI 2021), Springer. pp. 213–223.
- Xu, K., Huang, Q., Yang, X., 2023. Importance weighted variational cardiac mri registration using transformer and implicit prior, in: 26th International Conference on Medical Image Computing and Computer Assisted Intervention (MICCAI 2023), Springer. pp. 581–591.
- Xu, Z., Lee, C.P., Heinrich, M.P., Modat, M., Rueckert, D., Ourselin, S., Abramson, R.G., Landman, B.A., 2016. Evaluation of six registration methods for the human abdomen on clinically acquired ct. IEEE Transactions on Biomedical Engineering 63, 1563–1572.
- Xu, Z., Luo, J., Lu, D., Yan, J., Frisken, S., Jagadeesan, J., Wells III, W.M., Li, X., Zheng, Y., Tong, R.K.y., 2022. Double-uncertainty guided spatial and

- temporal consistency regularization weighting for learning-based abdominal registration, in: MICCAI22, Springer. pp. 14–24.
- Xu, Z., Luo, J., Yan, J., Pulya, R., Li, X., Wells, W., Jagadeesan, J., 2020. Adversarial uni-and multi-modal stream networks for multimodal image registration, in: 23rd International Conference on Medical Image Computing and Computer Assisted Intervention (MICCAI 2020), Springer. pp. 222–232.
- Xu, Z., Niethammer, M., 2019. Deepatlas: Joint semi-supervised learning of image registration and segmentation, in: 22nd International Conference on Medical Image Computing and Computer Assisted Intervention (MIC-CAI 2019), Springer. pp. 420–429.
- Yan, K., Cai, J., Jin, D., Miao, S., Guo, D., Harrison, A.P., Tang, Y., Xiao, J., Lu, J., Lu, L., 2022. Sam: Self-supervised learning of pixel-wise anatomical embeddings in radiological images. IEEE Trans. Med. Imag. 41, 2658–2669.
- Yan, P., Xu, S., Rastinehad, A.R., Wood, B.J., 2018. Adversarial image registration with application for MR and TRUS image fusion, in: Machine Learning in Medical Imaging: 9th International Workshop, MLMI 2018, Held in Conjunction with MICCAI 2018, Granada, Spain, September 16, 2018, Proceedings 9, Springer, pp. 197–204.
- Yang, H., Sun, J., Carass, A., Zhao, C., Lee, J., Prince, J.L., Xu, Z., 2020. Unsupervised MR-to-CT synthesis using structure-constrained CycleGAN. IEEE Trans. Med. Imag. 39, 4249–4261.
- Yang, H., Sun, J., Li, H., Wang, L., Xu, Z., 2018. Neural multi-atlas label fusion: Application to cardiac MR images. Medical Image Analysis 49, 60-75
- Yang, J., Wickramasinghe, U., Ni, B., Fua, P., 2022a. ImplicitAtlas: learning deformable shape templates in medical imaging, in: Proceedings of the IEEE/CVF Conference on Computer Vision and Pattern Recognition, pp. 15861–15871.
- Yang, T., Bai, X., Cui, X., Gong, Y., Li, L., 2022b. GraformerDIR: Graph convolution transformer for deformable image registration. Computers in Biology and Medicine 147, 105799.
- Yang, X., Kwitt, R., Niethammer, M., 2016. Fast predictive image registration, in: Deep Learning and Data Labeling for Medical Applications: First International Workshop, LABELS 2016, and Second International Workshop, DLMIA 2016, Held in Conjunction with MICCAI 2016, Athens, Greece, October 21, 2016, Proceedings 1, Springer. pp. 48–57.
- Yang, X., Kwitt, R., Styner, M., Niethammer, M., 2017. Quicksilver: Fast predictive image registration—a deep learning approach. NeuroImage 158, 378–396.
- Yao, Y., Liu, C., Luo, D., Zhou, Y., Ye, Q., 2020. Video playback rate perception for self-supervised spatio-temporal representation learning, in: Proceedings of the IEEE/CVF Conference on Computer Vision and Pattern Recognition, pp. 6548–6557.
- Ye, M., Kanski, M., Yang, D., Chang, Q., Yan, Z., Huang, Q., Axel, L., Metaxas, D., 2021. DeepTag: An unsupervised deep learning method for motion tracking on cardiac tagging magnetic resonance images, in: 2021 IEEE Conference on Computer Vision and Pattern Recognition (CVPR), pp. 7261–7271.
- Yin, W., Sonke, J.J., Gavves, E., 2023. Pc-reg: A pyramidal prediction—correction approach for large deformation image registration. Medical Image Analysis 90, 102978.
- Younes, L., 2010. Shapes and diffeomorphisms. volume 171. Springer.
- Yu, E.M., Dalca, A.V., Sabuncu, M.R., 2020a. Learning conditional deformable shape templates for brain anatomy, in: Machine Learning in Medical Imaging: 11th International Workshop, MLMI 2020, Held in Conjunction with MICCAI 2020, Lima, Peru, October 4, 2020, Proceedings 11, Springer. pp. 353–362.
- Yu, H., Chen, X., Shi, H., Chen, T., Huang, T.S., Sun, S., 2020b. Motion pyramid networks for accurate and efficient cardiac motion estimation, in: 23rd International Conference on Medical Image Computing and Computer Assisted Intervention (MICCAI 2020), Springer. pp. 436–446.
- Yu, H., Sun, S., Yu, H., Chen, X., Shi, H., Huang, T.S., Chen, T., 2020c. FOAL: Fast online adaptive learning for cardiac motion estimation, in: Proceedings of the IEEE/CVF Conference on Computer Vision and Pattern Recognition, pp. 4313–4323.
- Yuan, L., Chen, Y., Wang, T., Yu, W., Shi, Y., Jiang, Z.H., Tay, F.E., Feng, J., Yan, S., 2021. Tokens-to-token ViT: Training vision transformers from scratch on imagenet, in: Proceedings of the IEEE/CVF Conference on Computer Vision and Pattern Recognition, pp. 558–567.
- Zhai, M., Xiang, X., Lv, N., Kong, X., 2021. Optical flow and scene flow estimation: A survey. Pattern Recognition 114, 107861.
- Zhang, B., Faghihroohi, S., Azampour, M.F., Liu, S., Ghotbi, R., Schunkert, H.,

- Navab, N., 2023a. A patient-specific self-supervised model for automatic x-ray/ct registration, in: 26th International Conference on Medical Image Computing and Computer Assisted Intervention (MICCAI 2023), Springer.
- Zhang, J., 2018. Inverse-consistent deep networks for unsupervised deformable image registration. arXiv preprint arXiv:1809.03443.
- Zhang, M., Fletcher, P.T., 2019. Fast diffeomorphic image registration via fourier-approximated lie algebras. International Journal of Computer Vision 127, 61–73.
- Zhang, S., Liu, P.X., Zheng, M., Shi, W., 2020. A diffeomorphic unsupervised method for deformable soft tissue image registration. Computers in Biology and Medicine 120, 103708.
- Zhang, Y., Li, L., Wang, W., Xie, R., Song, L., Zhang, W., 2023b. Boosting video object segmentation via space-time correspondence learning, in: Proceedings of the IEEE/CVF Conference on Computer Vision and Pattern Recognition, pp. 2246–2256.
- Zhang, Y., Pei, Y., Zha, H., 2021a. Learning dual transformer network for diffeomorphic registration, in: 24th International Conference on Medical Image Computing and Computer Assisted Intervention (MICCAI 2021), Springer. pp. 129–138.
- Zhang, Y., Wu, X., Gach, H.M., Li, H., Yang, D., 2021b. GroupRegNet: a groupwise one-shot deep learning-based 4D image registration method. Physics in Medicine & Biology 66, 045030.
- Zhao, F., Wu, Z., Wang, F., Lin, W., Xia, S., Shen, D., Wang, L., Li, G., 2021a. S3reg: Superfast spherical surface registration based on deep learning. IEEE Trans. Med. Imag. 40, 1964–1976.
- Zhao, F., Wu, Z., Wang, L., Lin, W., Xia, S., Li, G., UNC/UMN Baby Connectome Project Consortium, 2021b. Learning 4D infant cortical surface atlas with unsupervised spherical networks, in: 24th International Conference on Medical Image Computing and Computer Assisted Intervention (MIC-CAI 2021), Springer. pp. 262–272.
- Zhao, L., Pang, S., Chen, Y., Zhu, X., Jiang, Z., Su, Z., Lu, H., Zhou, Y., Feng, Q., 2023. SpineRegNet: Spine Registration Network for volumetric MR and CT image by the joint estimation of an affine-elastic deformation field. Medical Image Analysis 86, 102786.
- Zhao, S., Lau, T., Luo, J., Eric, I., Chang, C., Xu, Y., 2019. Unsupervised 3D end-to-end medical image registration with volume tweening network. IEEE Journal of Biomedical and Health Informatics 24, 1394–1404.
- Zheng, Y., Sui, X., Jiang, Y., Che, T., Zhang, S., Yang, J., Li, H., 2021.SymReg-GAN: symmetric image registration with generative adversarial networks. IEEE Trans. Patt. Anal. Mach. Intell. 44, 5631–5646.
- Zhong, L., Huang, P., Shu, H., Li, Y., Zhang, Y., Feng, Q., Wu, Y., Yang, W., 2023. United multi-task learning for abdominal contrast-enhanced ct synthesis through joint deformable registration. Computer Methods and Programs in Biomedicine 231, 107391.
- Zhou, S., Hu, B., Xiong, Z., Wu, F., 2023. Self-distilled hierarchical network for unsupervised deformable image registration. IEEE Trans. Med. Imag. .
- Zhou, Z., Siddiquee, M.M.R., Tajbakhsh, N., Liang, J., 2019. Unet++: Redesigning skip connections to exploit multiscale features in image segmentation. IEEE Trans. Med. Imag. 39, 1856–1867.
- Zhu, H., Adeli, E., Shi, F., Shen, D., Initiative, A.D.N., 2020. FCN based label correction for multi-atlas guided organ segmentation. NeuroImage 18, 319–331.
- Zhu, J.Y., Park, T., Isola, P., Efros, A.A., 2017. Unpaired image-to-image translation using cycle-consistent adversarial networks, in: Proceedings of the IEEE/CVF Conference on Computer Vision and Pattern Recognition, pp. 2223–2232.
- Zhuang, X., Li, L., Payer, C., Štern, D., Urschler, M., Heinrich, M.P., Oster, J., Wang, C., Smedby, Ö., Bian, C., et al., 2019. Evaluation of algorithms for multi-modality whole heart segmentation: an open-access grand challenge. Medical image analysis 58, 101537.
- Zhuang, X., Rhode, K., Arridge, S., Razavi, R., Hill, D., Hawkes, D., Ourselin, S., 2008. An atlas-based segmentation propagation framework using locally affine registration–application to automatic whole heart segmentation, in: 11th International Conference on Medical Image Computing and Computer Assisted Intervention (MICCAI 2008), Springer. pp. 425–433.
- Zou, J., Gao, B., Song, Y., Qin, J., 2022. A review of deep learning-based deformable medical image registration. Frontiers in Oncology 12.